Morten Omholt Alver

Modelling, Instrumentation and Control in Marine Larviculture

DR.ING thesis

Norwegian University of Science and Technology

Acknowledgments

The work on this thesis has been funded through an NTNU (Norwegian University of Science and Technology) scholarship, and has formed part of the CODTECH project.

I would like to thank my supervisors, Jo Arve Alfredsen, Yngvar Olsen and Bård Holand, for sharing their enthusiasm, knowledge and good advice.

Thanks to Gunvor Øie at SINTEF Fisheries and Aquaculture for great leadership in running the CODTECH experiments, and for valuable ideas and feedback throughout these four years. Thanks to Atsushi Hagiwara at Nagasaki University, for letting me stay at his lab in September–December 2005, and for collaboration on rotifer modelling. This thesis would not have been written if not for Jens G. Balchen, who initiated fisheries and aquaculture related research at our department more than 35 years ago.

Thanks also go to Trygve Sigholt, Torodd Tennøy, Olav Vadstein, Erik Høy, Sunniva Kui, Tove Beate Leren, Ingrid Overrein, Werner Johansen and Per-Arvid Wold, for good cooperation in various experimental work, and all kinds of help and advice.

Contents

List of Papers

1. Alver, M. O., Alfredsen, J. A. & Olsen, Y., 2006. *An individual-based population model for rotifer (*Brachionus plicatilis*) cultures.* Hydrobiologia 560, 93–108.

2. Alver, M. O., Alfredsen, J. A. & Olsen, Y. *An individual-based model for predicting body composition of cultured* Brachionus plicatilis *rotifers.* Canadian Journal of Fisheries and Aquatic Sciences, submitted paper.

3. Alver, M. O., Tennøy, T., Alfredsen, J. A. & Øie, G. *Automatic measurement of rotifer* Brachionus plicatilis *densities in first feeding tanks.* Aquacultural Engineering, in press.

4. Alver, M. O., Alfredsen, J. A. & Øie, G., 2005. *A system for model based biomass estimation of larvae in intensive cod larvicultures.* Aquaculture International 13, 519–541.

5. Alver, M. O., Alfredsen, J. A. & Øie, G. *Estimating larval density in cod (*Gadus morhua*) first feeding tanks using measurements of feed density and larval growth rates.* Proceedings of the Larvi 2005 conference, Aquaculture, submitted paper.

6. Alver, M. O., Tennøy, T., Alfredsen, J. A. , Øie, G. & Olsen, Y. *Automatic control of rotifer density in larval first feeding tanks.* Control Engineering Practice, submitted paper.

Chapter 1

Introduction

The cold-water marine fish species Atlantic cod (*Gadus morhua* L.) and Atlantic halibut (*Hippoglossus hippoglossus* L.) are relatively new aquaculture species in Norway (Olsen, 1997). The development of culture methods for these species has been faced with significant challenges, particularly because of the complexity of the larval rearing process (Moksnes et al., 2004, pp. 1–5). Juveniles of both species have been produced in Norway since around 1990, but due to problems with productivity and predictability, the progress in production volumes was poor in the period 1990–2000 (Engelsen et al., 2004). Since year 2000, cod production has increased strongly, while the volumes of farmed halibut are not expected to increase rapidly during the next decade owing to the slow progress of juvenile production technology (Engelsen et al., 2004).

Predictable production and low production costs are keys for success, and in Norwegian marine larviculture there is still a lot to be gained in both respects. Hatcheries often rely on the personal experience of key employees to ensure stable production. Monitoring and control techniques have played an important part in improving predictability and reducing costs in other industries (Haley and Mulvaney, 1995; Jämsä-Jounela, 2001; Findeisen et al., 2003), but have apparently not been widely applied in aquaculture production. Dynamic modelling has also not been applied very extensively in aquaculture research, with some exceptions such as Slagstad et al. (1987), Conceição et al. (1998), Balchen (1999) and Alver et al. (2004). The present thesis is part of an effort to address these issues.

This work is part of the university programme *CODTECH — A process oriented approach to intensive production of juveniles with emphasis on cod.*

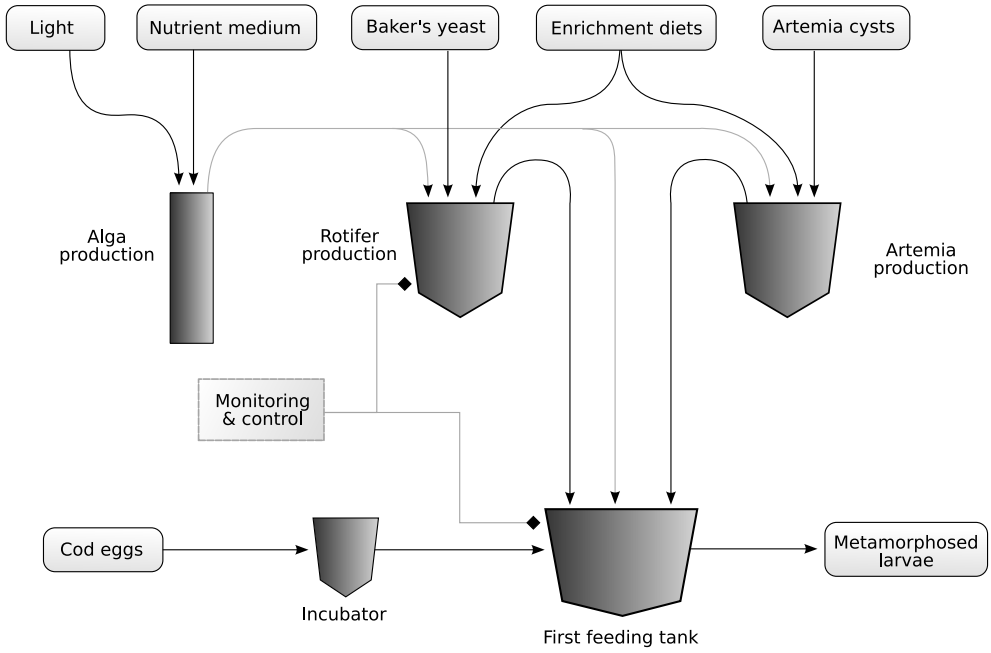

Figure 1.1: Overview of the production process from eggs to metamorphosed cod larvae.

The activities within CODTECH are divided into four projects: 1. Modelling, instrumentation, control and optimization of hatchery processes. 2. Larval feed components. 3. Microbial interactions and control. 4. Controlled intensive first feeding and weaning of cod larvae. The present thesis contributes primarily to Project 1, whose title implies the application of cybernetic methods to the juvenile production process. The basic processes involved in the production of juvenile marine fish are summarized in Figure 1.1. The box labeled *Monitoring & control* indicates which elements of the production process that this work is primarily focused on.

Mathematical modelling has an important role in this work, and as will be clear from the enclosed papers, the models are used for two purposes. First, they serve as tools for describing process dynamics. Model simulations can provide predictions for application in production planning and in assessing the effect of process parameters. Second, mathematical models are used as components

of model based control systems and state estimators. In this application, the models are run in parallel with the actual process and with instrumentation, providing estimates of the current process state beyond what can be readily measured.

1.1 Objectives

The main objectives of this work are to:

- Develop predictive models of central processes, such as larval first feeding and the cultivation and enrichment of live feed.
- Use instrumentation in combination with models to extract information from the production process for variables that are difficult to measure directly.
- Implement automatic control in order to improve predictability, optimize production and reduce manual labour.

1.2 Outline

- Chapter 2 provides background on the marine larviculture process, and highlights the challenges involved in the various subprocesses.
- Chapter 3 describes the methods that have been developed, in the form of mathematical models or physical equipment, and presents the main results that have been achieved. The contents of this chapter are mainly extracted from the enclosed published papers, which go into more detail on the various methods and results.
- Chapter 4 contains concluding remarks, a summary of the contributions of this thesis, and suggestions for further work.

Chapter 2

The Marine Larviculture Process

It is reasonable to draw comparisons between marine aquaculture and the culture of salmon and trout, which has been a remarkably successful industry in Norway, with a production of nearly 600.000 tonnes in 2005 (Anon., 2005). Despite the great amount of knowledge obtained and technology developed for salmonid aquaculture, and for the culture of other marine fish species such as sea bass (*Dicentrarchus labrax*) and sea bream (*Sparus aurata*) (Oliva-Teles, 2000), the development of culture techniques for cold-water marine species has posed significant challenges.

The challenges of cultivating the initial life stages of marine fish are different from those of salmonid production. The most important differences are in the size and developmental stage of the larvae at hatching, as marine fish typically hatch at a smaller size (Moksnes et al., 2004, Figure 1.2) and an earlier developmental stage. For instance, cod larvae at the time of hatching have not yet developed a stomach, and the digestive tract is only partly developed (Kjørsvik et al., 1991).

Marine fish larvae in aquaculture generally require live feed in the initial phase, for reasons that can be explained by several characteristics of the larvae. First, feed ingestion is triggered by visual and chemical stimuli (Cahu and Infante, 2001), and because of the larvae's limited visual range and movement at the earliest stage (Aksnes and Utne, 1997; Fiksen et al., 1998), the feed particles have to be suspended in the water column in order to be available. Formulated

feeds tend to have a high sinking rate, and must therefore be distributed in large excess to cover the larvae's requirements (Cahu and Infante, 2001). Live feed organisms, on the other hand, have active locomotion, and thus a better availability in the water column. Second, very small feed particle sizes are required to match the larvae's mouth sizes, and this may pose problems in formulating feeds. For sea bass at first feeding, Cahu and Infante (2001) used dry feed particles of 50–150 μm in diameter. Preventing nutrient leakage from particles of these sizes without reducing the digestibility of the feed is a significant manufacturing challenge (Baskerville-Bridges and Kling, 2000; Cahu and Infante, 2001). Third, since the larvae's digestive system is under development in the initial larval stage, the diet must contain the required components to support the induction of enzyme secretory mechanisms (Cahu and Infante, 2001). The live feed requirement may have other causes in addition to those mentioned here.

The requirement for live feed is not absolute, and some experimental diets have been shown to sustain growth and survival of larvae (Cahu and Infante, 2001). However, in the near future, it is not practically feasible to run a commercial farming process based on formulated feed only.

For several reasons, the use of live feed makes the culture process more complicated and costly.[1] First, the production of live feed requires significant amounts of tank space, equipment, feed and manual work. Hatcheries need to be prepared that rotifer cultures can sometimes unexpectedly suffer massive mortality, increasing the overall cost (Papakostas et al., 2006).

Second, live feed differs from formulated feed in that the organisms have their own metabolism and therefore a more volatile biochemical composition or nutritional value. There are few available choices of live feed organisms suitable for intensive culture, and therefore the body composition of the organisms in culture typically matches the requirements of the fish larvae poorly. This is especially true for cold-water species with a high requirement for $n-3$ HUFA (highly unsaturated fatty acids) (Olsen et al., 2004, pp. 282–284). To compensate for this the farmer needs to *enrich* the live feed with essential nutrients before use by providing a feed dosage containing the necessary nutritional additions (Rainuzzo et al., 1997). The effect of such an enrichment lasts for a limited time only, as the live feed organisms metabolize the nutrients after enrichment.

Third, live feed organisms carry their own bacterial flora into the larval rearing environment, and contribute in this way to a heavy microbial load in

[1] One study shows that for sea bass the live feed costs were 79% of the total costs during the first 45 days after hatching (le Ruyet et al., 1993).

the tanks (Skjermo and Vadstein, 1999). The digestive system of the larvae is initially sterile, and is colonized by bacteria from the eggs, the water and from ingested food (Vine et al., 2006). Short term enrichment procedures before use of the live feed provides an energy-rich environment which may increase the number of fast growing bacteria carried by the live feed. Some of these bacteria may be harmful to the fish. However, control of the microflora can also be utilized to the advantage of the larvae through the use of *probiotic* techniques, which is currently a field of active research (Skjermo and Vadstein, 1999; Huys et al., 2001; Shields, 2001; Planas et al., 2004; Vine et al., 2006).

2.1 Environmental Conditions

Marine fish larvae are cultured in cylindrical tanks with conical bottoms, with sizes ranging from just a few liters in research facilities up to 30 m^3 or more in commercial hatcheries. Different inside wall colours are used, and the colour can in fact have an important effect on the light conditions and the larvae's ability to detect prey. For instance, Downing and Litvak (2000) found significantly better growth and survival for haddock (*Melanogrammus aeglefinus*) larvae in white tanks compared to black tanks. Commercial scale tanks may be fitted with automatic cleaning arms that sweep dead larvae and feed particles into the drain.

Abiotic water quality parameters include temperature, salinity, dissolved oxygen and ammonia. Within lower and upper limits, the rate of biological processes increases with temperature, but above the optimum temperature deleterious effects become more significant and the rate falls (Howell and Baynes, 2004). Higher temperature can allow faster larval growth up to an optimum level, but because of decreasing feed utilization and survival, the temperature giving the most efficient growth is typically lower than that giving the fastest growth (Jordaan and Kling, 2003). For cod, the optimum temperature for growth rate has been shown to increase from 9.7 to 13.4°C as larvae grow from 73 to 251 μg (Howell and Baynes, 2004).

The salinity of seawater is typically around 35 ppt offshore, and can be 32–33 ppt in coastal areas affected by freshwater run-off from the land (Howell and Baynes, 2004). Salinity affects both the energy required for osmoregulation, and the buoyancy of eggs and larvae (Howell and Baynes, 2004). An increase in salinity from 32.3 ppt to 35.5 ppt has been shown to have a negative effect on the morphological development of halibut yolk sac larvae (Bolla and Ottesen, 1998).

Dissolved oxygen is required for the larvae's respiration, and the concentration needs to be above a certain minimum level, dependent on species. A concentration of 5 mg l^{-1} is considered acceptable to aquatic organisms in general (Howell and Baynes, 2004). The solubility of oxygen is strongly affected by a combination of temperature and salinity, with higher temperature and higher salinity giving lower solubility. The oxygen level also depends on the balance between consumption and supply, with consumption being especially dependent on feeding rate.

Ammonia (NH_3) and ammonium ions (NH_4^+) are excreted by the fish larvae, and these two forms exist in a chemical balance affected by pH in particular, but also by temperature and salinity (Howell and Baynes, 2004). Both NH_3 and NH_4^+ are toxic, but NH_3 to a much higher degree. Increasing pH leads to an increase in the concentration of unionized ammonia, which must be held below a species-dependent limit.

The exchange rate of water is typically in the interval 1–8 tank volumes per day, increasing throughout the first few weeks after hatching. The water exchange rate is important for the addition of oxygen and removal of ammonia, but a higher exchange rate leads to faster depletion of feed organisms, and causes stronger mechanical forces at the inflow and outflow points. These forces can cause damage to the larvae, and may put a limit on the maximum exchange rate that can be used.

Water treatment systems can be divided into flow-through systems and recirculation systems. In the former, water is mechanically filtered, heated or cooled to the correct temperature, aerated, and de-gassed to avoid gas supersaturation. For reducing bacterial numbers, the water may be treated by UV radiation or ozone injection. The water is only used once. In a recirculation system, a certain fraction of the outlet water is reused. This reduces the amount of water entering the facility, and thereby the load on the initial water treatment system. Nitrogenous compounds accumulating in recirculation systems are normally removed by biological filtering (van Rijn, 1996). Recirculation can allow a more constant and controllable water quality than flow-through systems (Attramadal, 2004). There is currently no general consensus as to which strategy is preferable, and the optimal choice depends on which species is cultured.

Developmental deformities are often encountered during the process of establishing culture methods for new species (Brown and Núñes, 1998), and this has also been the case with cod and halibut (Bolla and Ottesen, 1998; Olsen et al., 1999; Grotmol et al., 2005; Imsland et al., 2006). The susceptibility of cultivated fish to deformities may partly be caused by a high survival rate of less fit individuals, and partly by suboptimal environmental conditions and nutritional

deficiencies in the feed (Brown and Núñes, 1998).

2.2 Feeding

Under favorable rearing conditions cod larvae can show a high growth rate of more than 20% weight increase per day (Otterlei et al., 1999; Finn et al., 2002). This growth rate naturally leads to a rapid increase in food requirements, which on the population level is countered by a relatively high mortality rate. The food requirement for each larval tank is a function of both larval growth and development, and the number of surviving larvae.

2.2.1 Feeding Regime and Feed Intake

At a temperature of 6 °C, the yolk sac of cod larvae is absorbed in about 6 days after hatching (Finn et al., 1995a). Feeding with rotifers is initiated on day 3–5 post-hatch, and the rotifer feeding stage normally lasts between 20 and 40 days (Brown et al., 2003). If Artemia is used, its introduction is made gradually, replacing rotifers when the larvae reach about 8–9 mm in length (Rosenlund et al., 1993). However, it is also possible to introduce a formulated feed at the end of the rotifer phase, excluding the use of Artemia (Baskerville-Bridges and Kling, 2000). The majority of cod hatcheries in Norway do not use Artemia. For halibut larvae, even the largest rotifers are near the smallest acceptable feed particle size, and Artemia is commonly applied as the first and only type of live feed (Olsen et al., 2004).

In the rotifer period, cod larvae can be fed either in several batches per day, or more continuously. Batch feeding with 3–4 feedings per day is the most common method, both in commercial hatcheries and research facilities. Feed availability is strongly affected by the water exchange rate. The out-flowing water is filtered to retain the fish larvae, but the rotifers flow out freely. Together with feed ingestion by the larvae, this causes the rotifer density to decrease rapidly after each feeding. Figure 2.1 shows a measurement series demonstrating the highly dynamic concentration of rotifers in larval tanks. The water exchange ensures a limited residence time for the rotifers in the larval tank, even if the ingestion rate of the larvae is low.

Under a batch feeding regime, the optimal rotifer density for cod larvae with regard to larval survival and growth has been found to be 4000 l^{-1} (Puvanendran and Brown, 1999; Puvanendran et al., 2002). It is worth noting that the rotifer density in this case is only adjusted up to 4000 l^{-1} during each feeding,

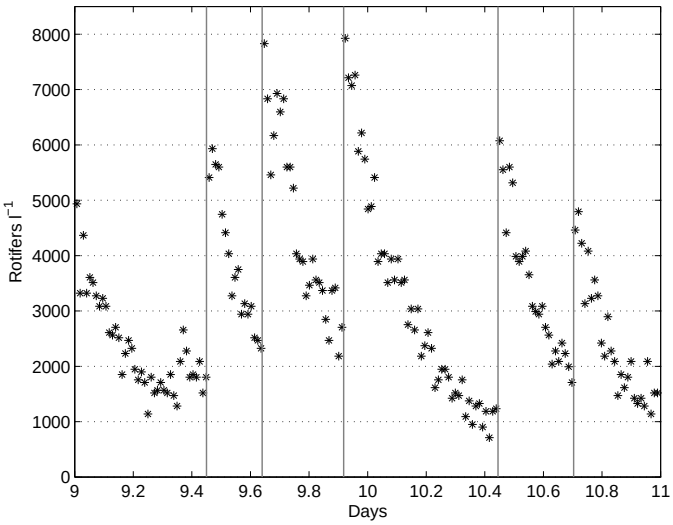

Figure 2.1: Automatic measurements of rotifer density in a cod larval first feeding tank. The gray lines indicate feeding times. The measurements are from days 9 and 10 of an experiment which is presented in Paper 5.

meaning that the average density will be significantly lower. The use of batch feeding has probably been motivated mostly by practical considerations, and there is no evidence of batch feeding being the optimal strategy for achieving high growth and survival. For red porgy (*Pagrus pagrus*), which has a high feed requirement, Papandroulakis et al. (2004) achieved favourable results with automated continuous feeding.

Fish larvae are believed to be *number maximizers*, which means that feed intake increases with prey density even at high densities, as opposed to reaching a saturation level (Lubzens et al., 1989; Hoehne-Reitan et al., 2001; Olsen et al., 2004). There is most likely an upper limit to the feed ingestion rate, and this limit is an effect of the minimum time required to capture and handle a prey organism. Several mathematical models have been published that describe the foraging behaviour of pelagic fish larvae (Fiksen et al., 1998, 2002; Fiksen and Folkvord, 1999; Fiksen and MacKenzie, 2002) based on such variables as visual range, reaction range and attack success rate. These models are primarily in-

tended for larvae in the wild, where food limitation is a significant risk, and may not be applicable for the aquacultural setting, where food is abundant most of the time. When food is abundant, the effect of handling time is more significant, and this element is typically ignored by the feed ingestion models. There is a limited amount of data from behavioural studies on the actual ingestion rate of live feed by cod larvae in culture tanks (Munk, 1995; Puvanendran et al., 2002).

2.2.2 Nutritional Requirements

The fish larvae require an adequate supply of the major nutrient classes to cover energy requirements and support growth, but the feed must also contain a number of specific essential components. There is a significant amount of data on the actual body composition of the larvae, e.g. Finn et al. (1995a) and Finn et al. (1995b), which can be expected to provide clues about their nutritional requirements. The fish larvae can to a certain degree metabolize components to cover their needs, but some fatty acids, amino acids and micronutrients such as vitamins and minerals, cannot be synthesized by the larvae, and need to be supplied in the feed. As mentioned earlier, deformities can often be linked to deficiencies in the nutritional value of the feed (Brown and Núñes, 1998).

The natural diet of the fish larvae, consisting largely of copepods for cold-water marine species, can be expected to provide a near perfect nutritional value. Copepods have been harvested and utilized as feed in extensive culture systems, but there has so far been slow progress towards mass-culture techniques for these organisms except in small-scale lab cultures of limited duration (Støttrup, 2000). Because of these difficulties, rotifers and Artemia are the most viable choices for intensive culture, and farmers must overcome the challenge of producing rotifers and Artemia manipulated to contain sufficient amounts of essential components.

Research on the nutritional requirements of marine fish larvae has to a large extent focused on lipids, and especially on two essential fatty acids: docosahexaenoic acid, 22:6$n-3$ (DHA), and eicosapentaenoic acid, 20:5$n-3$ (EPA). These fatty acids are abundant in the tissue of the larvae (Rainuzzo et al., 1992), and it appears that both a high content of DHA and a high ratio of DHA to EPA in the feed appear to be important for the development of cold-water marine larvae (Sargent et al., 1999; Kjørsvik et al., 2004). One very striking effect of low DHA content and low DHA:EPA ratio is malpigmentation of flatfish larvae such as turbot (Reitan et al., 1994). Arachidonic acid, 20:4$n-6$ (ARA), is another essential fatty acid. Both the content of ARA and the EPA:ARA ratio are probably important quality metrics of the feed (Sargent et al., 1999).

2.3 Live Feed Production

2.3.1 Algae

Microalgae such as *Isochrysis galbana*, *Nannochloropsis oculata*, and *Chlorella vulgaris* are used in the production of live feed. However, they can also be added to the larval tanks in what is known as the *green water* technique, to serve as feed both for the fish larvae and for the live feed (Reitan et al., 1997). Addition of microalgae has been shown to improve both growth and survival for turbot (*Schophtalmus maximus*) and halibut larvae (Reitan et al., 1993, 1997). There are probably several reasons for this effect, including the stabilization of the nutritional value of the live feed through preventing starvation, direct ingestion of algae by the fish larvae, and a positive effect of the algae on the bacterial flora of the tanks (Reitan et al., 1997). The moderate turbidity caused by the algae can also be a factor in enhancing the contrast of prey organisms against the background (Shaw et al., 2006).

Microalgae are typically produced in large, shallow tanks or in transparent tubes. The supply of light is an important growth regulator, along with pH, salinity, temperature, turbulence and the quality and quantity of nutrients provided. The combination of all these factors determine the maximum growth rate and the carrying capacity of a microalga culture. The growth curve of a batch culture follows several phases from the initial lag and exponential growth phases, until the culture stagnates and finally collapses because of nutrient depletion. The nutritional value of the algae changes with the growth phases, and is better in the initial phases than after growth stagnates at the end of the exponential phase (Coutteau, 1996). Algae can be grown semi-continuously in cultures with regular dilution and harvesting, which can improve the stability of their nutritional value by prolonging the rapid growth phase.

There are well established techniques for the production of microalgae, but it is labour intensive and expensive. Farmers commonly purchase *algae paste* or commercial condensed *Chlorella* rather than producing their own algae.

2.3.2 Rotifers

Rotifers of the species complex *Brachionus* are used as the first feed for cod larvae and numerous other marine species (Lubzens et al., 1989; Papakostas et al., 2006). Rotifers are filter-feeding planktonic organisms found in salinities from fresh water to seawater, in a wide range of temperatures. They vary significantly in size, with lengths of 150–270 μm being typical for rotifers used in

aquaculture. Rotifers in general can reproduce both asexually and sexually, with the latter mode resulting in the production of resting eggs (Pourriot and Snell, 1983). The frequency of sexual reproduction varies between strains, however, and the strains used as live feed for cod reproduce asexually only. Many rotifer strains lose the sexual reproduction mode after some time in culture, because the common culture methods favor asexual reproduction (Hagiwara, 1994).

Rotifer tanks are supplied with strong aeration, and feed is added either continuously or in batches. The culture growth dynamics can be described as having a lag phase with low growth in the beginning, then an exponential growth phase before growth stagnates due to food or other limitations. Maximum specific culture growth rates can reach 0.4–1.6 (Hagiwara et al., 1998; Olsen, 2004) depending on the rotifer strain and culture conditions such as temperature and salinity. To achieve steady growth one can harvest rotifers and replace the culture water either continuously or periodically. The alternative is to run pure batch cultures, which are harvested completely once they reach the end of their exponential growth phase.

The body composition of rotifers is influenced strongly both by their feed and by the culture growth rate (Frolov et al., 1991; Øie et al., 1997; Øie and Olsen, 1997; Lie et al., 1997), and their nutritional value must be ensured to be adequate for the fish larvae before use. Baker's yeast has a low cost, and is often used as the main feed. However, as the sole feed it leads to rotifers with too low lipid content and a shortage of essential $n-3$ HUFA (Lubzens et al., 1989). Typically, yeast is used with a 10% addition of an oil emulsion to improve the composition and amount of lipids (Olsen, 2004, pp. 80–81).

There are two main strategies suggested for obtaining a sufficient nutritional value of rotifers, called *short-term enrichment* and *long-term enrichment* (Rainuzzo et al., 1994; Coutteau and Sorgeloos, 1997). When using short-term enrichment, the rotifers can be cultured using a cheap diet, and enriched with a carefully selected and formulated feed for a period of 2–24 hours before use. The disadvantages of short-term enrichment are an excessive total lipid content, short retention time of the nutrients, and possible problems with water quality when adding the rotifers to the larval tanks (Dhert et al., 2001). Long-term enrichment is a combination of growth and enrichment, where $n-3$ HUFA is incorporated during growth. Long-term enrichment generally leads to a more balanced body composition with a lower lipid content (Rainuzzo et al., 1994).

2.3.3 Artemia

Artemia, or *brine shrimp*, is a crustacean with an adaptation to extremely high salinity levels. In nature, Artemia are found only at high salinity levels where their predators cannot survive (van Stappen, 1996), but despite this, Artemia can be cultured at the salinity level of normal seawater. One adaptation to their extreme natural environment is the ability to produce resting eggs called *cysts* in preparation of adverse environmental condition. The cysts can lay dormant for years before hatching, and can be spread to other locations with the help of migrating birds. Artemia cysts are harvested from the shores of hypersaline lakes at several locations in the world, and are available as a commercial product (van Stappen, 1996).

Artemia cysts used in production of larval fish are disinfected and decapsulated before being incubated for up to 24 hours, depending on temperature and hatching synchrony (van Stappen, 1996). After hatching, they need to be enriched for another 12–24 hours before use. Artemia can be grown for longer periods in order to obtain larger sizes. Use of successively larger sizes of Artemia during the period 0–60 days post-hatch has been found to improve the rate of complete pigmentation and metamorphosis of halibut larvae (Olsen et al., 1999).

Achieving a sufficient relative content of essential fatty acids such as DHA and EPA in Artemia is difficult, and also leads to a very high total lipid content compared to the feed organisms of the larvae in nature (Evjemo, 2001, p. 25).

Chapter 3

Methods and Results

3.1 Instrumentation

3.1.1 Rotifer Density Measurement

In the period when cod larvae are fed with rotifers, a sufficient density of rotifers is important to achieve a high growth rate. However, with manual sampling and counting only it is a labour intensive task to monitor this variable. According to the dynamics of the rotifer density in first feeding tanks this will require frequent measurements, as the density changes with a time scale on the order of 1 hour (see Figure 2.1). Monitoring the rotifer density could be equally important in rotifer culture tanks, where the densities are far higher.

Automatic counting and size measurement of rotifers using a Coulter counter has been applied by Boraas (1983) and Walz et al. (1997) in chemostat and turbidostat culture systems for rotifers. However, a general-purpose coulter counter is expensive, and is not a convenient instrument for use in a commercial fish hatchery. A dedicated instrument for measurement of rotifer densities has been developed under the CODTECH project, providing a system for regular measurements in a set of tanks without manual intervention (Tennøy, 2003). The counter is further described in Paper 3.

Figure 3.1 shows an overview of the rotifer counter. It is equipped with a number of tubes for extracting samples, and uses computer controlled magnetic valves to open for one tube at a time. Each tube is fitted with a 0.5 mm filter at the end to prevent fish larvae from being extracted. The pump pulls water from the tank through the object glass, where a known volume V [ml] is

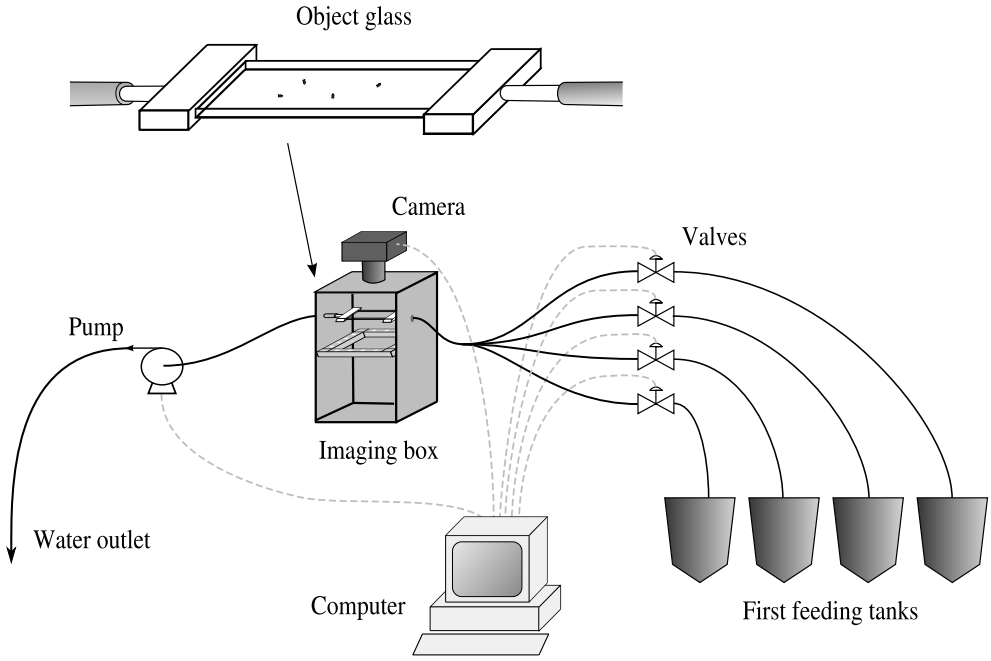

Figure 3.1: Overview of the rotifer counter system. The figure is from Paper 3.

photographed by a digital camera. Lighting is provided by yellow light emitting diodes mounted in a square with four diodes along each side. The square is set below the object glass in a plane parallel to the glass plates, at a distance chosen so the camera's angle of visibility falls between the LEDs (see Figure 2 in Paper 3). This setup provides darkfield lighting, where light is reflected by particles in the water, causing rotifers and other particles to appear in the images as bright spots against a dark background.

Images are captured in gray scale. To filter out stationary rotifers or other particles, the previous image is subtracted from each new image, removing all the light areas and particles that were also present in the previous image. The image is then thresholded (converted to binary form), and particles located and filtered by area, elongation and roundness. The remaining particles are counted, and the result divided by the volume V to achieve an estimate of the rotifer density. Filter intervals for the size and shape parameters are chosen

to represent the size and shape of the rotifers, and have to be adapted to the rotifer species used.

The counter takes images in rapid sequence, running the pump briefly between each image to replace the sample volume. After a sequence of N images (determined by the operator), the pump is run for a longer period to flush the entire tube. The mean density found in those N images is logged as a single data point.

The statistical properties of the measurements are derived in Paper 3. If the true rotifer density is ρ [rot. ml^{-1}] and the number of pictures used per measurement is N, the sampling variance will be given as:

$$\sigma^2 = \frac{\rho}{NV} \tag{3.1}$$

which means that the standard deviation is inversely proportional with $\sqrt{N}$ and with $\sqrt{V}$, and increases proportionally with $\sqrt{\rho}$. The coefficient of variance is inversely proportional to $\sqrt{\rho}$, and the measurements are therefore relatively more accurate at higher densities. We can influence accuracy by adjusting the N and V parameters.

After a series of test counts, the mean values and the sample variances can be studied to determine the precision and the repeatability of the measurements, respectively. Figure 3 in Paper 3 shows the automatic measurements plotted against the manual control counts. The results from the counter fall fairly close to the manually counted values. Figure 4 shows the sample standard deviation of the same measurements plotted against the theoretical minimum standard deviation. The observed variance is as expected, apart from a small positive bias. The bias indicates that some additional error is introduced in the counting process, but the statistical uncertainty due to sample size clearly dominates.

High density rotifer cultures

When the counter is used for monitoring rotifer cultures, densities may be on the order of 1000 rotifers ml^{-1} or higher. For densities of this magnitude, the process of counting rotifers as individual particles suffers increasing errors due to several rotifers forming clusters in the pictures. If these cannot be identified as such, the measurement will underestimate the density for high density samples. To address this error source, several alternative algorithms for high density measurements have been investigated by Bjørlykke (2006).

3.1.2 Automatic Feeding

For manual feeding of fish larvae in the rotifer period, the standard procedure is to estimate the number needed in each tank in order to reach a predefined feed density. An experienced operator can make an educated guess of the current density by visual inspection, and calculate the approximate number of rotifers to add. The density of rotifers in the enrichment tank is measured, and the correct amount extracted and washed, typically with an addition of 10% to account for handling loss. Finally the rotifers are added to each of the tanks by manually measuring out the correct amounts.

This procedure can be automated to considerably reduce the amount of manual work and the variability in rotifer density. One example of an automatic feeding system is that presented by Papandroulakis et al. (2002), which provided continuous feeding in a purely feed-forward manner based on feed requirement tables or manual dosage setup.

Paper 6 describes the application of feedback control in order to achieve appetite-based feeding. The advantage of feedback control over a feed-forward system is that the feed will not be depleted regardless of the ingestion rate of the fish larvae. The feedback controller thereby decouples feed supply from feed density, and provides a high degree of flexibility in the choice of feeding regime.

Figure 3.2 shows an overview of the control system. The automatic rotifer counter described in Section 3.1.1 provides measurements of the current feed density, using a valve manifold to pull samples from each of the larval tanks in turn. The controller pumps rotifers from a reservoir into the larval tanks, using a similar valve manifold to direct the flow. The only manual work involved is the regular refilling of the reservoir. The rotifer density in the reservoir is measured manually, but this measurement could also be automated.

The density controller is implemented using a model-based approach, for three reasons. First, when controlling several tanks using the same counter, new measurements are only available a few times per hour. The controller should be able to compute input values more frequently. Second, there can be significant measurement error in each single sample (see Paper 3), and a model based approach makes it possible to filter the data and reduce the impact of errors. Third, this structure allows the estimation of the total feed intake rate of the larvae, which is an important metric for the status and progress of larval growth.

The process model of the controller is very simple, corresponding to the rotifer density model described in Paper 5, but disregarding both reproduction, eggs and rotifers attaching to the wall. The remaining factors are the input and

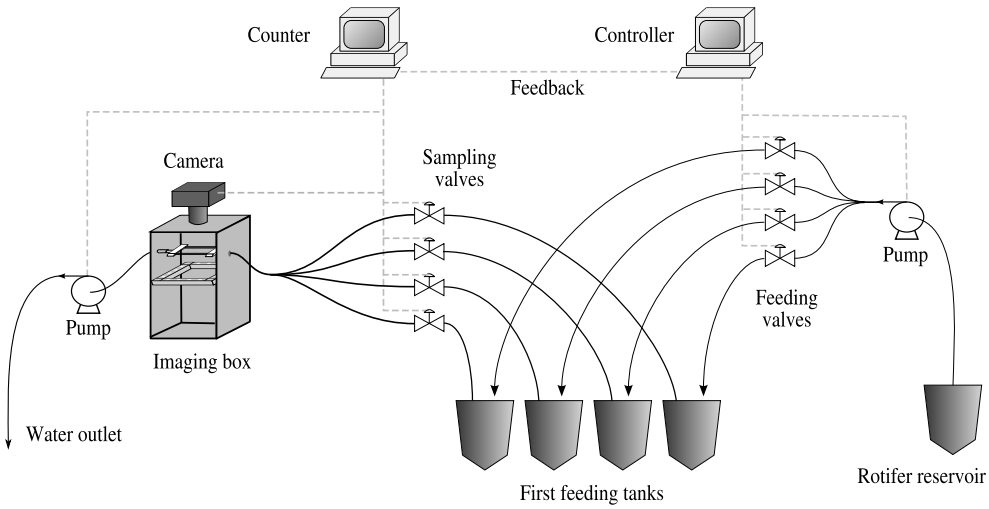

Figure 3.2: Overview of the control system. Solid curves represent tubes, while dashed lines represent data transmission and control lines. The "counter" and "controller" are both implemented in the same computer. The figure is from Paper 6.

the rotifer loss due to dilution and ingestion by the larvae. The dilution loss is assumed to be proportional to the measurable water dilution rate. The ingestion term is not directly measurable, but can be estimated by the controller. Adding the feed ingestion rate as a second model state results in the following linear model:

$$\dot{R}(t) = u(t) - q(t)R(t) - I(t) + v_D(t) \tag{3.2}$$

$$\dot{I}(t) = v_I(t) \tag{3.3}$$

where R is the rotifer density, I is the larval ingestion rate, q is the water exchange rate and v_D and v_I are random noise terms.

If we define the state vector $x = [R \quad I]^T$ and the noise vector $v = [v_D \quad v_I]^T$, we can express the system as follows:

$$\dot{x} = f(x, u) + I_{2\times 2} v \tag{3.4}$$

where $I_{2\times2}$ is the 2x2 identity matrix, and:

$$f(x,u) = \begin{bmatrix}1\\0\end{bmatrix} u + Ax \tag{3.5}$$

$$A = \begin{bmatrix}-q(t) & -1\\ 0 & 0\end{bmatrix} \tag{3.6}$$

We need to define a measurement model $y(t)$ to represent the prediction of measurements from the model. Our only measurement is of the rotifer density:

$$y(t) = R(t) + w(t) = Dx(t) + w(t) \tag{3.7}$$

where $D = [1 \quad 0]$ and w is the measurement noise. Given this measurement model the system is observable (see Paper 6), and by use of a Kalman filter (Jazwinsky, 1970) the deviation between predicted measurements $y(t)$ and actual measurements can be used to adjust the model and obtain estimates of the rotifer density $R(t)$ and the ingestion rate $I(t)$ close to the true values.

The controller computes the input value based on the current estimated rotifer density, denoted $\hat{R}(t)$. The control algorithm is a PI controller with an added feed-forward term to account for the loss of rotifers through the estimated ingestion rate ($\hat{I}(t)$) and the water exchange rate. Finally, the input is restricted to nonnegative values:

$$u(t) = max\left(0, \left[\hat{I}(t) + (q(t) + K_p)r(t) - K_p\hat{R}(t) + h(t)\right]\right) \tag{3.8}$$

where $r(t)$ is the reference density, K_p is the proportional gain and $h(t)$ is the integrator value.

The control system has been tested in a complete first feeding experiment with 9 tanks (80 l) kept at different rotifer density set points (1–9 rot. ml^{-1}). To verify the actual rotifer densities in the tanks, 50 ml samples were taken from each tank two times per day, and analyzed for rotifer density. Figure 3.3 shows both the manual measurements and the controller's measurements for all the 9 tanks.

The results demonstrated that the controller performed satisfactorily, with the exception of some deviations observed in connection to practical procedures such as addition of algae to the water, and cleaning of the tank bottoms. Both these procedures disturbed the controller's measurements temporarily.

The control system allows a reduction in manual labour by automating the feeding. Its usage is not restricted to constant feed densities as used in the experiment. It also allows any time-varying reference density, in order to emulate

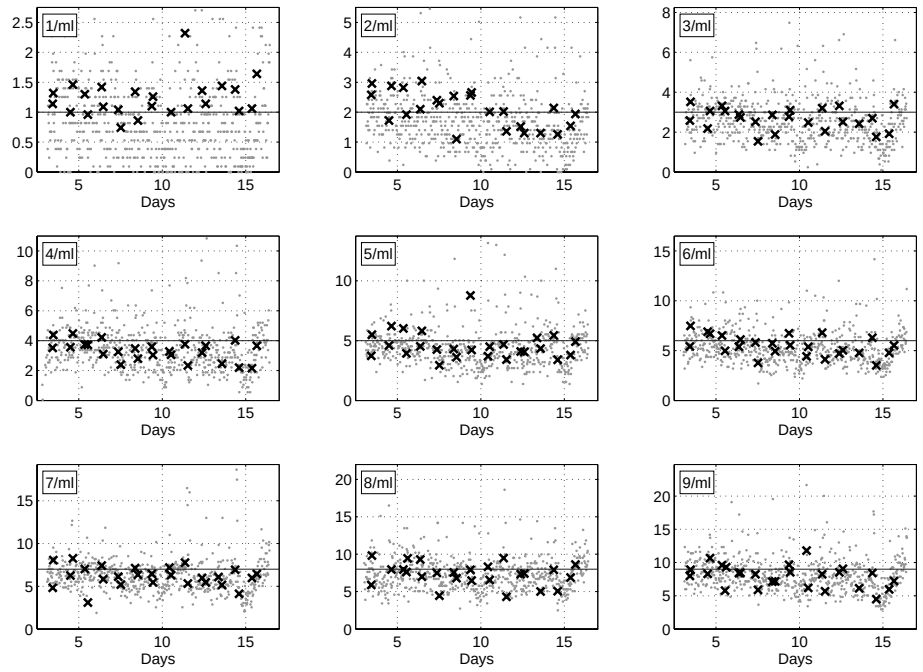

Figure 3.3: Manual rotifer density measurements (X) and automatic measurements (gray dots) in each of the experimental tanks. Tanks are ordered by increasing reference density. For comparison, a straight line shows the reference density for each tank.

batchwise feeding or other patterns. In addition to being a tool for commercial farmers, the controller provides wide opportunities for researchers in investigating feed ingestion patterns of the fish larvae, and in finding optimal feeding protocols for larval rearing.

3.2 Rotifer Population Models

Mathematical models describing population dynamics of rotifers have been developed for two different settings that impose different requirements: rotifer production cultures and rotifers after addition to first feeding tanks. In the first feeding scenario, the temperature is low, and there is strong predation pressure in addition to rotifers being removed due to water dilution. As a result, the residence time of each individual rotifer is low, and the dominant dynamical variable is the population density. In rotifer cultures the environmental and feeding conditions are optimized for fast population growth, and the egg ratio and age structure of the population have a marked influence on the expected growth rate for the near future.

3.2.1 Rotifers in First Feeding Tanks

Rotifers in first feeding tanks are modelled using a simple model that disregards most individual differences and internal dynamics of the rotifers. This model is used in Paper 4 and Paper 5, and in a simplified form in Paper 3. The model has 4 state variables:

- N_c : The number of rotifers in the water column.
- N_w : The number of rotifers attached to the tank wall.
- E_c : The number of eggs carried by rotifers in the water column.
- E_w : The number of eggs carried by rotifers attached to the tank wall.

The separation between rotifers in the water column and on the tank wall is made because rotifers attached to the wall are not subject to water dilution.

The state equations for the rotifer model, as presented in Paper 5, are as follows:

$$\frac{dN_c}{dt} = u + (E_c + E_w)h_e - M_w + M_c - p_c - q_c \tag{3.9}$$

$$\frac{dN_w}{dt} = M_w - M_c - p_w \tag{3.10}$$

$$\frac{dE_c}{dt} = ue_u - E_c h_e - \frac{E_c}{N_c}(M_w + p_c + q_c) + \frac{E_w}{N_w}M_c \tag{3.11}$$

$$\frac{dE_w}{dt} = -E_w h_e + \frac{E_c}{N_c}M_w - \frac{E_w}{N_w}(M_c + p_w) \tag{3.12}$$

where the controlled variables are u, the addition rate of rotifers into the water column, e_u, the egg ratio of the added rotifers, and Q_w, the exchange rate of the tank water (the turnover rate of the water volume per day). Q_w determines q_c, the loss rate of rotifers from the water column caused by the water exchange.

The model disregards mortality that is not caused by predation, because the short residence time eliminates any significant effect of this factor.[1] Predation by fish larvae is considered a disturbance, and affects all states through the variables p_c, predation rate in the water column, and p_w, predation from the tank wall. Migration rate of rotifers between the wall and water column states is represented by M_w and M_c. Rotifer reproduction is represented through the hatching rate h_e of eggs, but production of new eggs is disregarded. Paper 4 includes a term representing egg production, but due to the low temperature and short residence time this factor is of minor importance in a standard first feeding setting with cold-water fish.

The experiment discussed in Paper 3 provides data for evaluating the rotifer model. A 163 l tank was set up with temperature, lighting, aeration and water exchange rate similar to that of a first feeding tank, but without fish larvae. Rotifers were added to the water column several times. The rotifer counter was set up with sampling tubes at four different locations within the tank, and made measurements throughout the whole experimental period. We made the assumption that the arithmetic mean of the density measured at the four measurement locations was representative of the overall density in the water column, and plotted the mean in comparison to the model's output (Figure 3.4). Two model simulations are shown, one using the model as described above (solid line), and one where rotifers attaching to the wall were disregarded (dashed line). The comparison shows a very good fit for the complete model. It also shows that the density is clearly overestimated in the initial period when disregarding the wall state. Obviously, the significance of the wall state depends on the surface-area-to-volume ratio of the tank (in this case ca. 0.1 $\mathrm{cm}^2/\mathrm{cm}^3$), and will be less important for larger tanks than the one used in this experiment.

3.2.2 Rotifer Cultures

A model description of a rotifer culture where predation and water dilution are not dominant factors can be found by introducing factors such as maximum growth rate, carrying capacity and steady-state mortality rate (Olsen, 2004). To investigate population transients, however, such a model is insufficient. For

[1] Figure 2.1 gives an impression of the typical residence times.

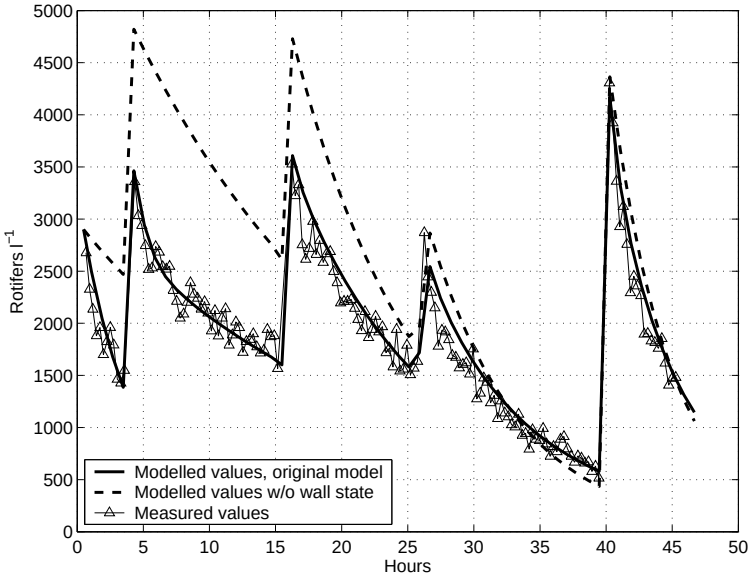

Figure 3.4: Automatic measurements made in a 48 hour experiment, compared with model simulations with and without a state value representing rotifers attached to the wall. The values are averages of measurements made at four different locations in a 163 l tank. The figure is from Paper 3.

instance, McNair et al. (1998) demonstrate the inability of classical chemostat population models to account for transient conditions and phenomena dealing with population structure. The authors also present a simple physiologically structured population model.

In Paper 1, an individual-based population model for rotifer cultures is derived based on dynamic energy budget (DEB) theory, as described by Kooijman (2000). In the model, a separation is made between *structural volume* and *energy reserve*. The energy reserve is energy available for maintenance, growth and reproduction, while the structural volume represents the irreversible investment in body structure. Figure 3.5 shows an overview of the individual model.

The state equation for the structural volume V is as follows:

$$\frac{dV}{dt} = (\kappa \dot{p}_C - \dot{p}_M)/[E_G] \tag{3.13}$$

where $\dot{p}_M = [\dot{p}_M]V$ (J cm^{-3} day^{-1}) is the temperature corrected maintenance rate, and $[E_G]$ (J cm^{-3}) is the volume-specific cost of growth. The flux $\dot{p}_C$ represents the consumption rate of energy from the reserve, and is referred to as the *catabolic rate*:

$$\dot{p}_C = \frac{[E]([E_G]\dot{v}V^{2/3} + \dot{p}_M)}{[E_G] + [E]\kappa} \tag{3.14}$$

This expression is chosen to obtain simple first-order dynamics for the reserve density E/V (Kooijman, 2000). The rate of change of the energy reserve E equals the difference between the assimilation rate $\dot{p}_A$ and the catabolic rate:

$$\frac{dE}{dt} = \dot{p}_A - \dot{p}_C \tag{3.15}$$

where the assimilation rate is modelled as a Holling Type 2 functional response (Holling, 1965) with a maximum rate proportional to $V^{2/3}$:

$$\dot{p}_A = \frac{X}{X + X_K}\{\dot{p}_{Am}\}V^{2/3} \tag{3.16}$$

where X is the feed density and X_K is the half-saturation constant for feed intake.

If the catabolic rate $\dot{p}_C$ is too low to support growth, i.e. Eq. (3.13) gives negative growth, the individual is considered to be starving. Starvation is modelled by assuming that all growth and reproduction is stopped, and energy is only expended to cover maintenance. Thus, $\frac{dV}{dt} = 0$, and $\frac{dE}{dt} = \dot{p}_A - ([\dot{p}_M] + [\dot{p}_J])V$, where $[\dot{p}_J]V$ represents *maturity maintenance* (Kooijman, 2000). If E reaches zero, the individual dies.

The rotifers attain their final size within the first couple of days (Korstad et al., 1989), and show little growth during their remaining lifetime. We therefore assume that once they reach a maximum structural volume V_p, growth stops and the rotifers start investing energy in reproduction. The energy flux invested in reproduction in this phase is:

$$\dot{p}_R = (1 - \kappa)\dot{p}_C - [\dot{p}_J]V \tag{3.17}$$

The flux $\dot{p}_R$ enters a reproductive buffer R representing the production of eggs. Once R reaches the required amount of energy for the production of a single egg, the buffer is emptied and an egg is produced. Each egg is carried by the female until it hatches after a temperature-dependent time. The average number of

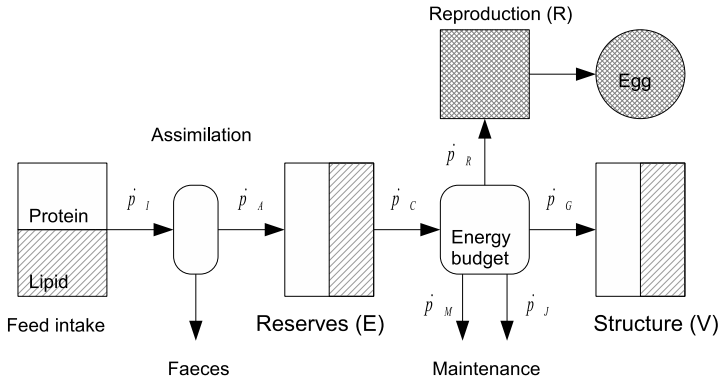

Figure 3.5: Overview of the individual rotifer model. Arrows represent fluxes, squared boxes represent energy or structure compartments, while rounded boxes represent the modelled relations between fluxes. The figure is from Paper 1.

eggs carried by each female (the *egg ratio*) is a useful indicator of the growth rate of a rotifer culture.

Senescence and natural mortality is important for the population dynamics, and is modelled by the method of Kooijman (2000): respiration is assumed to cause the production of *damage-inducing components* which in turn cause damage to DNA. Aging is expressed through the *hazard rate*, which represents accumulated cell damage, and increases as a function of the concentration of damage-inducing components. The amount of damage-inducing components, M_Q, has the following state equation:

$$\frac{dM_Q}{dt} = \eta_{QC}\dot{p}_C \tag{3.18}$$

where $\dot{p}_C$ is the catabolic rate of the rotifer, representing the respiration rate, and η_{QC} is the parameter defining its life expectancy. The hazard rate h, representing the probability per time unit of entering the senescent phase, has the following state equation:

$$\frac{dh}{dt} = \frac{M_Q}{V} \tag{3.19}$$

A senescent individual ingests less feed, and no longer produces eggs. After a temperature-dependent time, it dies of old age.

The individual model is used in a Lagrangian simulation to compute population dynamics, by simulating a number of parallel instances of the individual model. Each instance represents a number N of actual rotifers, and is referred to as a *super individual*. This principle is outlined by Scheffer et al. (1995). It is assumed that the rotifers in a culture do not interact, except for competing for the same feed resource. The availability of feed is modelled under the assumption that the feed is homogeneously distributed in the water column. This means that a single state variable X can represent the feed concentration:

$$\frac{dX}{dt} = \text{addition} - \frac{\text{ingestion}}{\text{tank volume}} - \text{dilution} \tag{3.20}$$

where the ingestion term is the sum of the ingestion of all super individuals.

Loss of rotifers due to mortality or water dilution can be handled in one of two ways; either super individuals live or die as a unit, determined by their probability of death, or mortality can be realized by reducing the N value of a super individual at a rate given by the probability of death. The latter strategy avoids the introduction of randomness in the simulation, and is a good way of representing e.g. water dilution, but leads to a monotonous decrease in the N values of the population. For a population of stable density this causes a corresponding increase in the number of super individuals needed to represent it, and thus a gradual slowdown in simulation speed. To counteract this the computer analyzes the population at regular intervals, combining super individuals that are sufficiently similar, thus reducing the model dimension.[2]

Model parameters have to be chosen with a specific rotifer strain in mind, because different strains have differences in size, growth rate and other characteristics. In Paper 1, we have chosen a set of parameter values for this model based on various published results for the SINTEF strain of *Brachionus plicatilis* (a Nevada strain which has been held in culture for a long time, and which is used in a number of cod hatcheries). Figure 3.6 shows a simulation of the population density and the egg ratio of a batch culture population, compared to the measurements from 6 cultures.

[2]For two individuals to be considered sufficiently similar, we require that they have the same number of eggs, and that the sum of relative differences in state values does not exceed a threshold level. This threshold level can be dynamically adjusted to keep the number of super individuals within our preferred range.

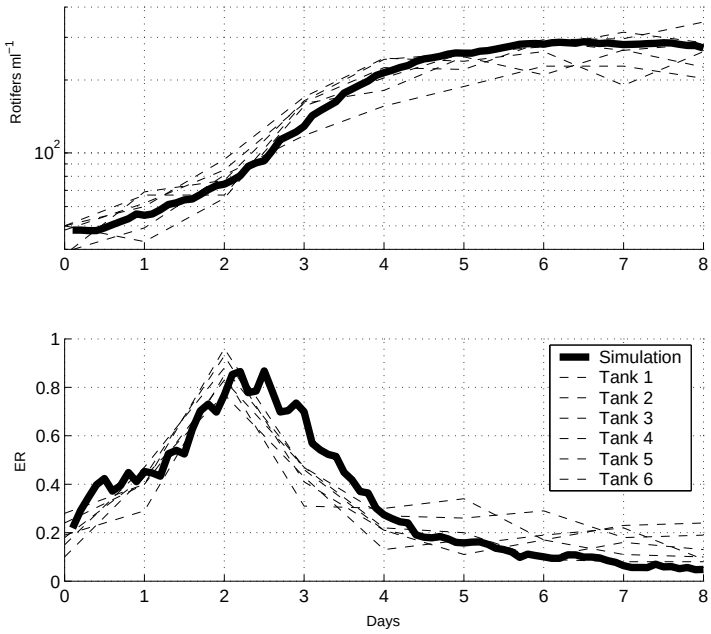

Figure 3.6: Growth and egg ratio of a batch culture, compared with experimental results from 6 cultures. The figure is taken from Paper 1.

3.2.3 Modelling Rotifer Body Composition

The model described in Paper 1 does not take feed composition into account, except for the consideration of the energy content of the feed. Because the nutritional value of rotifers is affected by feed composition (Maruyama et al., 1988; Lubzens et al., 1989; Frolov et al., 1991; Fernandez-Reiriz et al., 1993; Lie et al., 1997; Castell et al., 2003) and culture conditions (Øie and Olsen, 1997; Øie et al., 1997), we seek a model formulation that can take this into account.

In Paper 2, the model of Paper 1 is expanded to explicitly represent the balance between protein, lipid and carbohydrate in reserves. The reserve compartment E from Paper 1 is replaced by three compartments, E_P, E_L and E_C, representing energy reserves in the form of protein, lipid and carbohydrate. Figure 3.7 shows the basic structure of the expanded model. We assume that

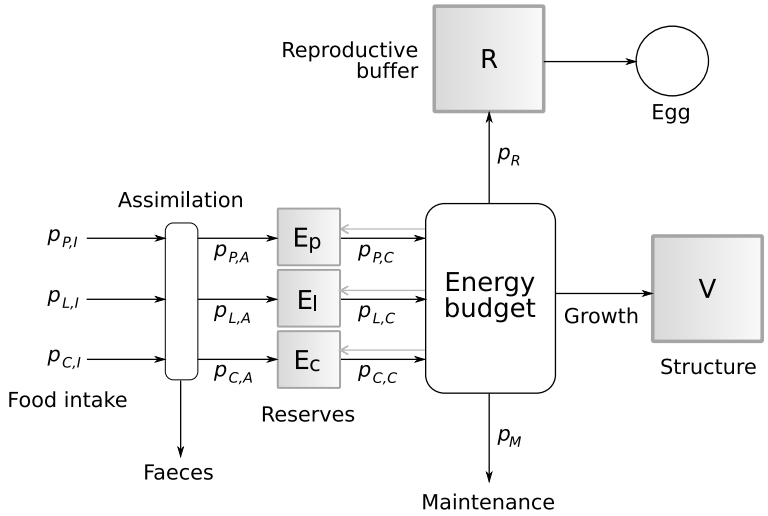

Figure 3.7: Overview of the individual model. Arrows represent energy flows, and rounded boxes represent modelled relations between these. The shaded squares represent model states. The gray arrows represent the returned fraction κ_R of rejected fluxes. The figure is taken from Paper 2, where the details of the model are presented.

structure has an approximately constant composition in terms of the main nutrient classes. The body composition of the rotifers depends on the balance between the state values E_P, E_L, E_C and V.

Feed intake and assimilation is treated the same way as in the original model, except that different assimilated fractions are allowed for the three nutrient classes. The main difference is in the determination of maintenance fluxes and growth or reproduction based on the balance between the energy reserves.

Analogous to the catabolic rate in the original model, we define a catabolic rate for each of the three reserve compartments. These rates are proportional to the reserve densities (reserve levels divided by structural volume). Part of each catabolic flux is used for covering maintenance requirements. The contribution from each depends on their relative magnitude, weighted by the *affinity* parameters ρ_P, ρ_L and ρ_C (Eqs. (11)–(13) in Paper 2). A higher affinity for one nutrient class means that a greater part of the corresponding catabolic flux will be utilized for covering maintenance.

After subtracting the maintenance fluxes from the catabolic fluxes, the remainders are available for growth or egg production. These processes are both modelled in the same way, with the composition of structure (P_V, L_V and C_V) representing the required contribution from each nutrient class per unit of growth. In addition, an overhead fraction of energy is required, which can be covered by any combination of nutrient classes. A side effect of the overhead requirement is to relax the stoichiometric balance dictated by P_V, L_V and C_V, because a limiting nutrient class will not be utilized to cover overhead. This principle is specified in Eqs. (14)–(27) in Paper 2.

The model presented in Paper 2 is still fairly basic, and treats all the three nutrient classes identically except for differences in parameter values. Despite this, the model can provide fairly good predictions after adapting parameter values to a specific rotifer strain. Figure 3.8 shows the model's predictions of rotifer dry weight and protein and lipid content after three different treatments, in comparison with measured values (Øie et al., 1997). In the P treatment, rotifers are short-term enriched after being grown at 20% dilution. In the L treatment, rotifers are short-term enriched, but dilution rate is only 5%, and in the N treatment, dilution rate is 5% and there is no enrichment. The main weakness of the model predictions as found in Paper 2 is a tendency to exaggerate the effect of feed composition on body composition.

Accounting for the effect of feed composition on growth rate and body composition has value in predicting the future state of rotifer cultures, but is also important when studying the nutritional value of rotifers in the first feeding scenario. Section 3.4.1 discusses this application of the model.

Rotifer resting egg production

In the model presented in Paper 1, it is assumed that the rotifers reproduce only asexually, and this is true for the SINTEF strain for which it is adapted. However, most rotifer strains found in nature initiate sexual reproduction under certain conditions, resulting in resting eggs that can lie dormant for extended periods under unfavorable conditions (Pourriot and Snell, 1983).

Commercial production of resting eggs as inoculum for rotifer cultures might be an interesting activity in the future (Lubzens et al., 1989), partly for the purpose of microbial control, since resting eggs can be disinfected before use (Dhert, 1996). Production methods for resting eggs have been studied in Japan (Hagiwara et al., 1993; Balompapueng et al., 1997; Hagiwara et al., 1997), and some modelling work has been undertaken for the resting egg formation process (Lubzens et al., 1993; Serra and Carmona, 1993). In a work related to this thesis,

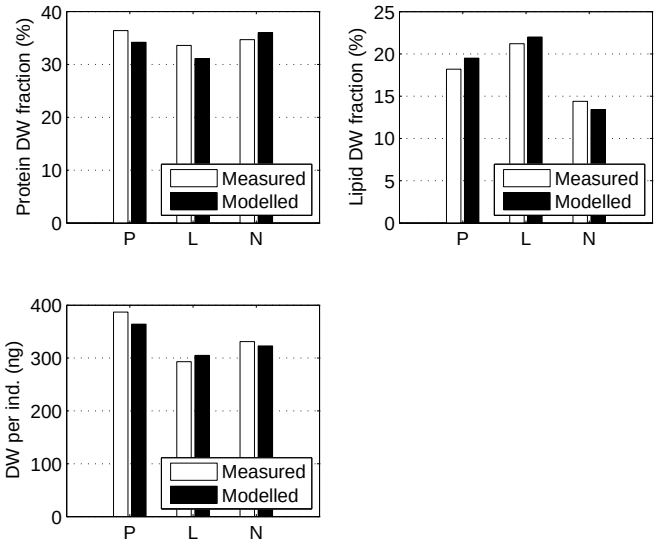

Figure 3.8: Relative protein content, relative lipid content and dry weight per individual of rotifers after the three different treatments P, L and N (Øie et al., 1997), compared to the model output. The figure is from Paper 2.

the model of Paper 1 has been expanded to describe the complete reproductive cycle leading up to the production of resting eggs (Alver, M. A. & Hagiwara, A., An individual-based population model for the prediction of rotifer population dynamics and resting egg production. Hydrobiologia, submitted paper).

3.3 Larval Model

There is a wide range of published work within mathematical modelling of fish physiology and behaviour, such as Balchen (1979), Olsen (1989), Olsen and Balchen (1992), Beer and Anderson (1997) and Fiksen and MacKenzie (2002). A large amount of modelling work, such as Aksnes and Utne (1997), Leising and Franks (1999) and van der Veer et al. (2003), has been motivated by an interest in the determinants of recruitment of commercially important species

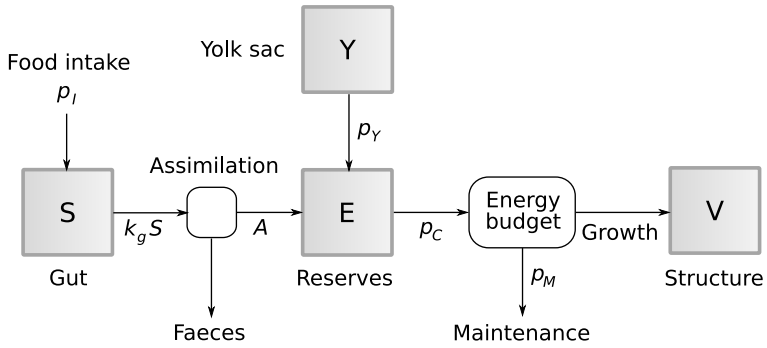

Figure 3.9: Overview of the larval model. Arrows represent energy flows, and rounded boxes represent modelled relations between these. The shaded squares represent model states.

in fisheries.

In Paper 5, an energetic model for cod larvae in aquaculture tanks is presented. This model is based on the same DEB principles as the individual rotifer model presented in section 3.2.2, but with several differences. Figure 3.9 shows the basic structure of the model.

Feed ingestion $\dot{p}_I$ is modelled as a Holling Type 2 functional response (Holling, 1965):

$$\dot{p}_I = \{\dot{p}_{Im}\} V^{2/3} f \tag{3.21}$$

$$f = \frac{X}{X + X_K} \tag{3.22}$$

where $\{\dot{p}_{Im}\}$ is the maximum surface-specific feed intake, X is the feed density and X_K is the half-saturation constant for feed intake. This formulation assumes that the feeding behaviour of the larvae is not appetite regulated, which is consistent with the general belief that marine fish larvae are *number maximizers* (Lubzens et al., 1989; Olsen et al., 2004). $\dot{p}_I$ represents an energy flux, and given the amount of nutritional energy per individual rotifer, E_r, we can calculate the number of rotifers ingested as:

$$p = \frac{\dot{p}_I}{E_r} \tag{3.23}$$

Ingested feed enters a *gut* compartment S, which is assumed to be evacuated exponentially with k_g representing the relative gut emptying rate:

$$\frac{dS}{dt} = \dot{p}_I - k_g S \tag{3.24}$$

The term $k_g S$ represents the energy flux available for digestion, and the assimilated flux A is a variable fraction of $k_g S$ in the interval $(0, k_{as})$, with higher energy flux resulting in lower assimilation efficiency (see Paper 5 for details).

Cod larvae carry a yolk sac at their point of hatching, which serves as a source of nutrition for a short period. When the yolk sac is depleted, the larva must be able to catch prey and digest the ingested food (Kjørsvik et al., 2004). The yolk sac is modelled as a compartment Y that is gradually emptied:

$$\frac{dY}{dt} = -\dot{p}_Y = \begin{cases} -\{\dot{p}_{Am,yolk}\}V^{2/3} & \text{if } Y > 0 \\ 0 & \text{otherwise} \end{cases} \tag{3.25}$$

where $\{\dot{p}_{Am,yolk}\}$ is the surface area-specific yolk assimilation rate. Energy drained from the yolk sac is available in the same way as energy assimilated from food, so the total energy acquisition rate is:

$$\dot{p}_A = A + \dot{p}_Y \tag{3.26}$$

The maintenance requirement is assumed to be proportional to the structural volume V with proportionality constant $[\dot{p}_M]$. The energy budget of the energy reserve E and the structural volume V are as follows:

$$\frac{dE}{dt} = \dot{p}_A - \dot{p}_C \tag{3.27}$$

$$\frac{dV}{dt} = \frac{\kappa \dot{p}_C - [\dot{p}_M]V}{[E_G]} \tag{3.28}$$

where the parameter $[E_G]$ specifies the energy expended per unit of volumetric growth. The parameter κ sets a fixed proportion of $\dot{p}_C$ that is spent on growth plus maintenance (the remaining portion $1-\kappa$ is available for development plus investment in reproduction).

Both $\frac{dV}{dt}$ and $\frac{dE}{dt}$ depend on $\dot{p}_c$, which is referred to as the catabolic rate, and represents the consumption rate of energy from the reserve. $\dot{p}_c$ is calculated as follows:

$$\dot{p}_C = \frac{[E]([E_G]\dot{v}V^{2/3} + \dot{p}_M)}{[E_G] + [E]\kappa} \tag{3.29}$$

which is analogous to Eq. (3.14) for the individual-based rotifer model.

The dry matter content of larvae depends on all larval states:

$$W_d = [W_V]V + (E + Y)/\mu_E + S/\mu_S \tag{3.30}$$

where $[W_V]$ relates structural volume to dry weight, and μ_E and μ_S are energy densities of reserves and gut contents, respectively.

In Paper 5, the energetic model is used to represent the entire larval population of a tank by simply adding the number of larvae, N, as an additional state value. This implies the approximation that all larvae are equal, or that the energetic model describes a representative average individual. It is also possible to run multiple instances of this model in a Lagrangian simulation in order to study the impact of differences in model parameters or state values (for instance, considering large vs. small individuals).

Figure 3.10 shows the state values of the larval model, as well as the computed dry weight, in a simulation of tank B1 in the experiment presented in Paper 5. Energy reserves increase as the yolk sac is depleted, and the gut content increases gradually from the onset of feeding. Dry weight decreases slightly initially, but starts increasing after feeding is initiated.

3.4 The First Feeding Scenario

3.4.1 Live Feed Quality Assessment

The nutritional value of enriched rotifers is volatile, and the actual balance and amount of nutrients acquired by the fish larvae depends both on the enrichment procedure and the residence time of the rotifers in the first feeding tank. Paper 1 and Paper 2 go a long way toward defining a model which can be used for predicting these dynamics, although they do not provide a description of the rotifers' content of individual fatty acids or amino acids. This model can be used in combination with the larval growth model of Section 3.3 to represent the entire food chain of the rotifer feeding phase. This approach allows closer investigation of both enrichment effects, and the effects of parameters such as water exchange rate and algal addition on the nutrition of the fish larvae.

We illustrate this method with simulation of a first feeding scenario where the results for clear water are compared to the results for green water. The following steps are used:

- Simulate pre-treatment of the rotifers using the model from Paper 2. A rotifer culture is simulated using the desired dilution rate, temperature

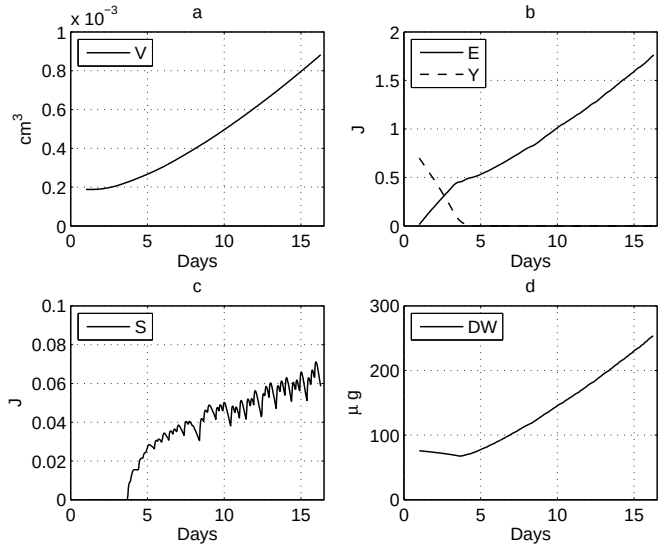

Figure 3.10: The output of the larval energetic model in a simulation of tank B1 in the experiment presented in Paper 5. a) Structural volume (V). b) Energy reserves (E) and remaining yolk energy (Y). c) Gut content (S). d) Larval dry weight (DW).

and feeding regime including any short-term enrichment. At the end of the simulation, the state values of the individuals are stored to disk.

- Simulate the first feeding scenario with a single super individual, modelled as in Section 3.3, representing the cod larvae. Addition of rotifers is handled by insertion of rotifer individuals with the state values stored from the pre-treatment simulation.

- The number of rotifers ingested by the larvae per time step is handled by first computing the larval ingestion rate p using Equations (3.21–3.23). Predation is resolved by repeatedly picking and removing random rotifer super individuals until p rotifers have been accounted for. The last super individual picked is likely to be only partly removed, by adjustment of its N value.

- In the process of removing rotifers, their body composition can be examined, allowing the model to compute the amount of nutrients ingested by the cod larvae.

In our simulations, the rotifers are pre-treated in a 20 day simulation with 10% daily dilution and 0.12 g liter^{-1} day^{-1} (wet weight) of a common yeast and Super Selco diet.[3] During the final 24 hours the rotifers were enriched with 0.16 g liter^{-1} day^{-1} (wet weight) of Super Selco (Paper 2 provides details on feed compositions). The first feeding tank initially contains 40 cod larvae liter^{-1}, and 5000 rotifers liter^{-1} are added three times daily. The water exchange rate is 1 day^{-1}. In the green water simulation *Isochrysis galbana* is added to achieve a concentration of ca. 2.5 mg C l^{-1}.

Figure 3.11 shows the mean relative protein content, lipid content, and dry weight, of the rotifers in the first feeding tank in the time period 3.5–6 days after hatching. In all cases, the values are close to the value of newly enriched rotifers immediately after each feeding batch, then drift up or down in the mean time, dependent on the tank conditions.

The difference between clear and green water is apparent in all three variables. Due to the lipid enrichment, the rotifers have a very high initial lipid content. In clear water, it decreases rapidly because lipid is metabolized by the rotifers. In green water, the high lipid content of the algae allow the rotifers to keep a steady lipid content. The relative protein content increases in both cases because the newly enriched rotifers have an unusually low value. The mean dry weight decreases in clear water, and increases in green water. On average, dry weight is around 6% higher in green water than in clear water.

3.4.2 Larval Biomass Estimation

Farmers may face high and unpredictable mortality rates during larval rearing of cod, and one way of addressing this problem is to acquire estimates of the mortality rate based on measurements from the larval tanks. An estimate of the density of larvae is useful for feeding, production planning, and economic management, and an early warning about high mortality can serve to minimize losses due to mortality. It is not easy to measure the density of cod larvae directly. Paper 4 demonstrates that by monitoring the live feed dynamics in the tanks as well as the larval growth rate, we obtain sufficient information to estimate the larval density in a model based estimator. The model can be used to estimate the loss rate of rotifers due to the water exchange in the tank, and

[3] INVE Aquaculture SA, Belgium.

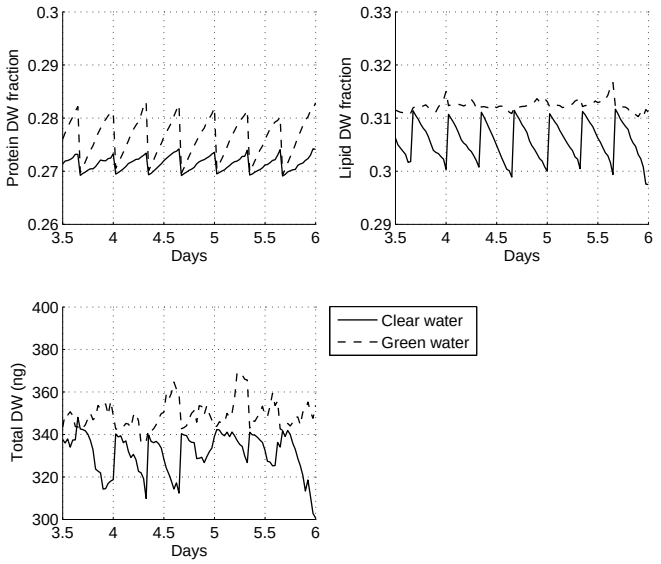

Figure 3.11: Averaged relative protein content, relative lipid content and dry weight of rotifers in a cod first feeding tank. Solid lines show values from a simulation without addition of algae, and dashed lines show a simulation with addition of *Isochrysis galbana*.

the monitoring of the live feed density thus provides information about the total ingestion rate of the larval population. Our knowledge of the size and feeding behaviour of the larvae provides indirect information about larval numbers.

The system consisting of the cod larvae and the rotifers added to the tank is described in a stochastic model, and a Kalman filter (Jazwinsky, 1970) is used to correct the model states whenever measurements are available, based on the deviation between the measured and modelled values. Two measurements are considered to be available: the density of rotifers in the water column, measured using the rotifer counter presented in Paper 3, and the average and standard deviation of the larvae's dry weight.

In order to test the larval biomass estimator principle, a first feeding experiment was conducted in which the larval tanks had different initial densities of

larvae (Paper 5). The experiment involved 9 tanks, divided into three groups with initial larval densities of 20 l^{-1}, 40 l^{-1} and 80 l^{-1}, respectively. To account for losses before and during hatching, 25% more than the nominal amounts of eggs were added to each tank. All groups were fed three times per day, to a rotifer density of 7000 l^{-1} for the high density group and to 5000 l^{-1} for the other groups. Two tanks from the high density group and one from each of the other groups were monitored throughout the experimental period using the automatic rotifer counter. The dry weight of the larvae was sampled from all tanks on days 0, 3, 5, 9 and 15, and the number of surviving larvae was counted in all tanks at the end of the experiment on day 16.

Figure 2 in Paper 5 sums up survival and growth rates for the three groups. The growth of the larvae was acceptable with an average specific growth rate (SGR) of 0.08–0.09 day^{-1}, with no significant differences between groups. Survival was also fairly good at 45–60 %, with significantly higher survival in the low density group than in the medium density group, and a survival rate in between for the high density group. The large difference in initial larval density between the groups was preserved throughout the experiment.

The system model was run for each of the four tanks monitored by the rotifer counter. The model inputs were temperature, water exchange rate, feeding times and amounts, all of which were recorded in the experimental log. Model corrections were made based on measurements of rotifer density and larval dry weight. The dry weight measurements were averaged within each group of tanks before being applied for model correction. The resulting estimate of larval numbers compared to the final survival count is shown in Figure 3.12. Figure 4 in Paper 5 shows the estimated dry weights along with the measurements.

Comparing the actual number of surviving larvae with the estimated survival, we see a very good agreement for all four tanks. Absolute agreement does not by itself indicate a conclusive result, because an important model parameter, $\{\dot{p}_{Im}\}$, regulating larval feed intake rate, was chosen based on the observations from this experiment. However, all model parameters were the same for all four tanks, and the results show that the estimator correctly detects the relative differences in larval density – even the small difference found between the two tanks from the high density group.

There is an unexpected increase during days 5–9 in the model prediction of the larval density in the low density tank. When studying the measured rotifer densities, this tank appears to have a particularly low rotifer density in the period 5–8.5 days, where the density barely reached 2500–3000 l^{-1} after feeding. The recorded feeding amounts are expected to give higher densities. This discrepancy explains why the estimator computes an increasing larval density,

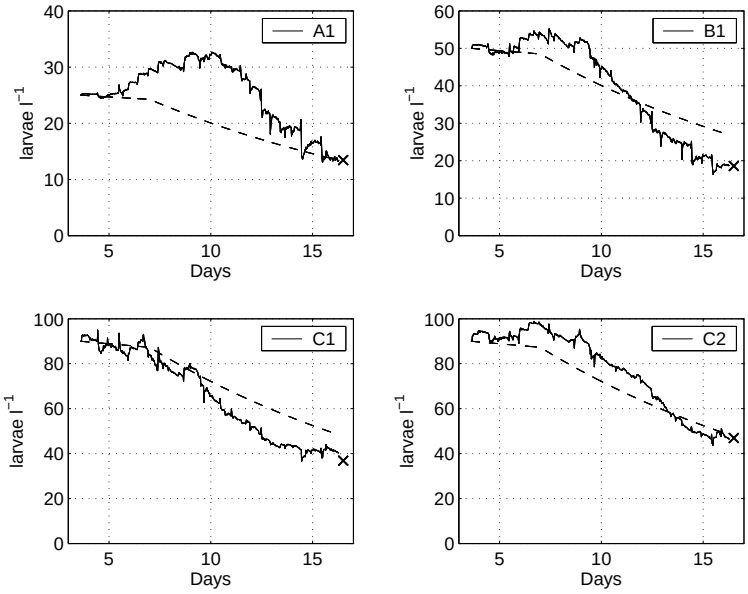

Figure 3.12: Estimated larval densities for the four tanks monitored by the rotifer counter. The dashed lines denote the estimates of the model running without corrections from the measurements, and the solid lines denote the estimates of the model when the measurements are used for state correction. The final survival count for each tank is shown with an X at day 16. This figure is taken from Paper 5

although the reasons for the deviations are not completely clear.

Chapter 4

Concluding Remarks

In this thesis, several applications of cybernetic methods for marine larviculture have been presented, targeting both production planning, process monitoring and automation. Mathematical models form a foundation for applying such techniques by providing a quantitative understanding of the production process. Several different but related mathematical models have been presented, along with some of their applications. The complexity of the models differ as a result of their purpose. For instance, the models of Paper 1 and Paper 2 can be used to describe the same scenario as the rotifer model of Paper 4, while providing estimates of many additional variables. However, their complexity makes them less suited for utilization in a biomass estimation system.

One of the main objectives of all methods that have been discussed in this thesis is to improve stability and predictability of the rearing process. Variability caused by the volatile nutritional value of live feed organisms is addressed by the development of predictive models that quantify nutritional value. Variability in feeding conditions for the fish larvae is addressed by feedback controlled feeding, with the additional benefit of reducing manual labour. Assessment of mortality rate through model based biomass estimation provides early information on the development of a batch of larvae, and can give early warning if adverse conditions of any kind cause increased mortality.

Optimization of result metrics such as survival, growth and juvenile quality is another important objective, which has been emphasized to a lesser degree in this thesis. The presented methods are equally relevant in this context, offering tools both for observation and quantification of the process dynamics, which are prerequisites for the application of optimization techniques.

4.1 Summary of Contributions

This thesis has four main contributions:

1. Development of an individual-based mathematical model describing population dynamics and quality parameters of rotifer cultures as well as rotifers in first feeding tanks.
2. Development of an individual-based mathematical model describing growth of cod larvae in the live feed period.
3. The development and testing of instrumentation for measurement and automatic control of the feed density in larval first feeding tanks.
4. Application of mathematical modelling in combination with instrumentation to provide online estimates of larval density in first feeding tanks.

4.2 Suggestions for Further Work

This thesis has dealt with instrumentation and process models, and their application in marine hatcheries. These are components serving as parts of an automated process. The interface of these components towards the human operators has not been addressed. Ideally, data gathered from all parts of the hatchery should be accessible from a central location, a process view that allows the operator to monitor the production and adjust all process set points. The specifics of models and controllers should not face the operators, but be utilized in the background for controlling the production and providing prognoses and the necessary information for planning. As the aquaculture industry matures, the usefulness of such a control system will increase as optimization of the production gets more important, and the process needs to rely on objective control targets rather than on the intuition of experienced employees.

In the shorter term, there are some specific items that should be addressed:

- A model describing the effect of feed quality on the growth, development and mortality of the cod larvae is still not available. A further development of the larval model in Paper 4 along the lines of what is done for the rotifer population model in Paper 2 is probably advisable. This is likely to require experimental work to supplement the currently available empirical data.
- The individual-based rotifer model presented in Paper 1, and refined in Paper 2, should be further improved, to describe body composition in

more detail, e.g. by including specific vitamins or essential fatty acids such as DHA and EPA.

- The measurement of larval dry weight is straightforward but time consuming. For a faster and less laborous measurement of larval growth, it is possible to develop a sensor to be placed in the water column, measuring the size of nearby larvae by image analysis. Length measures are strongly correlated with larval weight (Finn et al., 2002). Preliminary work on such a sensor has been initiated, focusing on the image processing for determination of larval size (Stensen, 2006).

- The rotifer feeding period is one of several production phases. In cod production, it is followed by the weaning period in which co-feeding with dry feed is initiated, and rotifers are gradually replaced. In halibut production, Artemia is the primary feed up until weaning. Some of the techniques discussed in the present thesis, such as the larval growth model, and the concept of estimating biomass based on feeding and growth dynamics, could and should be generalized for application beyond the rotifer phase.

Chapter 5

Errata

Paper 4:

- In the first paragraph of page 529, the sentence "the *a priori* estimates $\bar{X}_k$ and $\bar{X}_k$, and the *a posteriori* estimates $\hat{X}_k$ and $\hat{X}_k$." should be "the *a priori* estimates $\bar{x}_k$ and $\bar{X}_k$, and the *a posteriori* estimates $\hat{x}_k$ and $\hat{X}_k$."
- In the second paragraph of page 530, the sentence "The *a posteriori* estimates $\hat{X}_k$ and $\hat{X}_k$ (...)" should be "The *a posteriori* estimates $\hat{x}_k$ and $\hat{X}_k$ (...)"

References

Aksnes, D. L., Utne, A. C. W., 1997. A revised model of visual range in fish. Sarsia 82, 137–147.

Alver, M. O., Alfredsen, J. A., Sigholt, T., 2004. Dynamic modelling of pellet distribution in Atlantic salmon (*Salmo salar* L.) cages. Aquacultural Engineering 31, 51–72.

Anon., 2005. Tall og fakta 2005. Statistikkbilag til FHLs årsrapport. In Norwegian.

Attramadal, K. J. K., 2004. Water quality and microbial environment in a flow through and a recirculating system for intensive rearing of cod larvae (*Gadus morhua* L.). Master's thesis, Norwegian University of Science and Technology.

Balchen, J. G., 1979. Modeling, prediction, and control of fish behavior. In: Leondes, C. T. (Ed.), Control and Dynamic Systems. Advances in Theory and Application. Academic Press.

Balchen, J. G., 1999. Thirty years of research on the application of cybernetic methods in fisheries and aquaculture technology. Modeling, Identification and Control 21, 3–64.

Balompapueng, M. D., Hagiwara, A., Nishi, A., Imaizumi, K., Hirayama, K., 1997. Resting egg formation of the rotifer *Brachionus plicatilis* using a semi-continuous culture method. Fisheries Science 63, 236–241.

Baskerville-Bridges, B., Kling, L. J., 2000. Development and evaluation of microparticulate diets for early weaning of Atlantic cod *Gadus morhua* larvae. Aquaculture Nutrition 6, 171–182.

Beer, W. N., Anderson, J. J., 1997. Modelling the growth of salmonid embryos. Journal of Theoretical Biology 189, 297–306.

Bjørlykke, H., 2006. Instrument for måling av planktontetthet i høytetthetskulturer. Master's thesis, Norwegian University of Science and Technology, in Norwegian.

Bolla, S., Ottesen, O. H., 1998. The influence of salinity on the morphological development of yolk sac larvae of Atlantic halibut, *Hippoglossus hippoglossus* (L.). Aquaculture Research 29, 203–209.

Boraas, M. E., 1983. Population dynamics of food-limited rotifers in two-stage chemostat culture. Limnology and Oceanography 28, 546–563.

Brown, C. I., Núñes, J. M., 1998. Fish Diseases and Disorders. Vol. 2. CAB International, Ch. Disorders of Development, pp. 1–17.

Brown, J. A., Minkoff, G., Puvanendran, V., 2003. Larviculture of Atlantic cod (*Gadus morhua*): progress, protocols and problems. Aquaculture 227, 357–372.

Cahu, C., Infante, J. Z., 2001. Substitution of live food by formulated diets in marine fish larvae. Aquaculture 200, 161–180.

Castell, J., Blair, T., Neil, S., Howes, K., Mercer, S., Reid, J., Young-Lai, W., Gullison, B., Dhert, P., Sorgeloos, P., 2003. The effect of different HUFA enrichment emulsions on the nutritional value of rotifers (*Brachionus plicatilis*) fed to larval haddock (*Melanogrammus aeglefinus*). Aquaculture International 11, 109–117.

Conceição, L. E. C., Verreth, J. A. J., Verstegen, M. W. A., Huisman, E. A., 1998. A preliminary model for dynamic simulation of growth in fish larvae: application to the African catfish (*Clarias gariepinus*) and turbot (*Scophthalmus maximus*). Aquaculture 163, 215–235.

Coutteau, P., 1996. Micro-algae. In: Lavens and Sorgeloos (1996), pp. 7–48.

Coutteau, P., Sorgeloos, P., 1997. Manipulation of dietary lipids, fatty acids and vitamins in zooplankton cultures. Freshwater biology 38, 501–512.

Dhert, P., 1996. Rotifers. In: Lavens and Sorgeloos (1996), pp. 49–78.

Dhert, P., Rombaut, G., Suantika, G., Sorgeloos, P., 2001. Advancement of rotifer culture and manipulation techniques in Europe. Aquaculture 200, 129–146.

Downing, G., Litvak, M., 2000. The effect of photoperiod, tank colour and light intensity on growth of larval haddock. Aquaculture International 7, 369–382.

Engelsen, R., Asche, F., Skjennum, F., Adoff, G., 2004. Culture of Cold-Water Marine Fish, Ch. New species in aquaculture: some basic economic aspects. In: Moksnes et al. (2004), pp. 487–516.

Evjemo, J. O., 2001. Production and nutritional adaptation of the brine shrimp Artemia sp. as live food organism for larvae of marine cold water species. Ph.D. thesis, Norwegian University of Science and Technology.

Fernandez-Reiriz, M. J., Labarta, U., Ferreiro, M. J., 1993. Effects of commercial enrichment diets on the nutritional value of the rotifer (*Brachionus plicatilis*). Aquaculture 112, 195–206.

Fiksen, Ø., Aksnes, D. L., Flyum, M. H., Giske, J., 2002. The influence of turbidity on growth and survival of fish larvae: a numerical analysis. Hydrobiologia 484, 49–59.

Fiksen, Ø., Folkvord, A., 1999. Modelling growth and ingestion processes in herring *Clupea harengus* larvae. Marine Ecology Progress Series 184, 273–289.

Fiksen, Ø., MacKenzie, B. R., 2002. Process-based models of feeding and prey selection in larval fish. Marine Ecology Progress Series 243, 151–164.

Fiksen, Ø., Utne, A. C. W., Aksnes, D. L., Eiane, K., Helvik, J. V., Sundby, S., 1998. Modelling the influence of light, turbulence and ontogeny on ingestion rates in larval cod and herring. Fisheries Oceanography 7, 355–363.

Findeisen, R., Imsland, L., Allgöwer, F., Foss, B. A., 2003. State and output feedback nonlinear model predictive control: An overview. European Journal of Control 9, 190–206.

Finn, R. N., Fyhn, H. N., Evjen, M. S., 1995a. Physiological energetics of developing embryos and yolk-sac larvae of Atlantic cod (*Gadus morhua*). I. Respiration and nitrogen metabolism. Marine Biology 124, 355–369.

Finn, R. N., Henderson, J. R., Fyhn, H. N., 1995b. Physiological energetics of developing embryos and yolk-sac larvae of Atlantic cod (*Gadus morhua*). II. Lipid metabolism and enthalpy balance. Marine Biology 124, 371–379.

Finn, R. N., Rønnestad, I., van der Meeren, T., Fyhn, H. J., 2002. Fuel and metabolic scaling during the early life stages of Atlantic cod *Gadus morhua*. Marine Ecology Progress Series 243, 217–234.

Frolov, A. V., Pankov, S. L., Geradze, K. N., Pankova, S. A., Spektorova, L. V., 1991. Influence of the biochemical composition of food on the biochemical composition of the rotifer *Brachionus plicatilis*. Aquaculture 97, 181–202.

Grotmol, S., Kryvi, H., Totland, G. K., 2005. Deformation of the notochord by pressure from the swim bladder may cause malformation of the vertebral column in cultured atlantic cod *Gadus morhua* larvae: a case study. Diseases of Aquatic Organisms 65, 121–128.

Hagiwara, A., 1994. Practical use of rotifer cysts. Israel Journal of Aquaculture - Bamidgeh 46, 13–21.

Hagiwara, A., Balompapueng, M. D., Munuswamy, N., Hirayama, K., 1997. Mass production and preservation of the resting eggs of the euryhaline rotifer *Brachionus plicatilis* and *B. rotundiformis*. Aquaculture 155, 223–230.

Hagiwara, A., Hamada, K., Nishi, A., Imaizumi, K., Hirayama, K., 1993. Mass production of rotifer *Brachionus plicatilis* resting eggs in 50 m^3 tanks. Nippon Suisan Gakkaishi 59, 93–98.

Hagiwara, A., Yamamiya, N., Belem de Araujo, A., 1998. Effect of water viscosity on the population growth of the rotifer *Brachionus plicatilis* Müller. Hydrobiologia 387-388, 489–494.

Haley, T. A., Mulvaney, S. J., 1995. Advanced process control techniques for the food industry. Trends in Food Science & Technology 6, 103–110.

Hoehne-Reitan, K., Kjorsvik, E., Reitan, K. I., 2001. Bile salt-dependent lipase in larval turbot, as influenced by density and lipid content of fed prey. Journal of Fish Biology 58, 746–754.

Holling, C. S., 1965. The functional response of predators to prey density and its role in mimicry and population regulation. Memoirs of the Entomological Society of Canada.

Howell, B. R., Baynes, S. M., 2004. Culture of Cold-Water Marine Fish, Ch. Abiotic factors. In: Moksnes et al. (2004), pp. 7–27.

Huys, L., Dhert, P., Robles, R., Ollevier, F., Sorgeloos, P., Swings, J., 2001. Search for beneficial bacterial strains for turbot (*Scophthalmus maximus* L.) larviculture. Aquaculture 193, 25–37.

Imsland, A. K., Foss, A., Koedijk, R., Folkvord, A., Stefansson, S. O., Jonassen, T. M., 2006. Short- and long-term differences in growth, feed conversion efficiency and deformities in juvenile atlantic cod (gadus morhua) startfed on rotifers or zooplankton. Aquaculture Research 37, 1015–1027.

Jazwinsky, A., 1970. Stochastic Processes and Filtering Theory. Academic Press.

Jordaan, A., Kling, L. J., 2003. Determining the optimal temperature range for Atlantic cod (*Gadus morhua*) during early life. In: Browman, H. I., Skiftesvik, A. B. (Eds.), The Big Fish Bang: Proceedings of the 26th Annual Larval Fish Conference. Institute of Marine Research, Bergen.

Jämsä-Jounela, S. L., 2001. Current status and future trends in the automation of mineral and metal processing. Control Engineering Practice 9, 1021–1035.

Kjørsvik, E., Pittman, K., Pavlov, D., 2004. Culture of Cold-Water Marine Fish, Ch. From fertilisation to the end of metamorphosis - functional development. In: Moksnes et al. (2004), pp. 204–278.

Kjørsvik, E., van der Meeren, T., Kryvi, H., Arnfinnson, J., Kvenseth, P. G., 1991. Early development of the digestive tract of cod larvae, *Gadus morhua* L., during start-feeding and starvation. Journal of Fish Biology 38, 1–15.

Kooijman, S. A. L. M., 2000. Dynamic energy and mass budgets in biological systems, 2nd Edition. Cambridge University Press.

Korstad, J., Olsen, Y., Vadstein, O., 1989. Life history characteristics of *Brachionus plicatilis* (rotifera) fed different algae. Hydrobiologia 186/187, 43–50.

Lavens, P., Sorgeloos, P. (Eds.), 1996. Manual on the production and use of live food for aquaculture. FAO, Rome.

le Ruyet, P., Alexandre, J. C., Thebaud, L., Mugnier, C., 1993. Marine fish larvae feeding: Formulated diets or live prey. Journal of the World Aquaculture Society 24, 211–224.

Leising, A. W., Franks, P. J., 1999. Larval Atlantic cod (*Gadus morhua*) and haddock (*Melanogrammus aeglefinus*) growth on Georges Bank: a model with temperature, prey size, and turbulence forcing. Canadian Journal of Fisheries and Aquatic Sciences 56, 25–36.

Lie, Ø., Haaland, H., Hemre, G. I., Maage, A., Lied, E., Rosenlund, G., Sandnes, K., Olsen, Y., 1997. Nutritional composition of rotifers following a change in diet from yeast and emulsified oil to microalgae. Aquaculture International 5, 427–438.

Lubzens, E., Tandler, A., Minkoff, G., 1989. Rotifers as food in aquaculture. Hydrobiologia 186/187, 387–400.

Lubzens, E., Wax, Y., Minkoff, G., Adler, F., 1993. A model evaluating the contribution of environmental factors to the production of resting eggs in the rotifer *Brachionus plicatilis*. Hydrobiologia 255/256, 127–138.

Maruyama, I., Nakamura, T., Matsubayashi, T., Ando, Y., Maeda, T., 1988. Fatty acid composition of rotifers fed with *Chlorella* and yeast. Suisanzoshoku 63, 259–263, in Japanese.

McNair, J. N., Boraas, M. E., Seale, D. B., 1998. Size-structure dynamics of the rotifer chemostat: a simple physiologically structured model. Hydrobiologia 387/388, 469–476.

Moksnes, E., Kjørsvik, E., Olsen, Y. (Eds.), 2004. Culture of Cold-Water Marine Fish. Blackwell Publishing, Oxford.

Munk, P., 1995. Foraging behaviour of larval cod (*Gadus morhua*) influenced by prey density and hunger. Marine Biology 122, 205–212.

Oliva-Teles, A., 2000. Recent advances in European sea bass and gilthead sea bream nutrition. Aquaculture International 8, 477–492.

Olsen, A. I., Attramadal, Y., Jensen, A., Olsen, Y., 1999. Influence of size and nutritional value of *Artemia franciscana* on growth and quality of halibut larvae (*Hippoglossus hippoglossus*) during the live feed period. Aquaculture 179, 475–487.

Olsen, O. A., Balchen, J. G., 1992. Structured modeling of fish physiology. Mathematical Biosciences 112, 81–113.

Olsen, O. A. S., 1989. Structured modelling of fish physiology. Ph.D. thesis, Norwegian Institute of Technology.

Olsen, Y., 1997. Larval-rearing technology of marine species in Norway. Hydrobiologia 358, 27–36.

Olsen, Y., 2004. Culture of Cold-Water Marine Fish, Ch. Live food technology of cold-water marine fish larvae. In: Moksnes et al. (2004), pp. 73–128.

Olsen, Y., van der Meeren, T., Reitan, K. I., 2004. Culture of Cold-Water Marine Fish, Ch. First feeding technology. In: Moksnes et al. (2004), pp. 279–336.

Otterlei, E., Nyhammer, G., Folkvord, A., Stefansson, S. O., 1999. Temperature- and size-dependent growth of larval and early juvenile Atlantic cod (*Gadus morhua*): a comparative study of Norwegian coastal cod and northeast Arctic cod. Canadian Journal of Fisheries and Aquatic Sciences 56, 2099–2111.

Papakostas, S., Dooms, S., Triantafyllidis, A., Deloof, D., Kappas, I., Dierckens, K., Wolf, T. D., Bossier, P., Vadstein, O., Kui, S., 2006. Evaluation of DNA methodologies in identifying *Brachionus* species used in European hatcheries. Aquaculture 255, 557–564.

Papandroulakis, N., Dimitris, P., Pascal, D., 2002. An automated feeding system for intensive hatcheries. Aquacultural Engineering 26, 13–26.

Papandroulakis, N., Kentouri, M., Divanach, P., 2004. Biological performance of red porgy (*Pagrus pagrus*) larvae under intensive rearing conditions with the use of an automated feeding system. Aquaculture International 12, 191–203.

Planas, M., Vazquez, J., Marques, J., Perez-Lomba, R., Gonzalez, M., Murado, M., 2004. Enhancement of rotifer (*Brachionus plicatilis*) growth by using terrestrial lactic acid bacteria. Aquaculture 240, 313–329.

Pourriot, R., Snell, T. W., 1983. Resting eggs in rotifers. Hydrobiologia 104, 213–224.

Puvanendran, V., Brown, J. A., 1999. Foraging, growth and survival of Atlantic cod larvae reared in different prey concentrations. Aquaculture 175, 77–92.

Puvanendran, V., Leader, L. L., Brown, J. A., 2002. Foraging behaviour of Atlantic cod (*Gadus morhua*) larvae in relation to prey concentration. Canadian Journal of Zoology 80, 689–699.

Rainuzzo, J. R., Reitan, K. I., Jørgensen, L., 1992. Comparative study on the fatty acid lipid composition of four marine fish larvae. Comparative Biochemistry and Physiology B. 103B, 21–26.

Rainuzzo, J. R., Reitan, K. I., Olsen, Y., 1994. Effect of short- and long-term lipid enrichment on total lipids, lipid class and fatty acid composition in rotifers. Aquaculture International 2, 19–32.

Rainuzzo, J. R., Reitan, K. I., Olsen, Y., 1997. The significance of lipids at early stages of marine fish: a review. Aquaculture 155, 103–115.

Reitan, K. I., Rainuzzo, J. R., Olsen, Y., 1994. Influence of lipid composition of live feed on growth, survival and pigmentation of turbot larvae. Aquaculture International 2, 33–48.

Reitan, K. I., Rainuzzo, J. R., Øie, G., Olsen, Y., 1993. Nutritional effects of algal addition in first-feeding of turbot (*Scophthalmus maximus* L.) larvae. Aquaculture 118, 257–275.

Reitan, K. I., Rainuzzo, J. R., Øie, G., Olsen, Y., 1997. A review of the nutritional effects of algae in marine fish larvae. Aquaculture 155, 207–221.

Rosenlund, G., Meslo, I., Rødsjø, R., Torp, H., 1993. Large scale production of cod. In: Reinertsen, H., Dahle, L. A., Jørgensen, L., Tvinnereim, K. (Eds.), Fish Farming Technology. Balkema, Rotterdam, pp. 141–146.

Sargent, J., McEvoy, L., Estevez, A., Bell, G., Henderson, J., Tocher, D., 1999. Lipid nutrition of marine fish during early development: current status and future directions. Aquaculture 179, 217–229.

Scheffer, M., Baveco, J. M., DeAngelis, D. L., Rose, K. A., van Nes, E. H., 1995. Super-individuals a simple solution for modelling large populations on an individual basis. Ecological Modelling 80, 161–170.

Serra, M., Carmona, M. J., 1993. Mixis strategies and resting egg production of rotifers living in temporally-varying habitats. Hydrobiologia 255-256, 117–126.

Shaw, G., Pankhurst, P., Battaglene, S., 2006. Effect of turbidity, prey density and culture history on prey consumption by greenback flounder, *Rhombosolea tapirina*, larvae. Aquaculture 253, 447–460.

Shields, R. J., 2001. Larviculture of marine finfish in Europe. Aquaculture 200, 55–88.

Skjermo, J., Vadstein, O., 1999. Techniques for microbial control in the intensive rearing of marine larvae. Aquaculture 177, 333–343.

Slagstad, D., Olsen, Y., Tilseth, S., 1987. A model based system for control of live feed level for larval fish. Modeling, Identification and Control 8, 51–60.

Stensen, L., 2006. Instrument for størrelsesmåling av torskelarver. Master's thesis, Norwegian University of Science and Technology, in Norwegian.

Støttrup, J. G., 2000. The elusive copepods: their production and suitability in marine aquaculture. Aquaculture Research 31, 703–711.

Tennøy, T., 2003. Kamerabasert instrumentering for måling av individtetthet i rotatoriekulturer. Master's thesis, Norwegian University of Science and Technology, in Norwegian.

van der Veer, H. W., Kooijman, S. A. L. M., van der Meer, J., 2003. Body size scaling relationships in flatfish as predicted by Dynamic Energy Budgets (DEB theory): implications for recruitment. Journal of Sea Research 50, 257–272.

van Rijn, J., 1996. The potential for integrated biological treatment systems in recirculating fish culture–a review. Aquaculture 139, 181–201.

van Stappen, G., 1996. Introduction, biology and ecology of *Artemia*. In: Lavens and Sorgeloos (1996), pp. 79–106.

Vine, N. G., Leukes, W. D., Kaiser, H., 2006. Probiotics in marine larviculture. FEMS Microbiology Reviews 30, 404–427.

Walz, N., Hintze, T., Rusche, R., 1997. Algae and rotifer turbidostats: studies on stability of live feed cultures. Hydrobiologia 358, 127–132.

Øie, G., Makridis, P., Reitan, K. I., Olsen, Y., 1997. Protein and carbon utilization of rotifers (*Brachionus plicatilis*) in first feeding of turbot larvae (*Scophthalmus maximus* L.). Aquaculture 153, 103–122.

Øie, G., Olsen, Y., 1997. Protein and lipid content of the rotifer *Brachionus plicatilis* during variable growth and feeding condition. Hydrobiologia 358, 251–258.

Paper 1 is not included due to copyright.

An individual-based model for predicting body composition of cultured *Brachionus plicatilis* rotifers

Morten Omholt Alver*, Jo Arve Alfredsen*, Yngvar Olsen†

Abstract

An individual-based model describing body composition of rotifers has been derived by modification of a previously published model. The original model cannot account for the different balances of the main nutrients, protein, lipid and carbohydrate, which are observed as an effect of culture conditions and feed composition. Body weight and composition of rotifers are important quality metrics when rotifers are used as live feed in the culture of marine fish larvae. The new model addresses this by explicitly representing the nutrients in separate energy reserve compartments, and defining simple stoichiometric rules for growth based on the balance between these.

The model's output has been compared to data from the literature relating to body composition under steady-state semi-continuous culture, after enrichment with lipid emulsions and after addition to a first feeding tank with and without addition of microalgae. The model shows fairly good agreement with the experimental data.

*Department of Engineering Cybernetics, Norwegian University of Science and Technology (NTNU), Odd Bragstads plass 2D, 7491 Trondheim, Norway

†Department of Biology, Norwegian University of Science and Technology

1 Introduction

Rotifers of the species complex *Brachionus plicatilis* are widely used in aquaculture as live feed for the early larval stages of marine fish species (Lubzens et al., 1989). Rotifers are cultured in batch, semi-continuous or continuous cultures using different types of feed; baker's yeast with addition of oil emulsion, microalgae or alga paste, condensed *Chlorella vulgaris* or formulated feeds. The nutritional value of rotifers is strongly dependent on feed quality and on their treatment prior to being used as feed (Maruyama et al., 1988; Frolov et al., 1991; Øie and Olsen, 1997), and it is necessary to *enrich* the rotifers to ensure an acceptable nutritional value for the fish larvae. Short-term enrichment is a common approach, where the rotifers are cultured using a low-cost diet, and enriched with a carefully selected and formulated feed for a period of 2–24 hours before use. Alternatively, the rotifers can be enriched in the long term during cultivation, which typically leads to a more balanced body composition with a lower lipid content (Rainuzzo et al., 1994). For cold water marine species such as Atlantic cod (*Gadus morhua*), the amount and quality of lipids are especially important quality parameters (Sargent et al., 1999).

An individual-based model that can predict body composition under transient conditions can be combined with a predator-prey model predicting the ingestion of rotifers by fish larvae. This would allow us to estimate what residence times rotifers have in the first feeding tank prior to being ingested, and further estimate the nutritional value at the time of ingestion. More generally, the model could be used to predict rotifer nutritional value as an effect of the culture procedure.

A previously published individual-based model (Alver et al., 2006) is suitable for simulating scenarios such as rotifer culture and first feeding, but cannot predict the effect of changes in feed composition on population growth and the body composition of rotifers. In this study, we aim to make the necessary modifications to the existing model in order to make it useful for predicting the nutritional value of rotifers.

2 Materials and methods

2.1 Original model

The model presented by Alver et al. (2006) describes individual rotifer dynamics using a dynamic energy budget model for isomorphic organisms. The principles

of this type of model are described by Kooijman (2000). The original model has five state values. The structural volume V represents the body structure of the rotifer, and the energy reserve E represents the energy pool available for maintenance, growth, and reproduction. Food ingestion is modelled as a Holling Type II functional response (Holling, 1965), and the energy assimilation rate as a constant proportion of ingestion rate. Energy is mobilized from E at a rate referred to as the *catabolic flux*, which is dependent on the amount of reserves available. After maintenance requirements are subtracted, the remainder of the catabolic flux can be utilized for growth or reproduction.

The model designates three life phases. Initially, the rotifer grows in size until a maximum structural volume V_p is reached. At this point, growth is halted and the individual redirects growth energy to reproduction. The reproductive buffer R represents the energy invested in producing a new egg. R is emptied, and an egg produced, once it reaches the required amount of energy. Each egg is carried for a temperature-dependent time period before hatching, after which a newborn individual is added to the simulation. Finally, the individual reaches a senescent phase where neither growth nor reproduction takes place.

The last two states are used to describe aging - the accumulated amount of damage-inducing components, M_Q, and the hazard rate, h. M_Q increases proportionally with the catabolic rate (representing DNA damage to cells as a result of respiration), and h (representing wrong proteins accumulated as a result of damaged DNA) increases proportionally with M_Q (Kooijman, 2000). The hazard rate equals the risk per time unit of the individual entering the senescent phase, and is used to determine randomly at what time this occurs. After accumulating S_m day degrees (temperature in ℃ multiplied with time), a senescent individual dies from old age and is removed from the simulation.

A population of rotifers is represented by simulation of a large number of *super individuals*, which means instances of the individual model that each represent a number N of actual rotifers. Each super individual has its own state values, and the model can in this way represent a population of rotifers in various life phases. By using different values for N, populations of any size can be represented by a manageable number of super individuals.

2.2 New model

Temperature dependence and feed concentration are modelled as in Alver et al. (2006). All model changes are made on the individual level. Figure 1 shows an overview of the new model, which has three reserve compartments, E_P, E_L and E_C, instead of one:

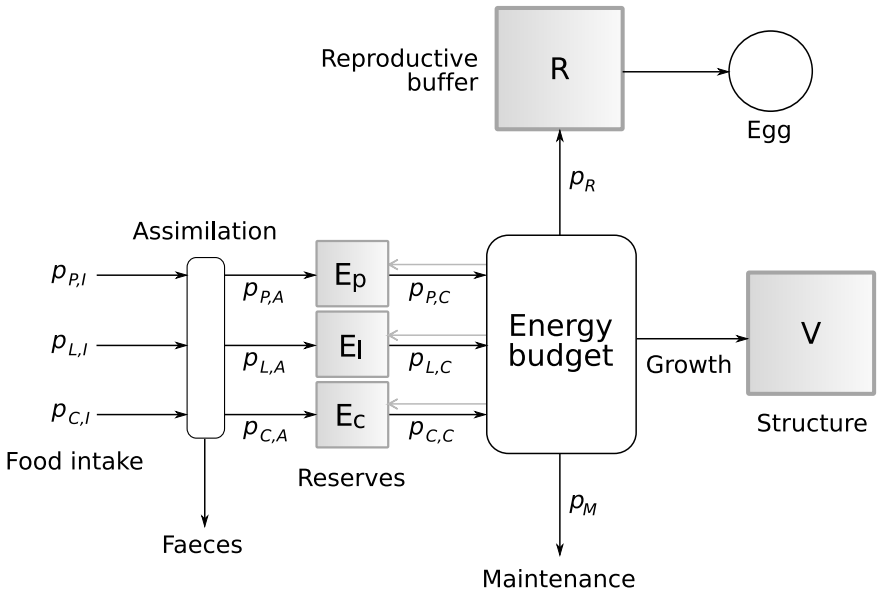

Figure 1: Overview of the individual model. Arrows represent energy flows, and rounded boxes represent modelled relations between these. The shaded squares represent model states. The gray arrows represent the returned fraction κ_R of rejected fluxes. The original model (Alver et al., 2006) had only a single reserves compartment.

- E_P: energy reserves, protein compartment
- E_L: energy reserves, lipid compartment
- E_C: energy reserves, carbohydrate compartment

In the following sections we will define the state equations for V, R, E_P, E_L, E_C, M_Q and h.

2.2.1 Feed intake and assimilation

We assume that maximum feed intake is given as a surface area-specific energy flux $\{p_{Im}\}$. This implies that maximum feed intake by weight will decrease with increasing energy density μ_I [J (g dry weight)$^{-1}$] of the feed, and that maximum

gross energy ingestion is independent of feed composition. Feed ingestion is modelled as a Holling type II functional response (Holling, 1965):

$$p_I = \{p_{Im}\} V^{2/3} \frac{X}{X + X_K} \tag{1}$$

where X is the feed concentration and X_K is the half-saturation constant for feed intake. Feed composition is defined by the input values P_X, L_X and C_X, which represent protein, lipid and carbohydrate content relative to dry weight. The ingestion rate of each of the nutrient classes is as follows:

$$p_{P,I} = \mu_P P_X \frac{p_I}{\mu_I} \tag{2}$$

$$p_{L,I} = \mu_L L_X \frac{p_I}{\mu_I} \tag{3}$$

$$p_{C,I} = \mu_C C_X \frac{p_I}{\mu_I} \tag{4}$$

where we use the same values for the energy density of the nutrient classes as in Sveier et al. (2000): $\mu_P = 23700$ J g^{-1}, $\mu_L = 39500$ J g^{-1} and $\mu_C = 17200$ J g^{-1}. The energy density of the food is $\mu_I = P_X \mu_P + L_X \mu_L + C_X \mu_C$.

The assimilated fraction of ingested feed is assumed to be independent of feed intake rate. The assimilated fractions are denoted $k_{P,as}$, $k_{L,as}$ and $k_{C,as}$ for protein, lipid and carbohydrate, respectively, giving the following assimilation fluxes:

$$p_{P,A} = k_{P,as} p_{P,I} \tag{5}$$

$$p_{L,A} = k_{L,as} p_{L,I} \tag{6}$$

$$p_{C,A} = k_{C,as} p_{C,I} \tag{7}$$

2.2.2 Catabolic fluxes

The catabolic fluxes represent the rate of expenditure of the energy reserves, and are calculated as first-order processes in terms of specific energy reserves (reserves relative to V):

$$p_{P,C} = \frac{E_P}{V} (\dot{v} V^{2/3} - \frac{dV}{dt}) \tag{8}$$

$$p_{L,C} = \frac{E_L}{V} (\dot{v} V^{2/3} - \frac{dV}{dt}) \tag{9}$$

$$p_{C,C} = \frac{E_C}{V}(\dot{v}V^{2/3} - \frac{dV}{dt}) \tag{10}$$

where $\dot{v}$ is referred to as the *energy conductance*, and determines the relative consumption rate of energy from reserves. The catabolic fluxes and the growth rate $\frac{dV}{dt}$ are interdependent and form an implicit set of equations in the growth phase, but the relative sizes of the catabolic fluxes can be computed readily.

2.2.3 Maintenance

The maintenance requirement is assumed to be proportional to V with proportionality constant $[p_M]$, so the total maintenance flux is $p_M = [p_M]V$. Maintenance is managed by a synthesizing unit (SU) that can operate on either protein, lipid or carbohydrate, but with a different preference for each. SUs are conceptual servers that receive units of nutrients, and follow set rules to transform these into a product (Kooijman, 2000). The maintenance SU is constrained to producing a flux equal to p_M by utilizing the available fluxes of protein, lipid and carbohydrate ($p_{P,C}$, $p_{L,C}$ and $p_{C,C}$). The contributions from the reserve compartments are as follows:

$$p_{P,M} = p_M \frac{\rho_P p_{C,P}}{\rho_P p_{C,P} + \rho_L p_{C,L} + \rho_C p_{C,C}} \tag{11}$$

$$p_{L,M} = p_M \frac{\rho_L p_{C,L}}{\rho_P p_{C,P} + \rho_L p_{C,L} + \rho_C p_{C,C}} \tag{12}$$

$$p_{C,M} = p_M \frac{\rho_C p_{C,C}}{\rho_P p_{C,P} + \rho_L p_{C,L} + \rho_C p_{C,C}} \tag{13}$$

where ρ_P, ρ_L and ρ_C are called *affinities*, and determine the relative priority of the nutrient classes for use in maintenance. A low affinity means that the nutrient class tends to get conserved for growth or reproduction instead of being used for maintenance. We note that $p_{P,M}$, $p_{L,M}$ and $p_{C,M}$ only depend on the relative sizes of $p_{P,C}$, $p_{L,C}$ and $p_{C,C}$, which can be determined from Equations (8–10).

2.2.4 Growth phase

We assume that after subtracting maintenance fluxes, the remainder of the catabolic fluxes are available for growth or reproduction. This contrasts with the model of Alver et al. (2006), which specifies that a fraction κ of the catabolic flux is available for growth plus somatic maintenance. However, since the κ factor is only relevant in the growth phase, the dynamics are not changed by representing

maturity and somatic growth as a single growth process, and combining somatic and maturity maintenance into a single maintenance requirement. The maturity growth term is represented as part of the overhead energy required for somatic growth. The fluxes available for growth are as follows:

$$p_{P,G} = p_{P,C} - p_{P,M} \tag{14}$$

$$p_{L,G} = p_{L,C} - p_{L,M} \tag{15}$$

$$p_{C,G} = p_{C,C} - p_{C,M} \tag{16}$$

Stoichiometric requirements for growth are set according to the dry weight fraction of protein, lipid and carbohydrate in structure (P_V, L_V and C_V, respectively) together with conversion factors:

$$n_P = \frac{P_V \mu_P}{\psi_P} \tag{17}$$

$$n_L = \frac{L_V \mu_L}{\psi_L} \tag{18}$$

$$n_C = \frac{C_V \mu_C}{\psi_C} \tag{19}$$

where ψ_P, ψ_L and ψ_C are the maximum conversion efficiencies of protein, lipid and carbohydrate, respectively.

We model growth using Liebig's principle, but allowing for an additional overhead cost by adding a fraction y to the energy cost. This overhead fraction can be covered by any combination of the catabolic fluxes, thus giving the stoichiometric requirement for growth some plasticity. Initially we calculate the growth rate in the absence of overhead:

$$\frac{dV'}{dt} = \min\left(\frac{p_{P,G}}{n_P}, \frac{p_{L,G}}{n_L}, \frac{p_{C,G}}{n_C}\right) \tag{20}$$

This growth rate leaves a rest of each energy flux:

$$rest_X = p_{X,G} - \frac{dV'}{dt} n_X \tag{21}$$

where the subscript X can be replaced by either P, L or C (the same applies to equations further below). The sum of rest fluxes is denoted $rest_\Sigma$:

$$rest_\Sigma = rest_P + rest_L + rest_C \tag{22}$$

The overhead energy requirement, given a growth of dV'/dt, is as follows:

$$Y = y(n_P + n_L + n_C)\frac{dV'}{dt} \tag{23}$$

If the available fluxes are sufficiently imbalanced ($Y \leq rest_\Sigma$), the rest fluxes for the nonlimiting nutrients will be sufficient to cover overhead, and dV'/dt will represent the actual growth rate:

$$\frac{dV}{dt} = \frac{dV'}{dt} \tag{24}$$

The fluxes actually utilized for growth are denoted $j_{X,G}$:

$$j_{X,G} = \frac{dV}{dt}n_X + Y\frac{rest_X}{rest_\Sigma} \tag{25}$$

The remaining part of the $p_{X,G}$ fluxes after subtracting the fluxes utilized for growth ($p_{X,G} - j_{X,G}$) will in part be excreted, and in part returned to their relevant energy reserves compartments. The excretion of part of the rejected fluxes ensures that the reserve density of a limiting nutrient will not be unbounded (Kooijman et al., 2004). We introduce the parameter κ_R which defines which fraction of the rejected fluxes is returned to energy reserves.

If the fluxes are balanced ($Y > rest_\Sigma$), the rest fluxes will be insufficient to cover Y, which means that the actual growth will be lower than dV'/dt. In this case growth is lowered to the point where all energy fluxes are expended completely:

$$j_{X,G} = p_{X,G} \tag{26}$$

Some calculation gives the following expression for the growth rate:

$$\frac{dV}{dt} = \frac{dV'}{dt} - \frac{Y - rest_\Sigma}{(n_P + n_L + n_C)(1 + y)} \tag{27}$$

The preceding equations define $\frac{dV}{dt}$ implicitly because the growth is interdependent with the catabolic rates $p_{X,C}$. Implementing these calculations is therefore easiest done iteratively, by computing catabolic rates based on last time step's $\frac{dV}{dt}$, then computing a more accurate $\frac{dV}{dt}$ based on those catabolic rates. This process can be repeated until the equations agree within a certain error margin.

The rate of change of each reserves compartment equals the assimilation flux minus the catabolic flux plus the fraction κ_R of the rejected part of the catabolic flux:

$$\frac{dE_P}{dt} = p_{P,A} - p_{P,C} + \kappa_R(p_{P,G} - j_{P,G}) \tag{28}$$

$$\frac{dE_L}{dt} = p_{L,A} - p_{L,C} + \kappa_R(p_{L,G} - j_{L,G}) \tag{29}$$

$$\frac{dE_C}{dt} = p_{C,A} - p_{C,C} + \kappa_R(p_{C,G} - j_{C,G}) \tag{30}$$

2.2.5 Reproductive phase

In the reproductive phase, $\frac{dV}{dt} = 0$. Equations (2–13) are valid also for this phase. Egg production is assumed to follow the same principles as growth, except that the result, expressed in energy units, is accumulated into the reproductive buffer R. Once the buffer holds the amount of energy required to produce an egg, it is emptied and an egg is immediately produced.

Stoichiometric requirements for egg production are assumed to be identical to those for growth. The contribution to the reproductive buffer is calculated by using Equations (14–27), except that the resulting $\frac{dV}{dt}$ value represents egg production instead of growth. The result is converted into an energy flux:

$$\frac{dR}{dt} = p_R = \mu_R \frac{dV}{dt} \tag{31}$$

where μ_R is the energy density of the egg tissue:

$$\mu_R = P_V \mu_P + L_V \mu_L + C_V \mu_C \tag{32}$$

Energy reserve dynamics are calculated from Equations (28–30), as in the growth phase. Production and hatching of eggs are otherwise handled as in Alver et al. (2006).

2.2.6 Aging and senescence

Aging is modelled as in Alver et al. (2006), with the sum of the catabolic fluxes determining the accumulation of damage-inducing components:

$$\frac{dM_Q}{dt} = \eta_{QC}(p_{P,C} + p_{L,C} + p_{C,C}) \tag{33}$$

where η_{QC} is a parameter regulating the organism's life expectancy. The hazard rate h increases as a function of the concentration of damage-inducing components:

$$\frac{dh}{dt} = \frac{M_Q}{V} \tag{34}$$

The hazard rate represents the rotifer's likelihood per time unit of entering the senescent phase, and the exact time when this occurs is determined randomly in the model. In the senescent phase, no energy is applied to egg production or growth, and feed ingestion rate is reduced by a factor k_S. The energy flux that would otherwise go to the reproductive buffer R is considered to be wasted.

2.3 Model parameters

There are many published data sets describing body composition of rotifers under various conditions and with varying feed compositions. However, there are significant differences between strains, and sometimes confusion about which strains or species have been used. For this reason it is not feasible to find a set of model parameters that equally well fit all the available data. We limit ourselves to experimental data for the SINTEF strain of *Brachionus plicatilis*, a Nevada strain long held in culture. This strain is used in a number of cod hatcheries, and is the subject of a wide body of research (Olsen et al., 1993; Øie et al., 1994; Øie and Olsen, 1997; Evjemo and Olsen, 1997; Makridis and Olsen, 1999; Olsen, 2004).

Through the model modification many new parameters have been introduced. We make a simplification by setting the efficiency parameters ψ_P, ψ_L and ψ_C all equal to 1. The affinity parameters ρ_P, ρ_L and ρ_C are the main determinants of the loss rate of energy reserves under starvation. The body contents of the modelled rotifers are determined by the structure composition parameters P_V, L_V and C_V together with the parameters affecting the balance between reserve compartments: the affinity parameters and the assimilation parameters $k_{as,P}$, $k_{as,K}$ and $k_{as,C}$. The variability of body composition depends on κ_R (the return rate of rejected nutrients), and on the balance between structure (with a constant composition) and the sum of reserves (with changing composition), determined by $\dot{v}$. The parameter $\dot{v}$ also influences survival times under starvation. Table 1 lists the parameter values chosen for the model based on comparisons with published data sets.

Table 1: Parameter values

Parameter	Value	Description
C_V	0.36	Carbohydrate DW fraction in structure
η_{QC}	1.3×10^{-6}	Aging rate factor
$k_{as,C}$	0.6	Assimilated fraction of ingested carbohydrate
$k_{as,L}$	0.8	Assimilated fraction of ingested lipid
$k_{as,P}$	0.7	Assimilated fraction of ingested protein
κ_R	0.5	Returned fraction of rejected nutrients
k_S	0.5	Multiplier for feed intake of senescent rotifers
k_{VM}	0.1 g cm^{-3}	Conversion factor, structure to dry weight
L_V	0.08	Lipid DW fraction in structure
$\{p_{Im}\}$	120 J $\mathrm{cm}^{-2}\mathrm{day}^{-1}$	Maximum surface area-specific feed intake
$[p_M]$	700 J $\mathrm{cm}^{-3}\mathrm{day}^{-1}$	Specific maintenance power
P_V	0.36	Protein DW fraction in structure
ρ_C	0.7	Affinity parameter for carbohydrate
ρ_L	0.8	Affinity parameter for lipid
ρ_P	0.6	Affinity parameter for protein
S_m	40 day °C	Duration of senescent period
$\dot{v}$	0.014 cm day^{-1}	Energy conductance
V_p	3.6×10^{-6} cm^3	Maximum structural volume
X_K	4.8×10^{-3} g l^{-1}	Half-saturation constant for feed intake
y	0.25	Growth overhead factor

Table 2: Feed compositions used in the model simulations (% of dry weight)

Feed type	P	L	C	Source
Chlorella vulgaris	55.0	10.2	29.0	Maruyama et al. (1988)
DHA Selco	0.0	94.2	0.0	same as Super Selco
ω-yeast	34.5	30.8	30.4	Maruyama et al. (1988)
Protein Selco	32.7	30.3	33.6	Fernandez-Reiriz et al. (1993)
Super Selco	0.0	94.2	0.0	Fernandez-Reiriz et al. (1993)
Yeast	47.1	2.1	44.9	Maruyama et al. (1988)
Yeast + 10% Super Selco	36.5	23.1	34.8	see text
Isochrysis galbana	35.0	36.6	10.0	Fidalgo et al. (1998)

2.4 Model testing

The model was simulated with the chosen model parameters in order to compare its output with experimental data published by Øie et al. (1997) and Olsen (2004). We reproduce the experimental conditions of Øie et al. (1997), and compare the protein and lipid content of rotifers after three treatments. In all treatments water temperature was 20℃, salinity was 20 ppt, and the culture feed was baker's yeast with 10% addition of Super Selco.[1] P-rotifers were grown at 20% daily dilution, and short-term enriched for 24 hours with 0.8 μg Protein Selco per individual. L-rotifers were grown at 5% daily dilution, and short-term enriched for 24 hours with 0.4 μg DHA Selco per individual. N-rotifers were grown at 5% daily dilution and not short-term enriched.

To simulate this experiment, we ran the model for 20 days to reach steady state, before switching feed composition and feeding amount for the P and L groups. After 21 days, the final protein and lipid contents were recorded for all three groups, as well as the average dry weight per individual. The feed compositions used are summarized in Table 2.

Rotifers from the N-group were subjected to a simulated first feeding scenario (Øie et al., 1997), where they were transferred to a tank at 18℃. In one treatment, *Isochrysis galbana* microalgae were added to the water ($>$ 2 mg C l^{-1}), and in the other, no algae were added. Rotifers were extracted for carbon and protein measurement at the beginning and after 12, 24, 48 and 72 hours.

To simulate this experiment, the model was run initially for 20 days with the N-rotifer treatment. Then the temperature was set to 18℃, the population density was reduced to $<$ 10 ml^{-1}, and the feed composition was switched to

[1] INVE Aquaculture SA, Belgium.

Table 3: Feed compositions used in steady-state lipid content simulations

Feed type	P	L	C
Yeast + 1% Super Selco	45.7	4.7	43.6
Yeast + 2% Super Selco	44.4	7.2	42.4
Chlorella vulgaris	55.0	10.2	29.0
Yeast + 5% Super Selco	41.0	13.8	39.0
Yeast + 10% Super Selco	36.5	23.1	34.8
ω-yeast	34.5	30.8	30.4
Yeast + 18% Super Selco	30.8	33.8	29.4

that of *I. galbana*. The feed concentration was set to 2.5 mg C l^{-1}.

Olsen (2004) shows data on the relationship between feed lipid content and rotifer lipid content in rotifers grown at a growth rate of 0.1–0.2 day^{-1} (Figure 4.10D). For comparison, the model was run at a dilution rate of 10% day^{-1}, which corresponds to a growth rate of 0.105 day^{-1}, with a variation of feed compositions providing a gradient of lipid contents (Table 3). In steady state, the relative lipid content was recorded. The composition of all yeast and Super Selco mixtures are based on the addition of a certain fraction of Super Selco by wet weight. Super Selco has 70% dry matter,[2] and yeast is assumed to have 24% dry matter.

3 Results

Some variables from the simulation of the P-rotifers during cultivation and enrichment are shown in Figure 2. During semi-continuous culture, the population density takes some time to stabilize (Figure 2a),[3] and the average weight of the rotifers (Figure 2b) tends to be negatively correlated with the variations in density. The protein level (Figure 2c) shows little variation when feeding conditions are constant, while the lipid level (Figure 2d) is positively correlated with the variations in dry weight. The daily variations in lipid level are caused by changes in the feed concentration leading to changing reserve levels. The lipid fraction in reserves is similar to that of the feed, and significantly higher than the lipid level L_V in structure, so the changing balance between structure and reserves affects the overall lipid fraction. The protein level shows comparatively very

[2]Source: http://www.inve.com/fish/index.asp?id=257 (retrieved 23 August 2006).

[3]The time to reach steady state increases with decreasing dilution rate, and for low dilution rates there will always be significant oscillations.

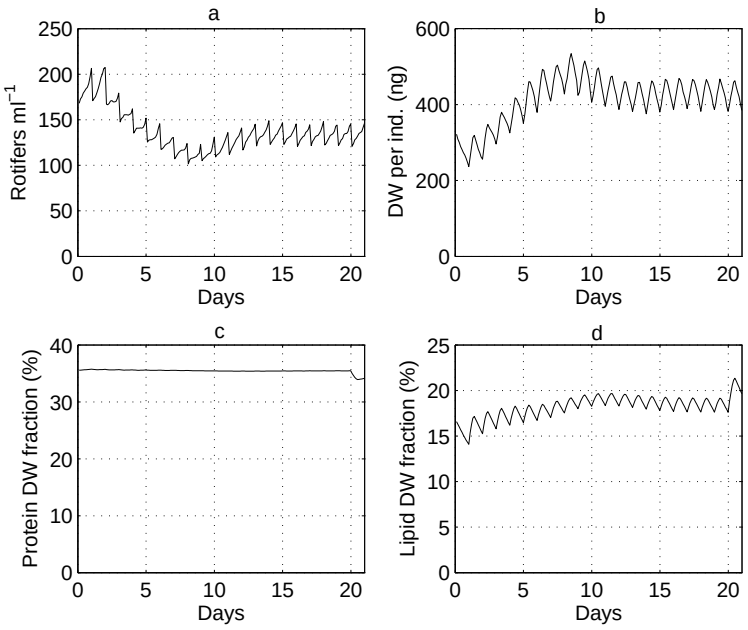

Figure 2: Population density (a), dry weight per individual (b), relative protein content (c) and relative lipid content (d) of rotifers in the simulation of the P group during culture (day 0–20) and enrichment (day 20–21).

small daily variations because the protein level in reserves in this case closely matches the level in structure. Both protein and lipid levels change abruptly during the enrichment on day 20–21.

The final protein content, lipid content and individual dry weight predicted by the model agree fairly well with the values from the literature (Figure 3). In the two enriched rotifer groups (P and L), the model underestimates protein content and overestimates lipid content. In the non-enriched group (N), the model overestimates protein content and underestimates lipid content. Dry weigths are slightly underestimated by the model in the P and N groups, and overestimated in the L group.

The transient changes in individual protein content predicted by the model after transfer to a first feeding tank agree quite well with the values from the

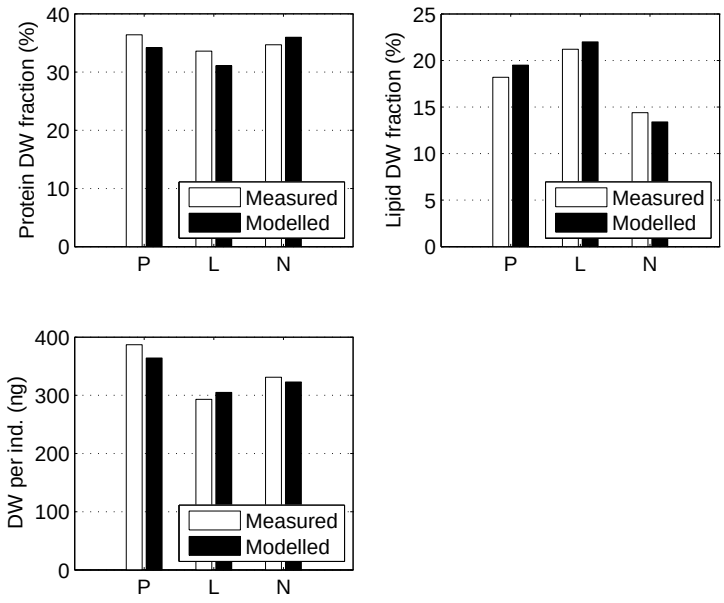

Figure 3: Relative protein content, relative lipid content and dry weight per individual of rotifers after the three different treatments (Øie et al., 1997), compared to the model output.

literature (Figure 4). The protein content increases steadily when algae are added, and decreases when algae are absent. Making the same comparison for the individual dry weigth (Figure 5) we see that the model overestimates dry weight after 72 hours in both cases. When algae are added, the model predicts a greater increase in dry weight. When algae are absent, the model predicts a smaller decrease that what was observed.

The model's prediction of the steady-state lipid content in rotifers as a function of feed lipid content (Figure 6) agrees fairly well with the experimental data for feed lipid contents of 10% and above. For lower lipid levels the model predicts a lower lipid content than that observed.

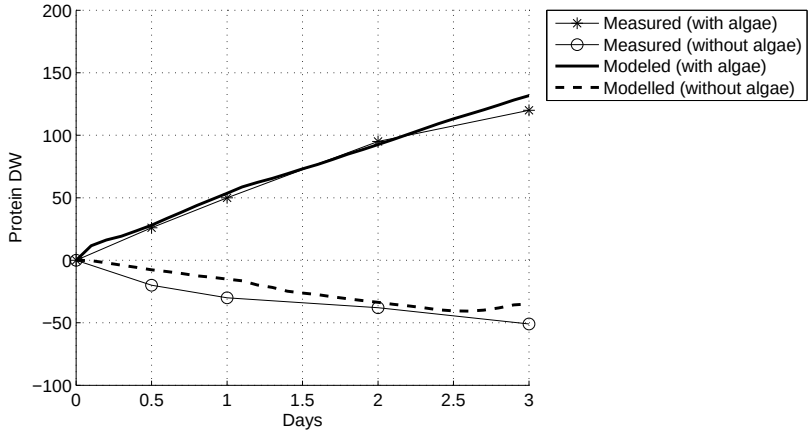

Figure 4: Relative change (%) in rotifer protein content in a simulated first feeding scenario with and without addition of *Isochrysis galbana*. The measured data (Øie et al., 1997) are compared to the model output.

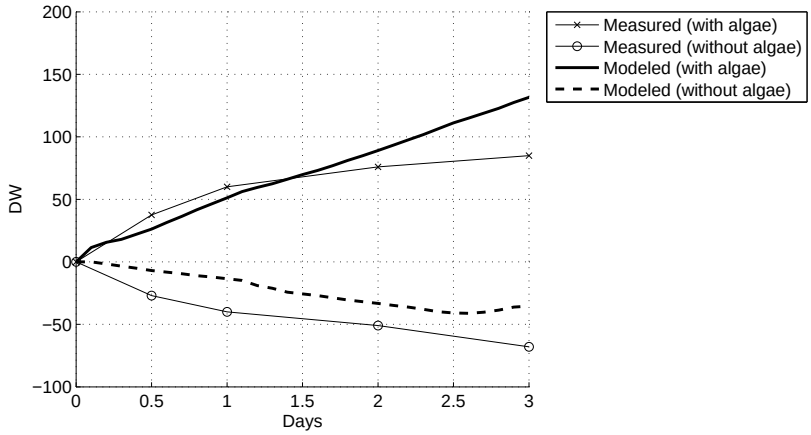

Figure 5: Relative change (%) in rotifer dry weight in a simulated first feeding scenario with and without addition of *Isochrysis galbana*. The measured data (Øie et al., 1997) are compared to the model output. We assume that dry weight is proportional to carbon content.

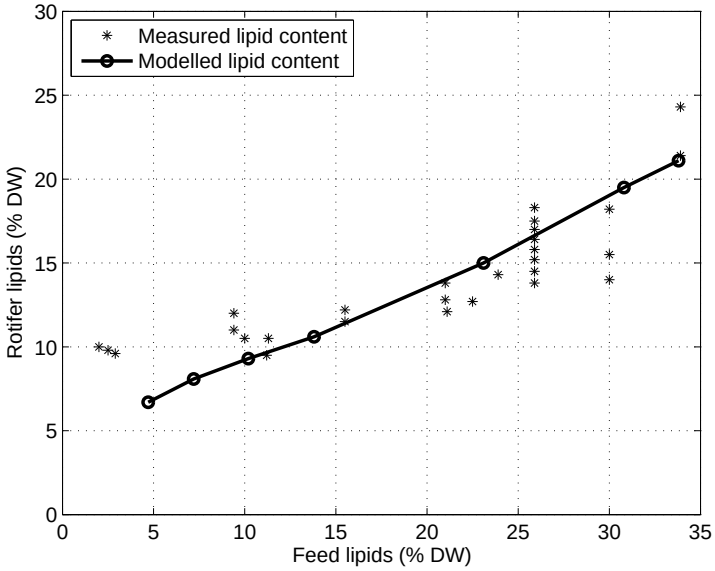

Figure 6: Relative lipid content in rotifers as a function of feed lipid content. Experimental data (Olsen, 2004) are compared to model output. The data have been copied manually from Figure 4.10D in Olsen (2004).

4 Discussion

The comparisons of the model output with the data from Øie et al. (1997) have shown fairly good overall agreement. The predicted body composition and dry weight of rotifers are close to the measured values both in the steady state semi-continuous culture and after two treatments ending with 24 hours short-term enrichment. The deviations observed indicate that the model tends to exaggerate the difference between body compositions as a result of different treatments.

The greatest deviation was seen when studying the change in individual dry weight after transfer of rotifers to a first feeding tank, where the model overestimated the dry weight after 72 hours. The model at the same time predicted the change in protein content much more accurately, so the deviations must originate in lipid or carbohydrate contents. *Isochrysis galbana* has a high lipid content (36.6% in our simulation), and therefore with algae present the model predicts some accumulation of lipids because these are not metabolised at a very high rate. Relative lipid content increases from ca. 14% to ca. 34% in the model during those 72 hours, and there may be an unmodelled effect that limits such large accumulation.

The model's predictions of steady-state lipid content as a function of food lipid content are too low at lipid levels below 10%. This may be caused by an unmodelled effect. One possible explanation is that rotifers synthesize lipid from glucose when glucose is abundant or when lipid is scarce. This would lead to higher lipid content, particularly when the feed lipid level is low.

Based on the comparisons with experimental data, we can conclude that the model, although relying on simple principles, provides a reasonably good representation of the effect of culture conditions on rotifer body composition. Some deviations between modelled and observed results are always to be expected, because small changes in the experimental setup can affect the results. There is significant variation in results between experiments, even when the same rotifer strain has been used.

4.1 Further work

For representing the effect of rotifer enrichment on their nutritional value when used in first feeding of marine fish larvae, the present model brings a clear improvement compared to the original model in Alver et al. (2006). However, the quality of lipids is as important as the quantity, and for cold water fish species the amount of docosahexaenoic acid (DHA) and eicosapentaenoic acid

(EPA) are especially important (Kjørsvik et al., 2004). The next step should be to extend the model to provide estimates of the amount of important fatty acids and possibly other nutrients.

References

Alver, M. O., Alfredsen, J. A., Olsen, Y., 2006. An individual-based population model for rotifer (*Brachionus plicatilis*) cultures. Hydrobiologia 560, 93–108.

Evjemo, J. O., Olsen, Y., Dec. 1997. Lipid and fatty acid content in cultivated live feed organisms compared to marine copepods. Hydrobiologia 358, 159–162.

Fernandez-Reiriz, M. J., Labarta, U., Ferreiro, M. J., 1993. Effects of commercial enrichment diets on the nutritional value of the rotifer (*Brachionus plicatilis*). Aquaculture 112, 195–206.

Fidalgo, J. P., Cid, A., Torres, E., Sukenik, A., Herrero, C., Jul. 1998. Effects of nitrogen source and growth phase on proximate biochemical composition, lipid classes and fatty acid profile of the marine microalga *Isochrysis galbana*. Aquaculture 166, 105–116.

Frolov, A. V., Pankov, S. L., Geradze, K. N., Pankova, S. A., Spektorova, L. V., Sep. 1991. Influence of the biochemical composition of food on the biochemical composition of the rotifer brachionus plicatilis. Aquaculture 97, 181–202.

Holling, C. S., 1965. The functional response of predators to prey density and its role in mimicry and population regulation. Memoirs of the Entomological Society of Canada.

Kjørsvik, E., Pittman, K., Pavlov, D., 2004. Culture of cold-water marine fish, Ch. From fertilisation to the end of metamorphosis - functional development. In: Moksnes et al. (2004), pp. 204–278.

Kooijman, S. A. L. M., 2000. Dynamic energy and mass budgets in biological systems, 2nd Edition. Cambridge University Press.

Kooijman, S. A. L. M., Andersen, T., Kooi, B. W., 2004. Dynamic energy budget representations of stoichiometric constraints on population dynamics. Ecology 85, 1230–1243.

Lubzens, E., Tandler, A., Minkoff, G., 1989. Rotifers as food in aquaculture. Hydrobiologia 186/187, 387–400.

Makridis, P., Olsen, Y., 1999. Protein depletion of the rotifer *Brachionus plicatilis* during starvation. Aquaculture 174, 343–353.

Maruyama, I., Nakamura, T., Matsubayashi, T., Ando, Y., Maeda, T., 1988. Fatty acid composition of rotifers fed with *Chlorella* and yeast. Suisanzoshoku 63, 259–263, in Japanese.

Moksnes, E., Kjørsvik, E., Olsen, Y. (Eds.), 2004. Culture of cold-water marine fish. Blackwell Publishing, Oxford.

Olsen, Y., 2004. Culture of cold-water marine fish, Ch. Live food technology of cold-water marine fish larvae. In: Moksnes et al. (2004), pp. 73–128.

Olsen, Y., Reitan, K. I., Vadstein, O., 1993. Dependence of temperature on loss rates of rotifers, lipids, and $\omega 3$ fatty acids in starved *Brachionus plicatilis* cultures. Hydrobiologia 255/256, 13–20.

Rainuzzo, J. R., Reitan, K. I., Olsen, Y., 1994. Effect of short- and long-term lipid enrichment on total lipids, lipid class and fatty acid composition in rotifers. Aquaculture International 2, 19–32.

Sargent, J., McEvoy, L., Estevez, A., Bell, G., Henderson, J., Tocher, D., 1999. Lipid nutrition of marine fish during early development: current status and future directions. Aquaculture 179, 217–229.

Sveier, H., Raae, A. J., Einar, L., 2000. Growth and protein turnover in atlantic salmon (*salmo salar* l.): the effect of dietary protein level and protein particle size. Aquaculture 185, 101–120.

Øie, G., Makridis, P., Reitan, K. I., Olsen, Y., 1997. Protein and carbon utilization of rotifers (*Brachionus plicatilis*) in first feeding of turbot larvae (*Scophthalmus maximus* L.). Aquaculture 153, 103–122.

Øie, G., Olsen, Y., 1997. Protein and lipid content of the rotifer *Brachionus plicatilis* during variable growth and feeding condition. Hydrobiologia 358, 251–258.

Øie, G., Reitan, K. I., Olsen, Y., 1994. Comparison of rotifer culture quality with yeast plus oil and algal-based cultivation diets. Aquaculture International 2, 225–238.

Automatic measurement of rotifer *Brachionus plicatilis* densities in first feeding tanks

Morten Omholt Alver*, Torodd Tennøy†,
Jo Arve Alfredsen*, Gunvor Øie‡

Abstract

Rotifers are an important live food in the culture of marine fish, but the process of measuring rotifer culture densities is time consuming. This is especially true at low densities such as those applied in first feeding tanks. A particle counter for making automatic measurements of rotifer densities has been designed. The instrument automatically extracts samples, and relies on a digital camera and image processing to measure the rotifer density. Due to its autonomous nature, the instrument is suited for use as a component in a process monitoring and control system.

The rotifer counter design is presented, and the statistical properties of the measurement derived. The accuracy achieved in practical countings is then investigated in a series of test counts. To assess the quality of measurements achieved in an actual first feeding tank with samples extracted from a single location, the rotifer counter is used in an experiment studying rotifer dynamics in a continuously diluted tank. The results indicate that the rotifers are approximately evenly distributed in the water column, and that one needs to consider rotifers attaching to the tank wall to be able to predict rotifer densities under these conditions. The experiment gives an example of the considerable potential for experimental work assisted by the automated rotifer counter.

*Department of Engineering Cybernetics, Norwegian University of Science and Technology, Odd Bragstads plass 2D, 7491 Trondheim, Norway

†Thelma AS, Box 6170 Sluppen, 7435 Trondheim, Norway

‡SINTEF Fisheries and Aquaculture AS, SINTEF Sealab, Brattørkaia 17B, 7010 Trondheim, Norway

1 Introduction

Monitoring of the live feed density is important in first feeding tanks as well as in the production of live feed, because the feed density has a significant effect on the growth and survival of the fish larvae (Lubzens et al., 1989). Experimental work on cod (*Gadus morhua*) larvae (Puvanendran and Brown, 1999) has shown that a feed density of ≥ 4000 rotifers liter^{-1} gives better survival and growth than lower densities. For turbot (*Scophthalmus maximus*) a density of 3000 rotifers liter^{-1} was found to give better growth than either 1000 rotifers liter^{-1} or 7500 rotifers liter^{-1} (Hoehne-Reitan et al., 2001). The monitoring of the feed densities in larval tanks makes it possible both to control feed availability for the larvae, and to estimate larval feed intake. Ultimately, such data can be used to estimate larval mortality (Alver et al., 2005).

Manual counting of rotifer densities is time consuming, and for this reason and others, the production of live food amounts to a significant part of the production costs for marine fish species.[1] To enable better monitoring of rotifer cultures and feed densities in larval tanks, a more efficient measurement method is needed. However, at present there are no commercially available instruments that automate the counting process.

By exploiting the fact that rotifers can be visually distinguished in size and shape from other particles present in culture water, the counting process can be automated. Digital camera technology has in the latest years become both more advanced and more affordable, making it a viable option for use in an automated rotifer counter. Computer controlled pumps and valves make it possible to automatically extract samples from one or several tanks. In this study, an autonomous rotifer counter based on image processing is designed, analyzed with respect to accuracy, and tested in practical use.

2 Materials and method

2.1 The rotifer counter

2.1.1 Measurement procedure

Figure 1 shows an overview of the rotifer counter. It is equipped with four tubes for extracting samples, and uses computer controlled valves to open for one tube at a time. Each tube is equipped with a 0.5 mm filter at the end to

[1] One study shows that for sea bass the live food costs were 79% of the total costs during the first 45 days after hatching (le Ruyet et al., 1993).

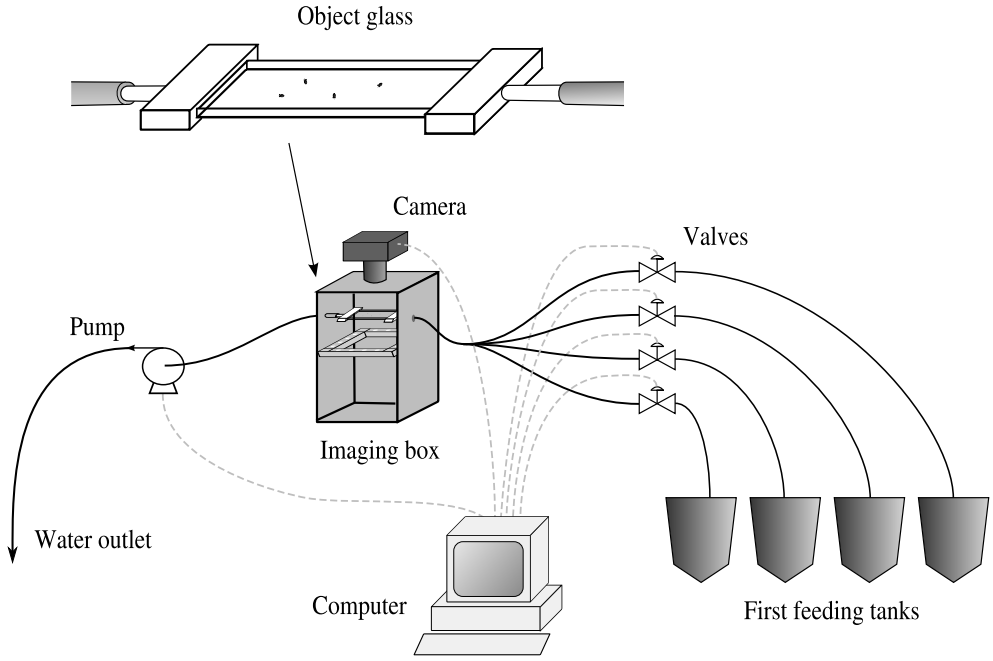

Figure 1: Overview of the rotifer counter. The imaging box is drawn without its front wall to indicate the lights and object glass inside. In the upper left a larger drawing of the object glass is shown.

prevent fish larvae from being extracted. The pump pulls water from the tank through the object glass, where a known volume V is photographed by a digital camera (Sumix SMX-100 USB2.0 CMOS camera). The object glass consists of two glass plates attached with metal spacings along the outer long edges giving a 2.9 mm distance between them.[2] The end pieces are made of plexiglass, and have nipples for attaching the tubes.

Lighting is provided by 16 light emitting diodes (587 nm yellow light, total 750 mcd) mounted in a square with four diodes along each side. The square is set below the object glass in a plane parallel to the glass plates, distanced

[2]The distance between the glass plates can be chosen depending on the desired sample volume, and the focus depth of the camera. For high densities a shorter distance should be chosen to reduce the risk of rotifers overlapping in the picture.

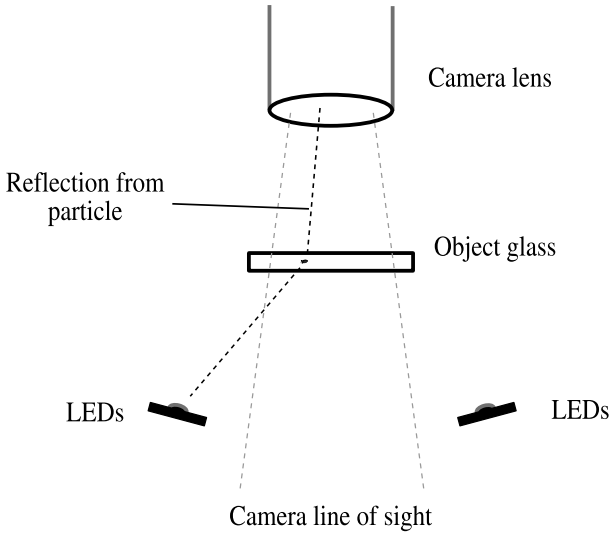

Figure 2: Darkfield lighting. The light sources are placed outside of the camera's line of sight. The only light reaching the camera is that reflected by particles in the object glass.

so the cone visible to the camera falls in between the LEDs (Figure 2). This setup provides darkfield conditions, where light is reflected by particles in the water, causing rotifers and other particles to appear in the images as bright spots against a dark background. This lighting was found to give images with better contrast than bright field conditions. Farmers often use *green water* (Shields, 2001), but the addition of microalgae in the culture water has a negligible effect on the contrast of the lighting setup.

Images were captured in gray scale. To filter out stationary rotifers or other particles, the previous image was subtracted from each new image, removing all the light areas and particles that were also present in the previous image. The image was then reduced to binary form by setting all pixels lighter than a certain threshold level to white, and all pixels below to black. Each particle (contiguous white area) in the image was then filtered out unless its area, elongation[3] and

[3]Elongation is defined as the particle's largest intercept divided by the mean perpendicular intercept.

roundness[4] indices were within preset intervals. These intervals were chosen to represent the size and shape of normal rotifers (40–600 pixels for area, 1.75–6.50 for elongation and 1.0–1.4 for roundness), and can to a certain degree distinguish rotifers from other particles such as air bubbles or detritus from the fish larvae. The area interval is fairly wide, to account for variation in size between rotifers of different ages and nutritional conditions. The remaining particles were counted, and the result divided by the volume V to achieve an estimate of the rotifer density. All image processing operations were performed using National Instruments IMAQ Vision running under LabView 7.0.

The counter takes images in rapid sequence, activating the pump for approximately one second between each image to replace the sample volume. To get a clear picure, the counter must pause after stopping the pump until the sample volume stops moving. After a sequence of N images (determined by the operator), the pump is activated for a longer period to flush the entire tube. The mean density found in those N images is logged as a single data point. The minimum time between data points depends primarily on transportation time for water samples and on the number of images used for each measurement. With the current setup, the total rate of measurements is approximately 15 data points per hour. Higher measurement rates could be achieved by replacing some of the equipment used.

The counter is entirely autonomous, and logs each data point for later retrieval, in addition to displaying the most recent measurements on a PC screen.

2.1.2 Measurement statistics

To assess the accuracy of measurements, we need a statistical model of the measurement process. We will in the following analysis assume that representative random samples are extracted from the tank, and that the counter correctly assesses the number of rotifers per image.

Each image analyzed by the counter contains a small sample of the water from the tank, and each rotifer found in such a sample may be considered an event. These events happen at random, but their frequency is dependent on the rotifer density in the water. Thus, the amount of rotifers found in each image is well modelled by the Poisson distribution $p(x; \lambda t)$ with x the number of rotifers, the water volume per image analogous to the time interval t, and the rotifer density analogous to the frequency λ. The mean and variance of the Poisson distribution $p(x; \lambda t)$ both have the value λt (Walpole et al., 1998, pp. 137).

[4] Roundness is defined as the particle perimeter divided by the perimeter of a circle with the same area as the particle.

Using compatible units, the rotifer density ρ is given as rotifers ml^{-1}, and the volume per image is V [ml]. From the Poisson distribution, the number of rotifers per image, x, will then be a random variable with both mean and variance equal to ρV.

It is clear that x/V is an unbiased estimate of ρ with variance ρ/V. However, as mentioned earlier, each data point is produced as an arithmetic mean of the densities of N images:

$$\hat{\rho} = \frac{1}{N} \sum_{i=1}^{N} \frac{x_i}{V} \tag{1}$$

Invoking the Central Limit Theorem (Walpole et al., 1998, pp. 217), for large enough N, $\hat{\rho}$ approximates a normal distribution with mean ρ and variance $\frac{\rho}{VN}$.

We can conclude that the inherent variance of the measurement is not fixed, but proportional to the true rotifer density. It is also inversely proportional to the sample volume and number of images per measurement, meaning that these variables can be increased to improve accuracy.

These are the parameters in the current setup:

$$V = 0.439 \text{ cm}^3 \tag{2}$$

$$N = 50 \tag{3}$$

which gives

$$\text{var}(\hat{\rho}) = 0.0456 \times \rho \tag{4}$$

The relative standard deviation, $\sqrt{\text{var}(\hat{\rho})}/\rho$, decreases with increasing density. If the rotifer counter is used in a situation with high densities, a lower N can therefore be used to increase the measurement speed.

2.2 Test counts

A series of 16 water samples with different rotifer densities in the interval 0–13000 rotifers l^{-1} were prepared. Each sample was measured 4 times by the rotifer counter, while being kept in a 1 l beaker, gently mixed by a magnetic stirrer. Water was extracted to the counter through a tube placed with its opening near the center of the water volume. For comparison, all samples were measured by manual counting. The manual counting was done by extraction of up to 72 ml samples using a 5 ml pipette, fixation of the samples using Lugol's solution, and visual determination of the total number of rotifers using a stereo microscope.

Table 1: Number of rotifers added to the tank, and water exchange rate (tank volumes day^{-1})

Time [h]	Rotifers liter^{-1}	Water exchange rate
0	3000	1.29
3.5	2500	1.29
15.5	2500	2.53
26	1500	3.53
40	4500	5.30

2.3 Long term test

An experiment was run over 48 hours, using the rotifer counter to investigate the rotifer density dynamics in an environment similar to a small scale first feeding setup for marine fish larvae.

One experimental tank was used, holding ca. 163 l. The tank walls were black, and illumination was provided by a 40 W light bulb hanging 25 cm above the surface. The temperature was held at approximately 10 ℃, and a continuous water exchange was set up, driven by a controlled inflow rate. The outflow passed through a perforated tube attached in the bottom center of the tank and reaching to the surface. The water exchange rate was measured regularly, and held at four different levels throughout the experiment. Table 1 shows the water exchange rates and times of adjustment.

The rotifer counter used four intake tubes placed at different locations in the tank. One was placed approximately 20 cm from the surface and 20 cm from the tank wall. The three remaining ones were attached to the center tube by the surface, halfway down, and at the bottom.

At five different times, three of them coinciding with adjustments of the water exchange rate, rotifers were added to the tank. The number of rotifers added each time is listed in Table 1. The rotifers were of the SINTEF strain of *Brachionus plicatilis*, and were cultured with a yeast and oil diet at 22 ℃ in a continuous culture at approximately 400 rotifers ml^{-1}. The rotifers were not acclimatized to the experimental tank's temperature before addition, and no algae or other feed substances were added to the test tank.

During the test period, a total of 695 measurements were made from the four measurement locations, at a rate of approximately 15.3 measurements per hour.

2.3.1 Mathematical model

A simple mathematical model of the rotifer density is used to compute expected values for comparison with the measurements. The model is described in detail in Alver et al. (2005), and will be only briefly described here.

Since no feed was provided for the rotifers, eggs are disregarded. Rotifers are known to use their foot to attach themselves to surfaces, and the model allows for this. The total amount of rotifers in the water column is denoted N_c, and the amount attached to the wall N_w. Given the tank volume V_w [cm^3] and the total wall surface area A_w [cm^2], we can express the measurable rotifer density as $\rho = N_c/V_w$, and the density on the tank wall as $\rho_w = N_w/A_w$.

The symbols M_w [day^{-1}] and M_c [day^{-1}] represent the migration rate of rotifers onto the wall and into the water column, respectively. Migration to the wall is represented by M_w:

$$M_w = N_c k_1 A_w / V_w \tag{5}$$

where k_1 [cm day^{-1}] is a constant. M_c imposes a soft upper bound ρ_{cap} [cm^{-2}] on the density on the wall:

$$M_c = N_w k_2 \left(\frac{N_w}{A_w \rho_{cap}} \right)^4 \tag{6}$$

where k_2 [day^{-1}] is a constant. This form is chosen arbitrarily to obtain a relationship where M_c is small for values of N_w smaller than $A_w \rho_{cap}$, and increasing steeply when N_w increases beyond $A_w \rho_{cap}$. The exponent determines how soft the density bound is, that is, how much the density can exceed ρ_{cap}.

Addition of rotifers is represented by the controlled variable u, which has the unit of rotifers added per day. Feeding often takes the form of instantaneous additions at discrete times - e.g. u_x rotifers added at time t_x. This can be represented as a burst lasting from time t_x to $t_x + \Delta t$, with an amplitude of $\frac{u_x}{\Delta t}$. Δt can be chosen equal to the time step in a numerical simulation. The relative water exchange rate is denoted Q_w [day^{-1}]. Assuming that the rotifers are homogeneously distributed, the outlet water will have the same rotifer density as the water column.

With these terms defined, we can set up the complete model:

$$\dot{N}_c = u - M_w + M_c - Q_w N_c \tag{7}$$

$$\dot{N}_w = M_w - M_c \tag{8}$$

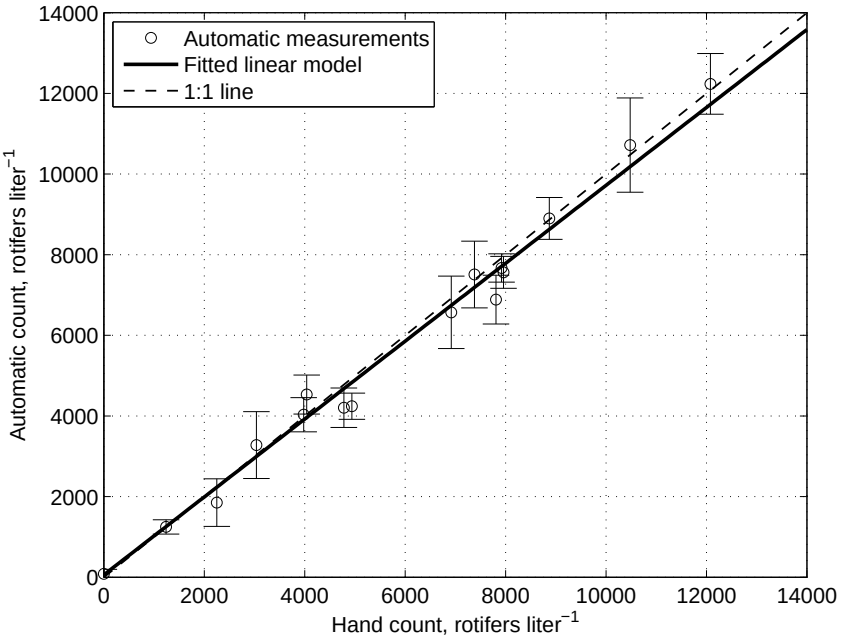

Figure 3: Results from test counts, with automatic measurements with error bars plotted against manual measurements. The regression line is $y = 0.97x+58$.

3 Results and discussion

3.1 Test counts

Figure 3 shows the automatic measurements plotted against the manual counts, along with a linear model fitted by weighted mean squares (weighted by the inverse of the manually counted density, because measurement variance is expected to be proportional to density), and a line showing the ideal measurement characteristic. It should be noted that the manual counts are also subject to error, due to limited sample size and possible counting errors or biased sampling.

We want to assess the observed variance in comparison with the theoretical calculations in Section 2.1.2. The true variance depends on the true rotifer density, and can therefore not be known at any point, but for each measure-

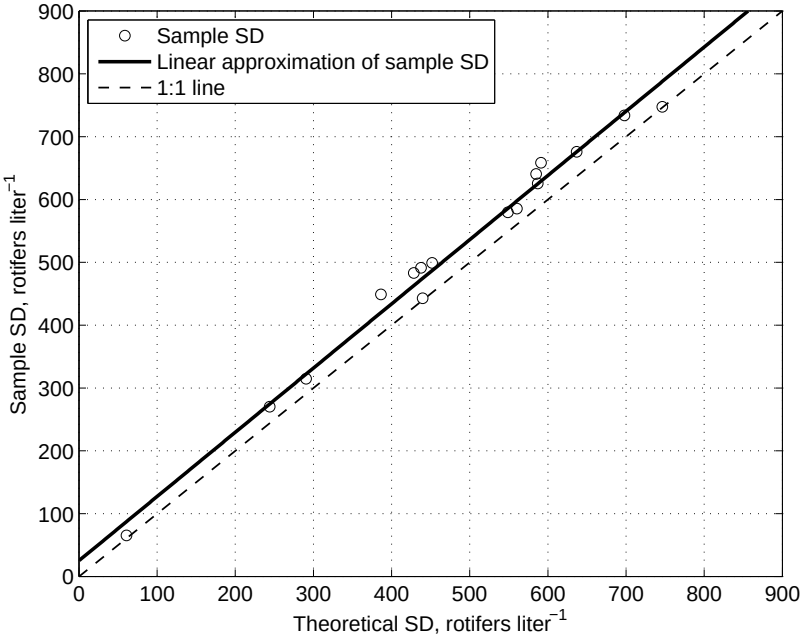

Figure 4: Comparison of observed sample SD in automatic measurements with estimated theoretical SD computed from Eq. (4). The regression line is $y = 1.02x + 25.0$ ($R^2 = 0.987$).

ment value $\hat{\rho}$, an unbiased estimate of the theoretical measurement variance is $\frac{\hat{\rho}}{VN}$. For each measurement point we have 4 samples, each consisting of 50 subsamples. Figure 4 shows the sample standard deviations of each such 200 subsample set, divided by $\sqrt{50}$ to account for the pooling of 50 subsamples into each measurement, plotted against the theoretical minimum standard deviation computed using Eq. (4). Also shown is a linear model fitted to the observed standard deviations by mean squares, which is found to be $y = 1.02x + 25.0$ with a good fit ($R^2 = 0.987$).

The observed SD increases roughly at the same rate as predicted by Eq. (4), but there is a small positive bias. The bias indicates that some variance is introduced in the sampling and image processing, beyond the theoretical

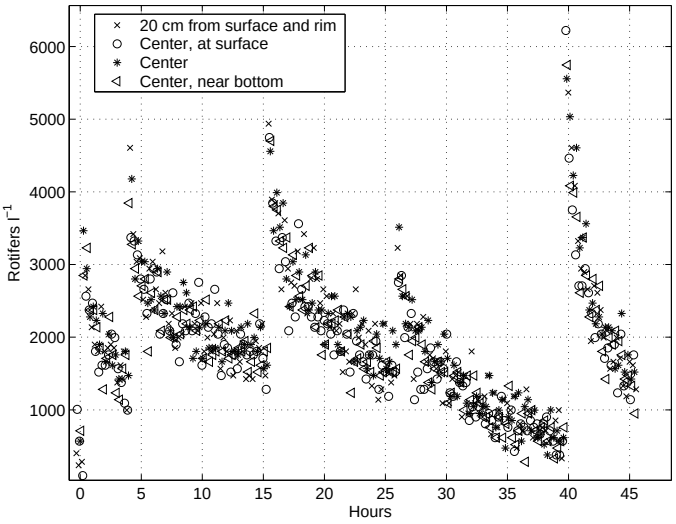

Figure 5: Complete measurement series from long-term experiment. All four measurement locations are shown.

minimum given by the sample size.

3.2 Long term test

Figure 5 shows the measurement series made by the automatic counter for all four measurement locations. Figure 6 shows how each of the measurement locations deviates from the average measurement.[5] The mean values measured at the individual locations showed the following deviations from the mean over all locations: +3.4% at 20 cm from the surface and the rim, -4.6% at the center near the surface, +3.8% at the tank center and -2.7% at the center near the bottom. The indication is therefore that the choice of measurement location does not have a large effect on measurements. The rotifers are approximately evenly distributed in the water column.

[5]The measurements at the four measurement locations were made sequentially, and not at identical times. To obtain comparable data series, the second, third and fourth series were resampled with linear interpolation to approximate the measured values at the time points of the first measurement location. The mean values and deviations were computed from these interpolated data series.

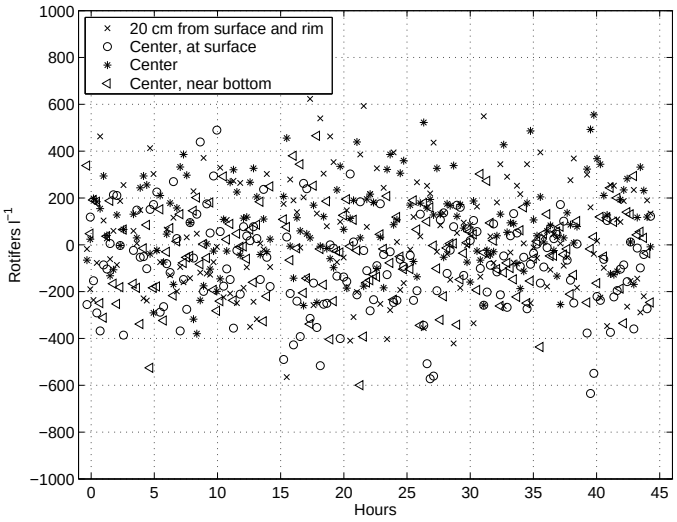

Figure 6: Deviations at each measurement location from the mean measurements.

The mathematical model is run with input parameters (addition of rotifers, and water exchange rate) given by the experiment. The parameter $A_w = 1.7 \times 10^4$ (based on a geometric evaluation of the tank area), $k_1 = 0.005$ and $k_2 = 1$. In an experiment with 10 l units, a maximum of approximately 14 rotifers cm^{-2} were found attached to the wall (Olav Vadstein, pers. comm.), so we choose $\rho_{cap} = 14$. In order to study the effect of rotifers attached to the wall, the model was run one additional time, with the wall state disabled by the following modification:

$$M_c = M_w = 0 \quad \Longrightarrow \quad N_W = 0 \tag{9}$$

Both model runs are shown together with the measured values, averaged over the four locations, in Figure 7. The difference is obvious, and the model with the wall state enabled shows a much better fit with the measured values than the modified model, especially in the first part of the period. This indicates that the wall state does in fact describe a significant property of the modelled system. In the initial days of start feeding, this means that the rotifer density in the water column will be lower than what is expected from the amount of rotifers added.

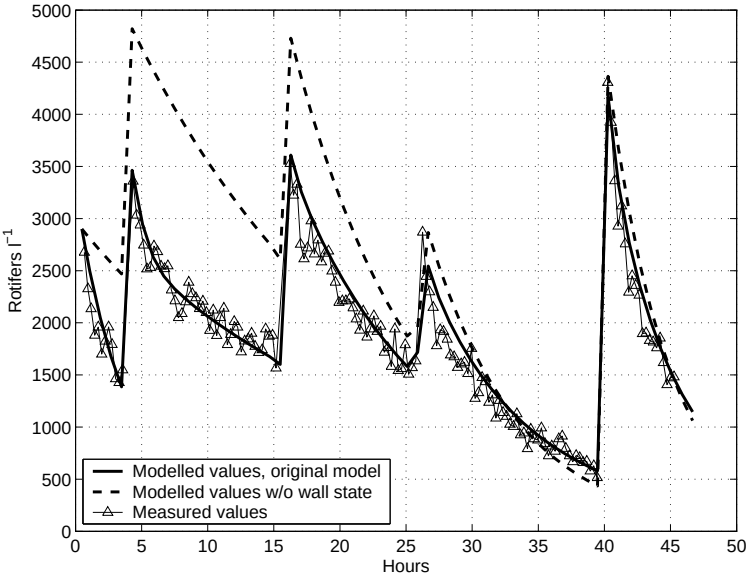

Figure 7: Measurements from long-term experiment, averaged over the four measurement locations, compared to model simulations with and without the wall state.

4 Conclusions

The automatic rotifer counter presented in this paper provides a means of monitoring rotifer densities with a minimum of manual work. Tests indicate that the accuracy of the density measurements is fairly close to the statistically possible accuracy determined by the sample size. By adjusting the sample volume and the number of images per measurement, the counter can be configured to achieve the user's required accuracy.

The long term test applies the rotifer counter in a realistic setting, and gives an indication of what research possibilities it offers. In this small experiment it has been shown that the spatial variations of the rotifer density are small, for tanks of the type used, in a typical larval first feeding setting. Additionally, using a simple mathematical model, the data clearly suggest the importance of the rotifers' tendency to attach to the tank wall.

5 Acknowledgments

The authors would like to thank two anonymous reviewers for their comments, which have helped improve the quality of this paper significantly.

References

Alver, M. O., Alfredsen, J. A., Øie, G., 2005. A system for model based biomass estimation of larvae in intensive cod larvicultures. Aquaculture International 13, 519–541.

Hoehne-Reitan, K., Kjorsvik, E., Reitan, K. I., 2001. Bile salt-dependent lipase in larval turbot, as influenced by density and lipid content of fed prey. Journal of Fish Biology 58, 746–754.

le Ruyet, P., Alexandre, J. C., Thebaud, L., Mugnier, C., 1993. Marine fish larvae feeding: Formulated diets or live prey. Journal of the World Aquaculture Society 24, 211–224.

Lubzens, E., Tandler, A., Minkoff, G., 1989. Rotifers as food in aquaculture. Hydrobiologia 186/187, 387–400.

Puvanendran, V., Brown, J. A., 1999. Foraging, growth and survival of Atlantic cod larvae reared in different prey concentrations. Aquaculture 175, 77–92.

Shields, R. J., 2001. Larviculture of marine finfish in europe. Aquaculture 200, 55–88.

Walpole, R. E., Myers, R. H., Myers, S. L., 1998. Probability and statistics for engineers and scientists. Prentice Hall International.

Paper 4 is not included due to copyright.

Estimating larval density in cod (*Gadus morhua*) first feeding tanks using measurements of feed density and larval growth rates

Morten Omholt Alver*, Jo Arve Alfredsen* & Gunvor Øie†

Abstract

Due to unpredictable mortality in larval cod rearing, a reasonably accurate estimate of the larval biomass in rearing tanks is important for production management such as determination of feed doses and planning of live feed production. A good estimate of larval numbers can also give an early warning if a larval group is suffering high mortality. Because direct measurement of the larval density is difficult, a model based estimator is developed to estimate the larval density from parameters that are simpler to measure, such as feed density and larval size. The estimator is based on an extended Kalman filter using measurements to update a process model.

The estimator was tested by aquiring data on feed densities and larval growth rates in a first feeding experiment on cod. Cod larvae were reared from hatching up to day 16 post hatch in nine 160 l tanks at three different densities. The larvae were fed with rotifers (*Brachionus plicatilis*) from day 3 until the end of the experiment. Results show that the estimator is able to correctly detect differences in larval density.

*Department of Engineering Cybernetics, Norwegian University of Science and Technology, Odd Bragstads plass 2D, 7491 Trondheim, Norway

†SINTEF Fisheries and Aquaculture AS, SINTEF Sealab, Brattørkaia 17B, 7010 Trondheim, Norway

1 Introduction

The principles of using model based estimation to estimate larval biomass in intensive cod larvicultures are described by Alver et al. (2005). A model of the process involving larval feed intake and growth, and the dynamics of the live feed density in the tanks, was described and investigated with regard to observability. The system model is run in real time, corrected by feedback from measurements of larval growth and live feed density. As a result we get approximate estimates of the larval density thoughout the live feed period.

The part of the process model dealing with the energetics of the cod larvae is developed further in this paper. The larval model is based on dynamic energy budget (DEB) theory as developed by Kooijman (2000), and includes both a yolk sac compartment and an energy reserve compartment, which is important in describing larval growth under varying feeding conditions.

To investigate the practical applicability of the larval density estimator, we run a start feeding experiment where cod larvae are reared at three different densities (20, 40 and 80 larvae l^{-1}). This makes it possible to test the estimator's ability to detect density differences between similarly treated tanks.

2 Material and methods

The experiment comprised 9 rearing tanks of 160 l. The tanks were arranged into three groups, denoted A, B and C, with different initial larval densities. The nominal densities were 20 larvae l^{-1} in the A tanks, 40 larvae l^{-1} in the B tanks, and 80 larvae l^{-1} in the C tanks.

2.1 Eggs and startup

Fertilized cod eggs were obtained from Cod Culture Norway AS, approximately 15 day degrees short of hatching. The average egg diameter was measured under the microscope, and used to determine the maximum number of eggs per volume unit based on an empirical relationship (Holm et al., 1991, p. 38). To account for losses before and during hatching, 25 % more eggs than the nominal amount were used. The total amount of eggs was measured by filtering out the estimated volume of eggs required. Eggs were kept in a well mixed bucket of water, and distributed into the tanks in the correct relative amounts. This was done before hatching had commenced, letting hatching take place within the rearing tanks.

2.2 Rearing conditions

The temperature was initially held at 7 ℃, and gradually increased to 12 ℃ through days 2–8. The temperature was measured daily in all tanks.

Water from 90 m depth in Trondheimsfjorden was filtered through a sandfilter and a protein skimmer with ozonation. Thereafter, the water was microbially matured in a biofilter. There was initially no water exchange in the larval tanks. At day 2 post hatch (p.h.) the exchange rate was set to 1 tank volume day^{-1}. The exchange rate was increased to 2 on day 5 and 4 on day 9.

All larval tanks were supplied with *Nannochloropsis oculata* alga paste (Reed Mariculture, 68×10^9 cells ml^{-1}) from day 2 p.h.. Initially, 2 ml alga paste was added per tank at each feeding. The amount was increased to 3 ml at day 6 and 4 ml at day 9. Feeding with rotifers was initiated with two feedings at day 3. On the following days the larvae were fed three times per day, up to a density of 5000 rotifers l^{-1} for the A and B tanks, and 7000 rotifers l^{-1} for the C tanks. The amount used per tank for each feeding was decided based on a quick assessment of the current density. The amount added was recorded for all tanks.

The rotifers used were of the SINTEF strain of *Brachionus plicatilis*. They were cultured with baker's yeast and Marol E, at approximately 22 ℃, 20 ppt salinity and densities between 200 and 500 rotifers ml^{-1}. At each feeding, rotifers were extracted from the culture tanks, washed and added directly to the larval tanks without additional enrichment.

The tanks were manually cleaned three times a week by siphoning out organic material such as dead eggs, larvae or rotifers, accumulated at the bottom of the tanks.

The experiment was terminated at day 16 p.h., and the remaining larvae were counted. The water level in each tank was lowered, to concentrate the larvae and make it possible to extract them and get an exact count. Finally the larvae were anesthetized and killed.

2.3 Measurements

The dry weight of larvae was sampled at days 0, 3, 5, 9 and 15 p.h. The first two samplings took place before feeding was initiated, and were conducted for the group as a whole. The remaining samplings were done by extracting 6 larvae at random from each tank. Each sampled fish was anesthetized, washed in fresh water, and put into a tin cup of known weight. The samples were dried for 48 h at 60 ℃, and their dry weight finally determined by measuring the weight

increase of each tin cup.

Four larval tanks (A1, B1, C1 and C2) were monitored using an automatic rotifer counter. The counter was equipped with tubes reaching into all four tanks, and computer controlled valves to open for one tank at a time. Rotifers were counted using a digital camera and image analysis, and the measured rotifer densities were logged at a rate of 3–4 data points per hour per tank.

Due to statistical uncertainty related to sample size, and uncertainty in distinguishing rotifers from other particles, each sample point has an expected standard deviation of approximately 480 rotifers liter^{-1} at a true density of 5000 rotifers liter^{-1}, and 300 rotifers liter^{-1} at 2000 rotifers liter^{-1}. The expected standard deviation increases proportionally with the square root of the true density.

The initial number of larvae in each tank has some uncertainty, due to an unknown loss of larvae through handling and hatching, and uncertainty in the empirical formula for the number of eggs per volume unit. The final larval count, on the other hand, has no significant error sources.

2.4 Mathematical model

A basic component of the state estimator is the mathematical model of the system, which allows the estimator to compute expected values for the rotifer density and larval dry weight under given conditions. The model covers both rotifer dynamics and larval growth. The following sections describe the model equations, and Table 1 summarizes model parameters and their values.

2.4.1 Larval model

The larval model is based on the Dynamic Energy Budget (DEB) model developed by Kooijman (2000). We make the significant simplification of simulating only one individual, which is considered to be an "average" individual. The model has the following state variables:

- N : Number of larvae
- S : Gut content [J].
- Y : Yolk energy [J].
- E : Energy reserves [J].
- V : Structural volume [cm^3].

Table 1: Summary of model parameter values used in simulations.

Symbol	Value	Unit	Description
A_w	1.7×10^4	cm^2	Tank internal surface area
$[E_G]$	2145	J cm^{-3}	Volume-specific cost of growth
E_r	6.1×10^{-3}	J	Energy content per rotifer
κ	0.8		Constant for energy allocation
k_{as}	0.8		Max assimilated fraction in larval gut
k_g	20	day^{-1}	Larval gut emptying rate
k_m	250	cm day^{-1}	Constant for rotifer migration to wall
μ_E	1.3×10^4	J g^{-1}	Energy density of larval energy reserves
μ_S	1.3×10^4	J g^{-1}	Energy density of larval gut content
M	variable		Relative mortality rate
$\{\dot{p}_{Am}\}$	90	J cm^{-2} day^{-1}	Max. surface area-specific assimilation rate
$\{\dot{p}_{Am,yolk}\}$	70	J cm^{-2} day^{-1}	Surface area-specific yolk absorption rate
$\{\dot{p}_{Im}\}$	135	J cm^{-2} day^{-1}	Max. surface area-specific feed intake rate.
$[\dot{p}_M]$	150	J cm^{-3} day^{-1}	Volume-specific cost of maintenance
ρ_{cap}	14	cm^{-2}	Soft upper boundary of wall rotifer density
T_A	5700	K	Arrhenius temperature
T_C	variable		Temperature correction factor
T_e	1.6	days	Hatching time of rotifer eggs
T_w	variable	℃	Water temperature
T_{ref}	8	℃	Reference water temperature
$\dot{v}$	0.02	cm day^{-1}	Energy conductance
V_w	160	l	Water volume
$[W_V]$	0.15	g cm^{-3}	Volume-specific dry weight of structure V
X_K	2500	l^{-1}	Half-saturation constant for larval feed intake

The larval numbers N is only affected by mortality. The mortality can be expected to vary with time, and is difficult to predict. Since our goal is to use measurements to improve the estimate of this value, a simple mortality model will be sufficient:

$$\frac{dN}{dt} = -M(t)N \tag{1}$$

Mortality is assumed to be proportional to the number of fish. We assume that mortality is low in the first period, up until the yolk sac is emptied, and higher

in the remaining period where starvation may occur:

$$M(t) = \begin{cases} 0.15 & \text{if } t < 7 \\ 1.05 & \text{otherwise} \end{cases} \tag{2}$$

The metabolic rates of cod larvae are strongly affected by water temperature. For simplicity, we specify the model for a reference temperature of 8 °C (281 K). For other temperatures, the parameters $\{\dot{p}_{Im}\}$, k_g, $\{\dot{p}_{Am,yolk}\}$, $\{\dot{p}_{Am}\}$, $\dot{v}$ and $[\dot{p}_M]$ introduced below are multiplied with a correction factor T_C:

$$T_C = \exp\left\{\frac{T_A}{T_{ref}} - \frac{T_A}{T_w}\right\} \tag{3}$$

where $T_{ref} = 281$ K, and T_A is called the Arrhenius temperature (Kooijman, 2000, p. 53). We choose $T_A = 7400$, which gives a temperature dependence approximately corresponding to a Q_{10} value of 2.5. This value agrees both with the values found by Finn et al. (2002) for metabolic rate (2.4–2.6), and with the range of values suggested by Buckley et al. (2000) for the ingestion rate of cod larvae (1.8–3.7).

The energy ingestion rate of the cod larvae is specified by:

$$\dot{p}_I = \{\dot{p}_{Im}\} V^{2/3} f \tag{4}$$

$$f = \frac{X}{X + X_K} \tag{5}$$

where $\{\dot{p}_{Im}\}$ is the maximum surface-specific feed intake. Figure 1 A illustrates the relation between X and f. This is an example of a Holling Type II response (Holling, 1965), which is appropriate for a predator with only one food source. This functional response does not take gut contents into account, implying that the larvae attempt to maximise their feed intake without any significant appetite effect. This is consistent with the general belief that marine fish larvae are *number maximisers*, as noted by Olsen et al. (2004). We choose the half-saturation constant $X_K = 2500$ rotifers liter^{-1} based on data from Puvanendran et al. (2002) that relate feeding behaviour to prey concentration. It is difficult to find good data on the long-term feed intake rate of cod larvae, so we have chosen the value $\{\dot{p}_{Im}\} = 135$ J cm^{-2} day^{-1} based on estimated total feed intake rates in the A1, B1, C1 and C2 tanks of this experiment.

In terms of number of rotifers, the predation rate p is specified by:

$$p = \frac{\dot{p}_I}{E_r} \tag{6}$$

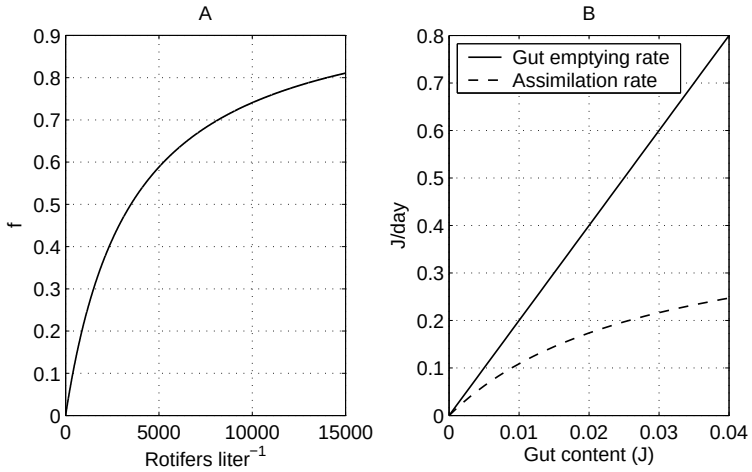

Figure 1: Functional responses for feed intake and assimilation. A) Fraction of maximum feed intake rate as function of rotifer density. B) Gut emptying rate and assimilation rate as function of gut content for a larva with $V = 5.0 \times 10^{-4}$ cm^3.

where E_r is the amount of nutritional energy per rotifer. The value of E_r is chosen based on data from Øie and Olsen (1997). Assuming that the rotifers have been cultured at a specific growth rate of 0.2, we can expect an individual dry weight of approximately 480 ng, protein content of 33% of DW and lipid content of 13% of DW. Using energy densities of 23600 J g^{-1} for protein and 39500 J g^{-1} for lipid, this gives an overall energy density of 13000 J g^{-1}, and we find the value $E_r = 6.1 \times 10^{-3}$ J.

Ingested energy enters the gut:

$$\frac{dS}{dt} = \dot{p}_I - k_g S \tag{7}$$

where k_g is the relative gut emptying rate. In one study it was estimated that it takes 4 h for cod larvae to empty their guts (Lough and Mountain, 1996). We choose an emptying rate of $k_g = 20$, which implies that remaining gut content after 4 h is approximately 3.5% of the initial value.

The yolk sac is absorbed gradually until it is exhausted:

$$\frac{dY}{dt} = \begin{cases} -\{\dot{p}_{Am,yolk}\}V^{2/3} & \text{if } Y > 0 \\ 0 & \text{otherwise} \end{cases} \tag{8}$$

where $\{\dot{p}_{Am,yolk}\}$ is the surface area-specific yolk assimilation rate. Finn et al. (1995) shows that the yolk is exhausted at day 6 p.h. at 6 ℃. With an initial value chosen from the same data (see below), an absorption rate of $\{\dot{p}_{Am,yolk}\} =$ 70 J cm^{-2} day^{-1} gives the same yolk absorption time.

The sum of assimilation fluxes from yolk and gut is denoted $\dot{p}_A$:

$$\dot{p}_A = A - \frac{dY}{dt} \tag{9}$$

where A is computed as a variable fraction of the gut emptying rate:

$$A = k_{as}\{\dot{p}_{Am}\}V^{2/3}\frac{k_g S}{k_{as}k_g S + \{\dot{p}_{Am}\}V^{2/3}} \tag{10}$$

where k_{as} is the maximum assimilated fraction, and $\{\dot{p}_{Am}\}$ is the surface area-specific maximum assimilation rate[1]. When gut content S is low, the assimilated fraction is close to k_{as}, and for increasing S the total assimilated flux approaches $\{\dot{p}_{Am}\}V^{2/3}$, giving a decreasing assimilated fraction for increasing ingestion rates. The relationship between gut emptying rate $k_g S$ and A is illustrated by Figure 1 B. We choose $k_{as} = 0.8$ and $\{\dot{p}_{Am}\} = 90$ J cm^{-2} day^{-1}, which typically gives an assimilated fraction of 40-60 % in the start feeding regimes used in this experiment.

Before finding the state equations for structure V and energy reserves E, we set up the expression for the total catabolic power, $\dot{p}_C$. Kooijman (2000) uses the assumptions of strong and weak homeostasis and the partitionability requirement to derive the following expression for $\dot{p}_C$:

$$\dot{p}_C = [E](\dot{v}V^{2/3} - \frac{dV}{dt}) \tag{11}$$

where $[E] = E/V$ is the reserve density, and $\dot{v}$ is the energy conductance, which determines how rapidly energy in reserves is mobilized, and affects how much of the larvae's dry weight is in reserves versus structure. We choose the value $\dot{v} = 0.02$ cm day^{-1}, which leads to reserves making up around 45 % of dry weight under the feeding regimes of this experiment.

[1]The cod larvae are assumed to grow *isomorphically*, which implies that surface area is proportional to $V^{2/3}$.

The maintenance requirement is assumed proportional to the structural volume V with proportionality constant $[\dot{p}_M]$.The energy budget for structural growth is as follows:

$$\frac{dV}{dt} = \frac{\kappa \dot{p}_C - [\dot{p}_M]V}{[E_G]} \tag{12}$$

where the parameter $[E_G]$ specifies the energy spent per unit of volumetric growth. The value of $[E_G]$ will be specified later. The parameter κ sets a fixed proportion of $\dot{p}_C$ that is spent on growth plus maintenance (the remaining portion $1 - \kappa$ is available for development plus investment in reproduction). The rapid growth of cod larvae indicate that growth is given high priority, so we choose the value $\kappa = 0.8$.

The maintenance rate $[\dot{p}_M]$ can be chosen after looking at survival time for starved larvae. Jordaan and Brown (2003) found that larvae starved at 7.7±0.6 ℃ from day 0 had close to 100% mortality after 10-11 days. We assume that the model enters a starvation mode if Eq. 12 gives negative growth, where $dV/dt = 0$ and mobilization from reserves is limited to that required for maintenance. The time until the energy reserves E is exhausted under starvation should be comparable to the time when the larval group reaches 100% mortality. With $[\dot{p}_M] = 150$ J cm^{-3} day^{-1}, $E = 0$ J at day 11, which seems reasonable in comparison with the starvation times of Jordaan and Brown (2003).

Substituting Eq. (12) into Eq. (11) gives:

$$\begin{array}{c} \dot{p}_C = [E](\dot{v}V^{2/3} - \frac{\kappa \dot{p}_C - [\dot{p}_M]V}{[E_G]}) \\ \Updownarrow \\ \dot{p}_C = \frac{[E]([E_G]\dot{v}V^{2/3} + \dot{p}_M)}{[E_G] + [E]\kappa} \end{array} \tag{13}$$

The values of dV/dt and dE/dt can now be calculated, the former from Eq. (12), and the latter from:

$$\frac{dE}{dt} = \dot{p}_A - \dot{p}_C \tag{14}$$

The dry weight of larvae depends on all larval states, and is comparable with the measurement of larval dry weight, denoted y_{DW}.

$$W_d = [W_V]V + (E + Y)/\mu_E + S/\mu_S \tag{15}$$

where $[W_V]$ relates structural volume to dry weight. Since the larvae are neutrally buoyant the wet weight should be approximately 1 g cm^{-3}. Finn et al. (2002) found that DW of larvae in this phase is approximately 15% of wet

weight, so we choose $[W_V] = 0.15$ g cm^{-3}. μ_E and μ_S denote the energy per g DW of reserves and gut content, respectively. We assume that these are both similar to the energy density of the feed, which was estimated at 13000 J g^{-1} earlier.

To find a reasonable estimate for the cost of growth, $[E_G]$, we assume that the energy density per DW unit is the same in structure as in reserves, and add a 10% overhead. Thus, $[E_G] = 1.1 \times [W_V] \times \mu_E = 2145$ J cm^{-3}.

2.4.2 Rotifer model

We use a simple rotifer model that accounts for addition, dilution by water exchange, predation and egg hatching, as well as the rotifers' tendency to attach to the tank walls. If microalgae are added to the tank, one can expect the rotifers to produce new eggs after having been added to the fish tank. However, at the temperatures and water exchange rates used for cod larvae, the egg production rate is too low to affect the rotifers' egg ratio significantly. Therefore we simplify the model by assuming that there is no production of new eggs.

This model is described in detail in Alver et al. (2005), so only a brief overview will be given here. The model has 4 state variables:

- N_c : The number of rotifers in the water column.
- N_w : The number of rotifers attached to the tank wall.
- E_c : The number of eggs on rotifers in the water column.
- E_w : The number of eggs on rotifers attached to the tank wall.

The automatic measurement from the rotifer counter accounts for N_c, the only directly observable state in the rotifer model. The measurement of rotifer density is denoted y_X.

The controlled variables are u (addition rate of rotifers to the water column), e_u, egg ratio of the added rotifers, and Q_w, the exchange rate of the tank water (the turnover rate of the water volume per day).

The rotifer state equations are as follows:

$$\frac{dN_c}{dt} = u + (E_c + E_w)h_e - M_w + M_c - p_c - q_c \quad (16)$$

$$\frac{dN_w}{dt} = M_w - M_c - p_w \quad (17)$$

$$\frac{dE_c}{dt} = ue_u - E_c h_e - \frac{E_c}{N_c}(M_w + p_c + q_c) + \frac{E_w}{N_w}M_c \quad (18)$$

$$\frac{dE_w}{dt} = -E_w h_e + \frac{E_c}{N_c} M_w - \frac{E_w}{N_w}(M_c + p_w) \tag{19}$$

where the various symbols are computed as described in Eqs. (20) – (25).

The hatching rate of rotifer eggs is approximately equal to the inverse of the development time of eggs, T_e:

$$h_e = 1/T_e \tag{20}$$

Dhert (1996) reports embryonic development times of 1.0 days at 20 ℃ and 1.3 days at 15 ℃. Since temperatures are 10–12 ℃ in the larval tanks, we choose $T_e = 1.6$ days as a rough estimate.

The total predation pN_l can be split into predation on rotifers in the water column, p_c, and on rotifers on the wall, p_w, proportionally to the distribution of rotifers:

$$p_c = pN_l \frac{N_c}{N_c + N_w} \tag{21}$$

$$p_w = pN_l \frac{N_w}{N_c + N_w} \tag{22}$$

Eggs are also subject to predation, and we calculate the predation rate on eggs by multiplying the predation rate on rotifers with the egg ratio for each of the two subpopulations.

The symbols M_w and M_c represent the migration of rotifers onto the wall and into the water column, respectively. Migration to the wall is represented by M_w:

$$M_w = N_c k_m A_w / (10000 V_w) \tag{23}$$

where A_w is the wall area of the tank, and k_m is a constant. $A_w/(10000V_w)$ describes the area/volume ratio of the tank, and k_m describes the product of how close to the wall (cm) a rotifer must be to be able to attach, and the rate of "close enough" rotifers attaching. As in Alver et al. (2005), we set $k_m = 250$.

M_c imposes a soft upper bound ρ_{cap} to the density on the wall:

$$M_c = N_w \left(\frac{N_w}{A_w \rho_{cap}} \right)^4 \tag{24}$$

where this specific form is chosen simply to get a relationship where M_c is small for values of N_w smaller than $A_w \rho_{cap}$, and increasing steeply when N_w increases beyond $A_w \rho_{cap}$. As in Alver et al. (2005), we set $\rho_{cap} = 14$ cm^{-2}.

The rate of rotifer loss through the water outlet per time unit is denoted q_c. Rotifers making up the N_c state are assumed to be homogeneously distributed

throughout the water column, and consequently the loss of rotifers due to water exchange is proportional to N_c and the water exchange rate Q_w:

$$q_c = Q_w N_c \tag{25}$$

2.5 Initial values

Simulations are started on day 3 p.h. at noon ($t = 3.5$). All the rotifer states start out at 0 because feeding has not yet been initiated. The initial number of larvae varies between simulations, and their gut content S is initially set to 0. Using data from Finn et al. (1995) on cod egg composition and yolk volume we can estimate that the yolk initially contains approximately 1.76 J of chemical energy. Comparing the relative yolk volume initially with that three days after hatching, we find $Y(3.5) = 0.4$ J as a reasonable initial value. We choose the initial values $V(3.5) = 2.35 \times 10^{-4}$ cm^3 and $E(3.5) = 0.06$ J that give an initial dry weight of 6.6×10^{-5} g and a relatively small energy reserve.

2.6 Kalman filter

The extended Kalman filter is the state estimator algorithm that will be used. The Kalman filter, when used on linear systems, gives the optimal least-variance state estimates for a given system and measurement setup (Jazwinsky, 1970). The Kalman filter equations are presented in detail in Alver et al. (2005).

The model equations are integrated using the fourth order Runge-Kutta method (Hartley et al., 1994). At time steps where measurements are available, the deviation between estimated and actual measurements, termed the *innovation*, is used together with a covariance matrix for the model states to calculate corrections for the states values. The covariance matrix is integrated in parallell with the model equations.

To apply this technique we need to make certain assumptions regarding the variability (or uncertainty) of model states and measurement values. Each model state and measurement is assumed to be affected by an additive white noise term, each with a given variance, and all of them independent of each other. The estimator will work optimally if these assumptions are exactly correct, but that is difficult to achieve in practical terms. A reasonable approximation of these values is sufficient, and we have chosen values based on a fraction of a typical value for each state. Table 2 shows the noise standard deviations that were used.

Table 2: Standard deviation of additive noise terms for all model states.

State	Noise std.dev.	Unit
N_l	280	larvae
V	7.0×10^{-6}	cm^3
E	2.2×10^{-4}	J
Y	2.2×10^{-4}	J
S	7.1×10^{-5}	J
N_c	1.7×10^{5}	rotifers
N_w	1.7×10^{5}	rotifers
E_c	5.5×10^{4}	rotifers
E_w	5.5×10^{4}	rotifers

Table 3: Standard deviation of additive noise terms for measurements.

Measurement	Noise std.dev.	Unit
y_X	300	rotifers $liter^{-1}$
y_{DW}	5.5×10^{-6}	g

The measurement uncertainty for y_X (the rotifer counter) is variable, but we choose a fixed standard deviation of 300 rotifers $liter^{-1}$]. For y_{DW} (dry weight) we assume a standard deviation of 5.5×10^{-6} g, which amounts to approximately 5% of the measured values in the middle of the period. Table 3 summarizes the assumed measurement standard deviations.

The effect of the noise terms on the Kalman filter is to determine how much the model estimates are weighted versus the measurements. Generally speaking, the model corrections resulting from a given deviation will be greater the greater the model uncertainty and the lower the measurement uncertainty, and uncertain states will be given relatively greater corrections than less uncertain states.

3 Results

3.1 Survival and growth

Survival and growth data are summarized in Tables 4 and 5. Due to an error in the sampling procedure, dry weight measurements are incomplete at day 9 for the A group.

Table 4: Number of larvae at the termination of the experiment on day 16.

Tank	Larvae	Larvae l^{-1}	Initial larvae l^{-1}	Survival %
A1	2191	13.4	20	67.2
A2	1699	10.4	20	52.1
A3	1998	12.3	20	61.3
B1	3030	18.6	40	46.5
B2	2923	17.9	40	44.8
B3	3005	18.4	40	46.1
C1	6004	36.8	80	46.0
C2	7652	46.9	80	58.7
C3	6863	42.1	80	52.6

Table 5: Measured larval dry weight [μg].

Tank	Day 0	Day 3	Day 5	Day 9	Day 15
A1	75.5	70.1	114	-	165
A2	75.5	70.1	137	-	230
A3	75.5	70.1	67.0	89.8	204
B1	75.5	70.1	80.8	112	211
B2	75.5	70.1	71.2	153	252
B3	75.5	70.1	78.9	146	177
C1	75.5	70.1	73.7	105	223
C2	75.5	70.1	71.7	133	202
C3	75.5	70.1	102	208	183

Dead larvae were removed at each tank cleaning, but due to their small size they decompose quickly, making it very difficult to obtain reliable mortality data throughout the period. At the end point at day 16 p.h., however, the larval count is reliable. Survival is calculated relative to the nominal starting densities for each group. The B group showed a significantly lower survival than the A group ($p \approx 0.03$), but no significant difference could be found between the A and C groups and between the B and C groups. Figure 2 sums up the survival and growth rates for the three groups. Growth rate is averaged over the period from the initial feeding at day 3 until the last measurement at day 15.

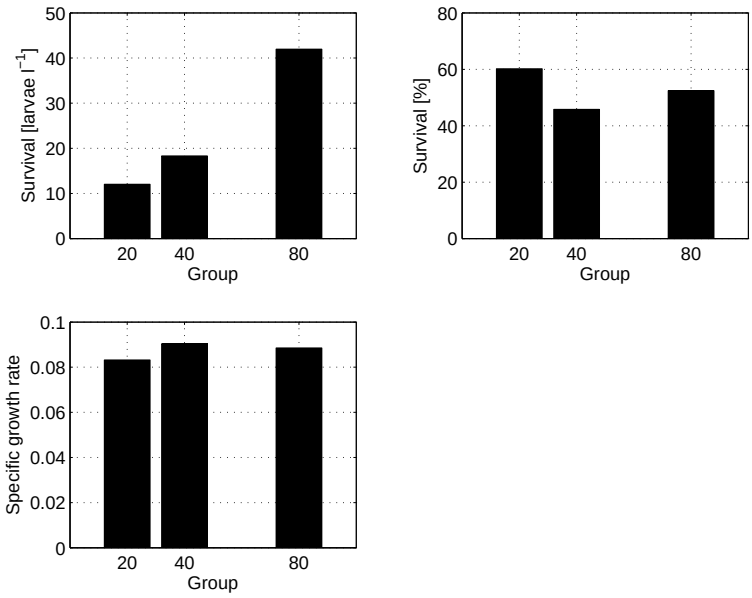

Figure 2: Survival at day 16 and average growth from day 3–15 for the three groups.

3.2 Estimator runs

Each estimator run produces estimated values for all model states throughout the simulation period, and all derived output values can be computed.

Figures 3 and 4 show the larval density and dry weight from an estimator run for each of the four tanks monitored by the automatic rotifer counter. Figures 5 and 6 shows part of the rotifer density measurement series for tanks B1 and C1, compared to modelled values[2]. One can see indications, in comparison with Figure 3, of how model adjustments come as reactions to deviations in rotifer density.

[2]The complete series are quite extensive, and would require too much space to present in entirety.

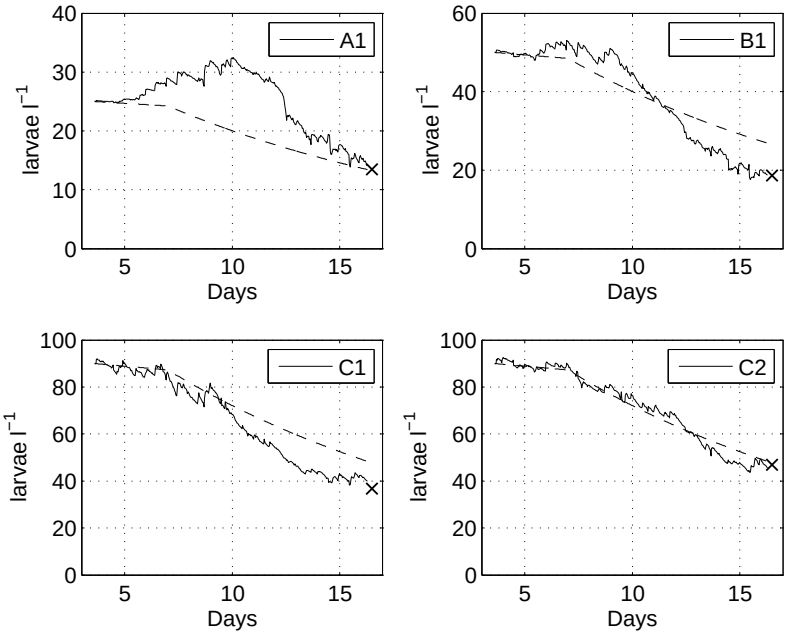

Figure 3: Estimated larval densities for tanks A1, B1, C1 and C2. Dashed lines show uncorrected modelled values, and solid lines show corrected estimates. For comparison the individual count at the end of the experiment is marked with an asterisk (*) for each tank.

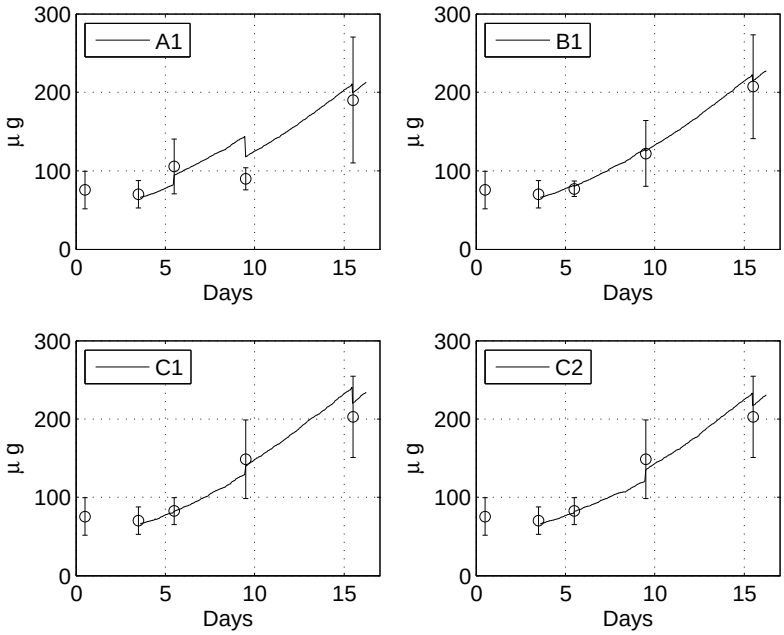

Figure 4: Estimated larval growth for tanks A1, B1, C1 and C2, and group-averaged dry weight measurements used for estimator correction. Error bars show sample standard deviation for larval weight.

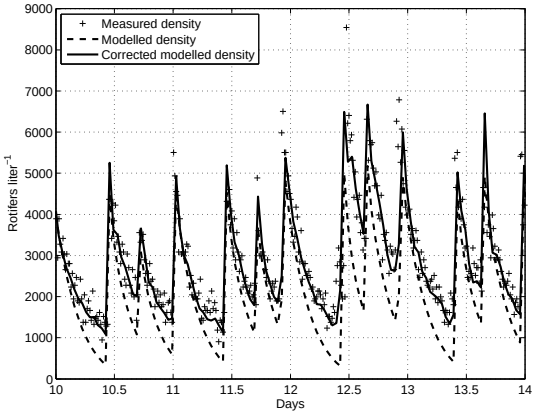

Figure 5: Measured rotifer densities in tank B1 for days 10–13. The dashed line shows uncorrected modelled values, and the solid line shows corrected model estimates.

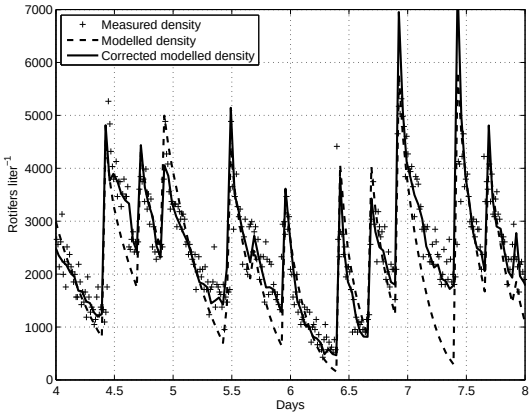

Figure 6: Measured rotifer densities in tank C1 for days 4–7. The dashed line shows uncorrected modelled values, and the solid line shows corrected model estimates.

4 Discussion

4.1 Experimental results

There were no apparent problems related to water quality or microbial condition in the tanks, and survival was good (ranging 44–67 %) in all tanks. Survival was highest in the low density group, which had significantly better survival than the medium density group. The average specific growth rate (SGR) in the period 3–15 days p.h. was 0.09 day^{-1}, and the average DW at day 15 was 200 μg. In comparison, Otterlei et al. (1999) fitted growth curves in the larval period for cod fed with live zooplankton, which predict approximately the same DW on day 15 at a temperature of 12 °C.

Both growth and survival were close to the average values for the highest density group, meaning that no adverse effects of using that density compared to lower densities could be seen.

4.2 Estimator performance

The ultimate goal of the larval density estimator is to provide objective and correct estimates of the larval density. However, at this point we must look at the simpler task of detecting relative differences in larval density. There is still too much model uncertainty, especially related to feed intake and conversion rate, to be able to directly estimate the absolute densities. In this experiment observations were used to adjust the model's feed intake parameter $\{\dot{p}_{Im}\}$, which means that the estimator's larval densities are not quite objective estimates.

However, what has been shown in this experiment is that the estimator correctly detects differences in larval density between tanks with all model parameters unchanged. The differences are detected based on inputs and measured values only, and the results firmly establish that the estimator principle is valid for this process.

Time series of estimated values show some random variation (noise), which is caused by measurement errors affecting the adjustments made by the Kalman filter.

One interesting feature of Figure 3 is the increase in the larval density estimate of tank A1 during days 5–10. Even though the model only allows reduction in larval density over time, the estimator is allowed to increase the density to compensate for too low estimates. Since a maximum of 25 larvae liter -1 should have been added to tank A1, the estimator overestimates the density significantly in this period. This could be a sign that appetite was unusually

high in this tank in the first period – the growth data do indicate fast growth initially for this tank. It is also possible that more than the nominal number of larvae by accident has been added to this tank. Finally, this could indicate an unmodelled density-dependent effect which is more pronounced at lower larval densities.

5 Conclusions

No clear conclusions about the effect of larval densities on growth and survival can be drawn from the experimental results, although we note that the highest density used, 80 larvae liter^{-1}, does not appear to have caused any adverse effects.

The results of the estimator runs are more interesting, since it is clearly demonstrated that the model based estimator can provide approximate estimates of larval density based on readily available measurements. Relative differences in density are detected, although to obtain truly objective biomass estimates, more experimental work must be done to produce more reliable estimates for the model's most important parameters.

6 Acknowledgments

Thanks to Elin Kjørsvik and Per-Arvid Wold (Department of Biology, NTNU) who participated in the start feeding experiment.

This work is part of the strategic university programme CODTECH at the Norwegian University of Science and Technology.

References

Alver, M. O., Alfredsen, J. A., Øie, G., 2005. A system for model based biomass estimation of larvae in intensive cod larvicultures. Aquaculture International 13, 519–541.

Buckley, L. J., Lough, R. G., Peck, M. A., Werner, F. E., 2000. Comment: Larval atlantic cod and haddock growth models, metabolism, ingestion, and temperature effects. Canadian Journal of Fisheries and Aquatic Sciences 57, 1957–1960.

Dhert, P., 1996. Rotifers. In: Lavens, P., Sorgeloos, P. (Eds.), Manual on the production and use of live food for aquaculture. FAO, Rome, pp. 49–78.

Finn, R. N., Fyhn, H. N., Evjen, M. S., 1995. Physiological energetics of developing embryos and yolk-sac larvae of atlantic cod (*Gadus morhua*). i. respiration and nitrogen metabolism. Marine Biology 124, 355–369.

Finn, R. N., Rønnestad, I., van der Meeren, T., Fyhn, H. J., 2002. Fuel and metabolic scaling during the early life stages of atlantic cod gadus morhua. Marine Ecology Progress Series 243, 217–234.

Hartley, T. T., Beale, G. O., Chicatelli, S. P., 1994. Digital Simulation of Dynamic Systems - A Control Theory Approach. PTR Prentice Hall.

Holling, C. S., 1965. The functional response of predators to prey density and its role in mimicry and population regulation. Memoirs of the Entomological Society of Canada.

Holm, J. C., Svåsand, T., Wennevik, V. (Eds.), 1991. Håndbok i torskeoppdrett. Stamfiskhold og yngelproduksjon. Havforskningsinstituttet, in Norwegian.

Jazwinsky, A., 1970. Stochastic processes and filtering theory. Academic Press.

Jordaan, A., Brown, J. A., Oct. 2003. The risk of running on empty: the influence of age on starvation and gut fullness in larval atlantic cod (*Gadus morhua*). Canadian Journal of Fisheries and Aquatic Sciences 60, 1289–1298.

Kooijman, S. A. L. M., 2000. Dynamic energy and mass budgets in biological systems, 2nd Edition. Cambridge University Press.

Lough, R. G., Mountain, D. G., 1996. Effect of small-scale turbulence on feeding rates of larval cod and haddock in stratified water on georges bank. Deep Sea Research Part II: Topical Studies in Oceanography 43, 1745–1772.

Olsen, Y., van der Meeren, T., Reitan, K. I., 2004. First feeding technology. In: Moksness, E., Kjørsvik, E., Olsen, Y. (Eds.), Culture of Cold-Water Marine Fish. Blackwell Publishing, Oxford, pp. 279–336.

Otterlei, E., Nyhammer, G., Folkvord, A., Stefansson, S. O., 1999. Temperature- and size-dependent growth of larval and early juvenile atlantic cod (*gadus morhua*): a comparative study of norwegian coastal cod and northeast artctic cod. Canadian Journal of Fisheries and Aquatic Sciences 56, 2099–2111.

Puvanendran, V., Leader, L. L., Brown, J. A., 2002. Foraging behaviour of atlantic cod (*Gadus morhua*) larvae in relation to prey concentration. Canadian Journal of Zoology 80, 689–699.

Øie, G., Olsen, Y., 1997. Protein and lipid content of the rotifer *Brachionus plicatilis* during variable growth and feeding condition. Hydrobiologia 358, 251–258.

Automatic control of rotifer density in larval first feeding tanks

Morten Omholt Alver[*], Torodd Tennøy[†], Jo Arve Alfredsen[*], Gunvor Øie[‡], Yngvar Olsen[§]

Abstract

Larvae of many marine fish species in aquaculture require live plankton as feed. Under the common feeding regimes the density of live feed shows significant variation throughout the day. We present a feedback control system for keeping feed density at a desired level or following a trajectory. Such a system allows more flexibility in experimental designs for research on feed intake patterns, and can reduce manual labour and increase stability of the feeding conditions in commercial hatcheries. The system has been tested in a first feeding experiment and shown to perform satisfactorily.

[*]Department of Engineering Cybernetics, Norwegian University of Science and Technology, Odd Bragstads plass 2D, 7491 Trondheim, Norway

[†]Thelma AS, Box 6170 Sluppen, 7435 Trondheim, Norway

[‡]SINTEF Fisheries and Aquaculture AS, SINTEF Sealab, Brattørkaia 17B, 7010 Trondheim, Norway

[§]Department of Biology, Norwegian University of Science and Technology, 7491 Trondheim, Norway

1 Introduction

Larvae of marine fish species such as Atlantic cod (*Gadus morhua*), turbot (*Scophthalmus maximus*), sea bream (*Sparus aurata*) and many other in aquaculture are fed live plankton in the initial feeding period (Yoshimura et al., 1996; Shields, 2001). In intensive culture, the first feed is usually rotifers of one of a few species of the *Brachionus* species complex (Lubzens et al., 1989; Papakostas et al., 2006).

A water exchange rate of one or more tank volumes per day is typically used in larval tanks. This serves to remove food organisms in order to limit their residence time, and to prevent accumulation of toxic substances. We therefore see a continuous loss of live feed, typically of the same order of magnitude as the combined ingestion rate of the larvae. With only two to four feedings per day, the result is a significant diurnal variation in feed density (see Figure 1). Systems for automatic feeding have been presented by other authors (Kolkovski et al., 2004; Papandroulakis et al., 2002; Rabe and Brown, 2000), but these are feed-forward systems only. In feed-forward systems, the rotifer density observed in the tanks is a direct consequence of the feed addition rate used, so density and feed supply are interdependent. This dependency can be broken by the introduction of feedback controlled feeding, in which the controller supplies exactly the amount of feed needed to hold the density at the desired level. The feed supply will cover demands regardless of the chosen density, and consequently density and supply are decoupled.

Feedback control is achieved by utilizing online measurements of the process variables when computing input. In our process we can measure the feed density using an automatic plankton counter (Alver et al., in press). The counter works autonomously, and can monitor the rotifer density in a set of up to 10 tanks. Figure 1 shows an example of measurements made in a cod start feeding experiment with batch feeding. A feedback controller would make it possible to remove the diurnal density variations or dictate the desired variation pattern. A significant reduction in manual labour can be achieved, but other benefits may prove to be of equal importance. First, the ability to keep a constant, optimal, feed density could result in significantly higher ingestion rates, and consequently better growth and survival – cod larvae have been demonstrated to have a growth potential exceeding 25% per day (Otterlei et al., 1999). Automation makes it possible to investigate feed intake patterns of the larvae much more closely, and to find the optimal feeding regimes for each species. If good results can be achieved with a low, constant feed density, the amount of live feed wasted due to the water exchange can be reduced significantly. Further-

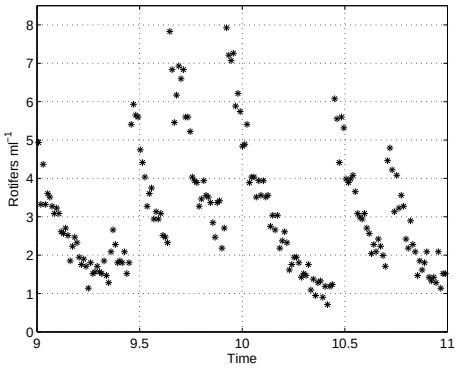

Figure 1: Automatic measurements of rotifer density in larval first feeding tank. Measurements from days 9 and 10 of a cod start feeding experiment (Alver, M. O., Alfredsen, J. A. & Øie, G., unpublished results).

more, the live feed contributes to a high microbial load in the first feeding tanks (Skjermo and Vadstein, 1999), and feedback controlled feeding may reduce this effect by preventing over feeding. Second, when combining measurements and information about the amount of rotifers added, the controller can produce an estimate of the feed ingestion rate in the tank, which has a substantial value for the farmer as a metric for assessing the status of a larval group.

In this study, a system for feedback control of rotifer density in first feeding tanks is developed. The system is tested in a first feeding experiment in order to investigate its accuracy, and to discover which disturbances need to be handled in practical use of the control system.

2 Material and methods

2.1 The control system

Figure 2 shows an overview of the control system. It is designed so that one controller and one plankton counter can handle a set of larval tanks. For measurement, one sampling tube is attached within each tank. A valve manifold is used to lead water from one of these at a time into the counter. The sampled water is not returned to the larval tanks. For addition of rotifers, water is

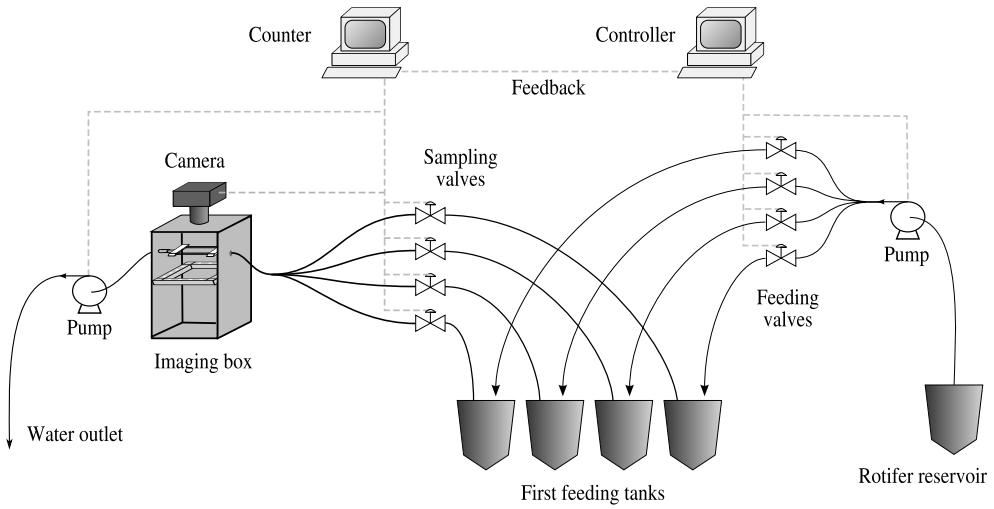

Figure 2: Overview of the control system. Solid curves represent tubes, while dashed lines represent data transmission and control lines. The "counter" and "controller" are both implemented in the same computer.

pumped from a rotifer reservoir and through another valve manifold that routes the input into the correct tank. The pumps are peristaltic pumps (Watson-Marlow), which set up a flow with a minimum of harm to the rotifers in the water, and without risk of contamination of the water from the pump.

Rotifer addition is managed by pulse width modulation. The controller cycles repeatedly through all tanks, allocating a predetermined time slot per tank. A fraction of each slot, as determined by the controller, is used for pumping rotifers into the tank.

Since the rotifer counter alternates between tanks, new measurements are not available very frequently (2–3 per hour per tank in our experimental setup). The controller must be able to compute input values at any time, and since the true density can change significantly in the time interval between measurements, we choose a model based approach to provide estimates of the rotifer density. In the model based controller, we use a Kalman filter (Jazwinsky, 1970) for correcting the model state based on measurements. In order to predict the depletion rate of rotifers in the tanks, the larval ingestion rate needs to be included in the model.

2.2 System model

We formulate a simple model of the larval tank, where the first state variable is the rotifer density R. R is only affected by the addition rate u, the known water exchange rate q and the larvae's ingestion rate. Since we need to estimate the ingestion rate, we introduce it as a second state variable I. We further define the state vector $x = [R \quad I]^T$.

The model's state equations are as follows:[1]

$$\dot{R}(t) = u(t) - q(t)R(t) - I(t) + v_D(t) \tag{1}$$

$$\dot{I}(t) = v_I(t) \tag{2}$$

where v_D and v_I are random noise terms. Typically, the ingestion rate as a function of feed density is modelled according to the Holling Type II functional response (Holling, 1965). In this model we make the simplifying assumption that the ingestion rate of the fish is independent of the feed density.

If we define the noise vector $v = [v_D \quad v_I]^T$, we can express the system as follows:

$$\dot{x} = f(x, u) + I_2 v \tag{3}$$

where I_2 is the 2x2 identity matrix, and

$$f(x, u) = \begin{bmatrix} 1 \\ 0 \end{bmatrix} u + Ax \tag{4}$$

where

$$A = \begin{bmatrix} -q(t) & -1 \\ 0 & 0 \end{bmatrix} \tag{5}$$

We need to define a measurement model $y(t)$ to represent the prediction of measurements from the model. Our only measurement is of the rotifer density:

$$y(t) = R(t) + w(t) = Dx(t) + w(t) \tag{6}$$

where $D = [1 \quad 0]$ and $w(t)$ is the measurement noise.

The noise terms $v_1(t)$, $v_2(t)$ and $w(t)$ are assumed to be mutually independent white noise terms. We define the covariance matrices V and W:

$$V = E\left\{ \begin{bmatrix} v_1(t) & v_2(t) \end{bmatrix} \begin{bmatrix} v_1(t) \\ v_2(t) \end{bmatrix} \right\} = \begin{bmatrix} 5 & 0 \\ 0 & 5 \end{bmatrix} \tag{7}$$

$$W = E\{w(t)w(t)\} = [0.5^2] \tag{8}$$

[1] The ingestion rate I is assumed to have no deterministic dynamics. A more detailed model could contain factors describing the expected changes in ingestion rate due to larval size and mortality.

where the values for V are chosen based on simulations of the system, and the value of W is near the expected variance of measurements at low densities.

To check for observability, we compute the observability matrix of the linear system:

$$O = \begin{bmatrix} D \\ DA \end{bmatrix} = \begin{bmatrix} 1 & 0 \\ -q & -1 \end{bmatrix} \tag{9}$$

which has full rank, showing that the system is observable (Jazwinsky, 1970).

2.3 Kalman filter

In the Kalman filter, an estimate of the covariances between the states is utilized to compute optimal model corrections. The matrix $X(t)$ denotes the covariance matrix, and has the following differential equation:

$$\dot{X}(t) = AX(t) + X(t)A^T + V = F(X) \tag{10}$$

The model derived above is time-continuous. We use a time-discrete formulation in the Kalman filter, where the time step is denoted Δt, and start by defining two new sets of state vectors:

- $\bar{x} = [\bar{R} \quad \bar{I}]^T$: *a priori* estimates
- $\hat{x} = [\hat{R} \quad \hat{I}]^T$: *a posteriori* estimates

for which we indicate the time step using subscripts. We similarly introduce $\bar{X}$ and $\hat{X}$ for the covariance matrix.

We integrate the model by alternating between two steps, *prediction* and *filtering*. In the prediction step we compute the *a priori* estimates for time step $k+1$ from the *a posteriori* estimates of time step k, replacing the noise term v_k by its expectation value (0). Since the model's dynamics are slow and we can afford to use a sufficiently small time step, we discretize the model using the simple Euler's method:

$$\bar{x}_{k+1} = \hat{x}_k + \Delta t f(\hat{x}_k, u_k) \tag{11}$$

$$\bar{X}_{k+1} = \hat{X}_k + \Delta t F(\hat{X}_k) \tag{12}$$

Before filtering we advance k by one time step, so that the *a priori* estimates just computed are now denoted $\bar{x}_k$ and $\bar{X}_k$. In the filtering step we compute the *a posteriori* estimates for time step k. If there are no measurements available

at time k, $\hat{x}_k = \bar{x}_k$ and $\hat{X}_k = \bar{X}_k$. If there is a measurement vector y_k, a model correction is computed:

$$\hat{x}_k = \bar{x}_k + K_k(y_k - D\bar{x}_k) \tag{13}$$

$$\hat{X}_k = (I - K_k D)\bar{X}_k \tag{14}$$

where the matrix K_k is given by:

$$K_k = \bar{X}_k D^T (D\bar{X}_k D^T + W)^{-1} \tag{15}$$

K_k is the matrix that describes what relevance each measurement has to each state value, and also how much weight should be put on the measurements as opposed to the model estimates. Both the state equations and our assumptions about the system's stochastic inputs influence the elements of K_k.

2.4 Controller

The controller uses the estimated rotifer density and ingestion rate when setting the input value. Since rotifers cannot be removed from the tank by the controller, $u(t)$ is restricted to nonnegative values. The reference value is denoted $r(t)$.

We define the errors in our estimates $\hat{R}$ and $\hat{I}$ as $e_R = R - \hat{R}$ and $e_I = I - \hat{I}$. We define the deviation of the true density from the reference value as z: $z(t) = R(t) - r(t)$. In the absence of any addition of rotifers, we estimate the rate of change of the rotifer density to be $-(\hat{I}(t) + q(t)\hat{R}(t))$, so it is reasonable to seek to cancel out this term with an equal opposite feed-forward term. After adding a proportional compensation term, $K_p(r(t) - \hat{R}(t))$, this gives:

$$u(t) = K_p r(t) + \hat{I}(t) + (q(t) - K_p)\hat{R}(t) \tag{16}$$

and the following equation for the true deviation in the absence of noise terms:

$$\dot{z}(t) = u(t) - I(t) - q(t)(r(t) + z(t)) = -K_p z(t) - e_R(t)(K_p + q(t)) - e_I(t) \tag{17}$$

which would give asymptotic convergence with a time constant of $1/K_p$ if the state estimates were perfect. However, we achieve faster convergence and less interference from e_R by using the feed-forward term $\hat{I}(t) + q(t)r(t)$, based on the reference density, giving:

$$u(t) = \hat{I}(t) + (q(t) + K_p)r(t) - K_p\hat{R}(t) \tag{18}$$

and

$$\dot{z}(t) = -(K_p + q(t))z(t) - e_R(t)K_p - e_I(t) \tag{19}$$

An increase in K_p increases the convergence rate if the state estimates are perfect. Generally, however, $|e_R| > 0$, and a larger K_p also amplifies the effect of this error on the density deviation.

The feed-forward term prevents stationary deviation if the estimate of the feed ingestion rate is correct. However, the ingestion rate is expected to increase with time, which can lead to a stationary deviation in its estimate. To improve the handling of estimation errors, an integral term is needed. We introduce the state variable h in the controller to keep track of the integral term:

$$\dot{h}(t) = K_{int}(r(t) - \hat{R}(t)) \tag{20}$$

Finally, we restrict $u(t)$ to nonnegative values, and get the following expression:

$$u(t) = max\left(0, \left[\hat{I}(t) + (q(t) + K_p)r(t) - K_p\hat{R}(t) + h(t)\right]\right) \tag{21}$$

The controller cycles through N tanks with a time slot of Δt_u seconds each. The pumping time per time slot must be calculated from $u(t)$, which is expressed as rotifers ml^{-1} day^{-1}, and calculated as if the input were continuous. We define V_w [ml] as the tank volume, R_{res} [rot. ml^{-1}] as the rotifer density in the reservoir and q_u [ml s^{-1}] as the pumping rate from the reservoir. The number of rotifers to add in each N tank cycle is:

$$u_{cycle} = \frac{\Delta t_u N}{86400} V_w u(t) \tag{22}$$

where 86400 is the number of seconds in a day. For each tank's time slot, this gives a pumping period of U seconds:

$$U = \frac{u_{cycle}}{q_u R_{res}} \tag{23}$$

If $U > \Delta t_u$, the pumping time is limited to the entire time slot of Δt_u seconds, and the value of $u(t)$ must be similarly limited before being applied to the mathematical model.

Based on simulations of the system, we choose the controller parameters $K_p = 100$ and $K_{int} = 1$, and add the limitation $|h(t)| \leq 6$.

2.5 Hardware and software implementation

The software for the rotifer counter and the controller is implemented in LabView 7.0 and run on a laptop PC with Microsoft Windows XP. The density counter captures images using a Sumix SMX-150 black and white machine vision camera. The camera is connected to the PC's USB port, allowing the LabView software to retrieve and analyze the images. The relays for activating lights and the pumps and valves are controlled from the LabView software through two I/O modules that communicate with the PC using an RS-232 serial connection.

2.6 First feeding experiment

The control system was tested in a complete first feeding experiment with 9 tanks (80 l) kept at different rotifer density set points. We number the tanks 1–9, where tank 1 had a set point of 1 rot. ml^{-1}, tank 2 of 2 rot. ml^{-1}, etc., up to 9 rot. ml^{-1} in tank 9.[2] The positions of the tanks in the laboratory were randomized. The experiment also included a 10th tank (the control tank) which was batch fed three times per day up to 5000 rot. ml^{-1} initially, and to 7000 rot. ml^{-1} from day 11.

Rotifers were grown in 250 l tanks under semi-continuous conditions at 20°C with 20% daily dilution, and fed 1.4 μg yeast per individual (up to 120 g per tank) with addition of 5% Marol E and 10% alga paste.

Cod eggs were acquired from Marinebreed AS, and hatched in an egg incubator. Near the completion of hatching, 40 larvae l^{-1} were transferred into each of the tanks. Each tank was equipped with aeration from the bottom center. Feeding was initiated on day 2 post hatch. Water exchange was initiated at the same time, and set to 1 tank volume per 24 h. The rate was doubled on day 4, and doubled again on day 10. All tanks were cleaned four times throughout the period by siphoning up organic matter accumulated on the tank bottoms. A number of live larvae were carried out during the siphoning, and these were immediately returned to the tanks.

The controller pumped water from a reservoir into the experimental tanks. The reservoir was refilled each morning with a high density (400–1000 rot. ml^{-1}) of rotifers, and *Isochrysis galbana* alga paste was added to boost the nutritional quality of the rotifers. The reservoir density was measured after each refill

[2] In a standard batch feeding regime one typically adjusts the rotifer density up to a density of 4000-7000 rotifers l^{-1} three times per day. Puvanendran and Brown (1999) found that 4000 rotifers l^{-1} was the optimal density.

and again in the evenings, and the density entered as the parameter R_{res} in the controller. The controller cycled through the tanks with a time slot of 30 seconds each.

To verify the actual rotifer densities in the tanks, 50 ml samples were taken from each tank two times per day, and analyzed for rotifer density. The samples were taken near the center of the tanks using a glass tube fitted with a filter at the end to prevent larvae from being extracted. The number of rotifers in each sample was determined visually using a stereo microscope after fixation with Lugol's solution.

3 Results

Survival at the end of the experiment was in the range 30–50% for all tanks except tanks 4 and 8, which had only 14% and 23%, respectively. The growth of the larvae was fairly good, with mean standard length increasing from ca. 5.1 mm to ca. 7.0 mm.

The densities observed in manual measurements show a fairly stable density for each of the 9 tanks (Figure 3), although some negative drift can be seen e.g. for tanks 2 and 4. Taking the arithmetic mean of all manual measurements for each tank (Figure 4), we see that the average density is somewhat high for tank 1, and low for tanks 3–9. The densities observed from the controller's point of view can be summarized by taking the arithmetic mean of all automatic measurements for each tank (Figure 5). The averages of the automatic measurements are lower than the set points for tanks 2–9.

The number of rotifers added per day to each tank (Figure 6) shows that the feed usage increases strongly, although less than proportionally, with the density set point. For comparison, the total amount of feed added to the control tank was approximately 17.7 million rotifers, which is slightly less than the amount added to tank 2.

The agreement between automatic and manual measurements (Figure 7) is fairly good. The linear approximation indicates a slight positive bias in the automatic measurements, and the density-dependent measurement uncertainty is indicated by the scatter of the measurement points.

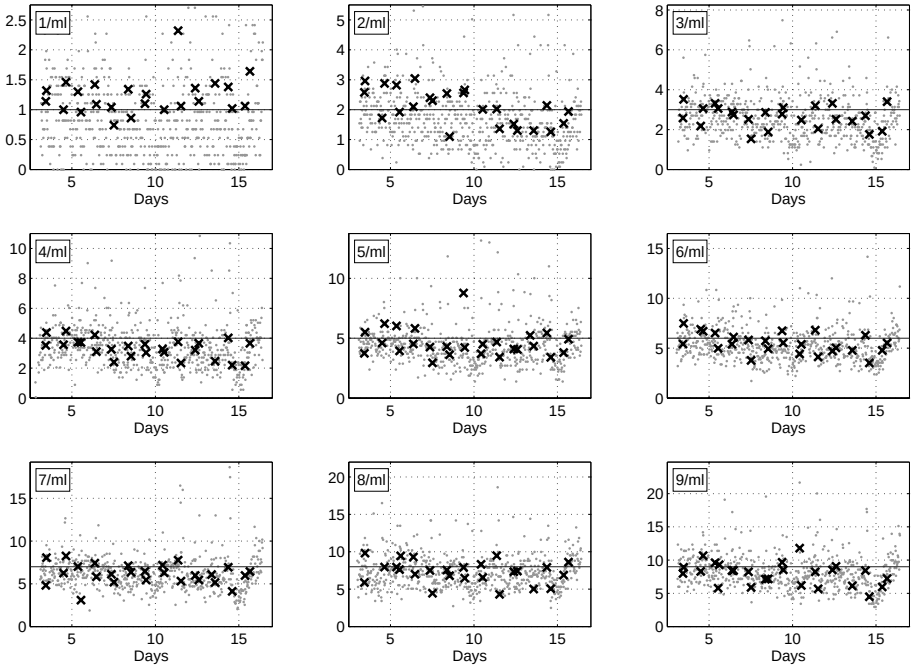

Figure 3: Manual rotifer density measurements (marked with X) and automatic measurements (marked with gray dots) in each of the experimental tanks. Tanks are ordered by increasing reference density. For comparison, a solid line shows the reference density for each tank. Note that the y axis scaling is different for each tank

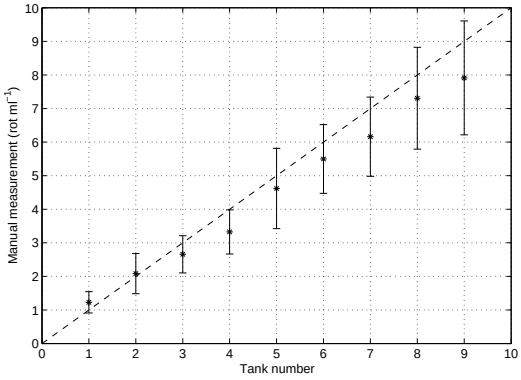

Figure 4: Average and standard deviation of manual rotifer density measurements in all tanks. Tanks are ordered by increasing reference density. For comparison, the dashed line shows the desired rotifer densities in each of the tanks.

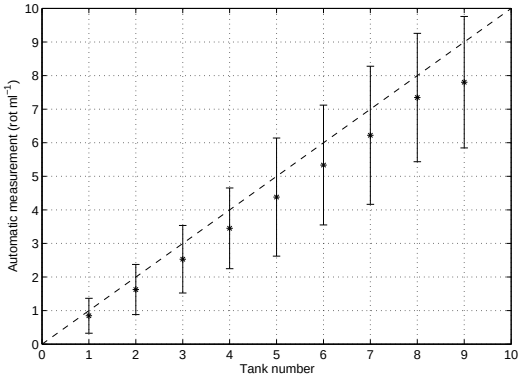

Figure 5: Average and standard deviation of automatic rotifer density measurements in all tanks. Tanks are ordered by increasing reference density. For comparison, the dashed line shows the desired rotifer densities in each of the tanks.

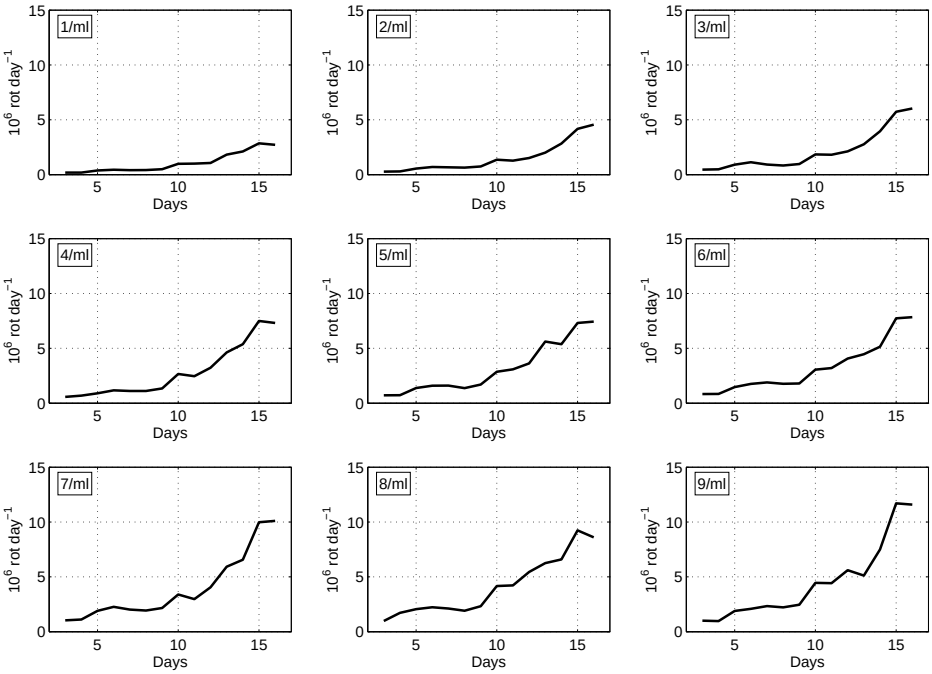

Figure 6: Total number of rotifers added to each tank during each day of the experiment.

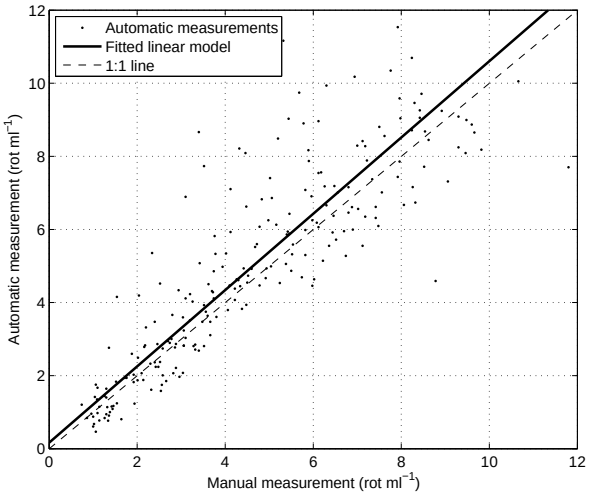

Figure 7: Manual measurements plotted each against the average of the 3 closest automatic measurements. The solid line shows a linear approximation of the relationship ($y = 1.04x + 0.17$), calculated by weighted mean squares. For comparison, the dashed line shows the ideal 1:1 line.

4 Discussion

4.1 Feeding amounts

In the period from day 9–10 until the end of the experiment, the feed addition rates are increasing rapidly for all tanks. This is reasonable, given that the larvae's feed requirements increase as they grow. However, it is likely that rotifer addition by the controller is overestimated toward the end of the experiment because the tube from the reservoir became clogged by organic matter from the alga paste used for enrichment. The flow rate provided by the pump decreases as the counter-pressure increases. This problem can be corrected by replacing the pump or modifying tube dimensions.

The comparison of feeding amounts in batch feeding versus feedback controlled feeding is skewed because of this deviation. It is likely that less feed was used in several of the tanks with the lowest densities compared to the batch feeding tank, but the available data do not allow this to be determined.

4.2 Model accuracy

The increase in feed consumption with time leads to some negative offset in the observed rotifer densities, even as the controller adjusts its estimate of feed ingestion rate and steadily increases addition rate. This effect could to some degree have been suppressed by assuming a larger noise level for feed ingestion in the Kalman filter (through modification of V in Eq. (7)) to give more rapid correction of this state variable.

Another model limitation is that the effect of rotifers attaching to the tank wall and bottom is neglected. For small tanks, the number of rotifers attached to the wall can be large enough to significantly affect the density of rotifers in the water column (Alver et al., in press). This can be expected to give some bias initially, because rotifers attached to the wall are not lost through the water exchange, and are not detected when measuring rotifer density. However, as long as the rotifer density is held at a near-constant level, this will only be a transient effect.

4.3 Accuracy and variability of measurements

We have calculated the standard deviations of the automatic measurements, and compared these to the theoretical statistical variability due to sample size (Alver et al., in press) in Figure 8. To get more accurate information on the

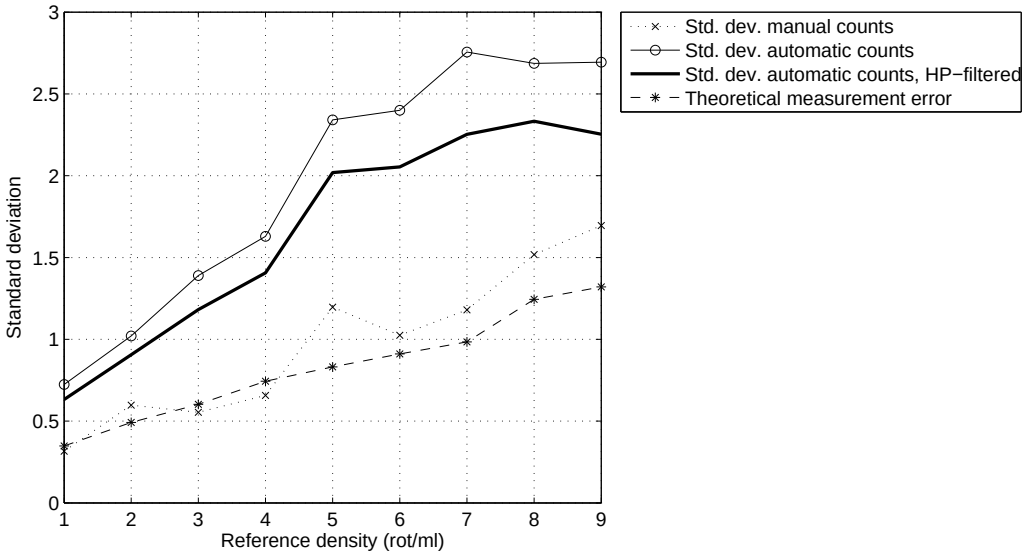

Figure 8: Comparison of standard deviation of manual counts, automatic counts (actual and high-pass filtered) and theoretical standard deviation for each of the tanks.

measurement error of the counter, we also compare with high-pass filtered measurement series to remove slow density changes which are likely to represent real fluctuations. The standard deviation of the measurements appears to be 70–130% higher than the theoretical standard deviation. This difference may be caused by imperfect mixing in the tanks due to added feed pulses.

The standard deviation of the manual measurements is similar to the theoretical standard deviation, however, which indicates that the controller to a certain degree suppresses the effect of the measurement error.

4.4 Procedures causing measurement errors

Addition of algae is done by pouring along the tank wall to minimize strain on the cod larvae. This process tears loose rotifers attached to the tank wall and bottom, causing a temporary increase in rotifer density in the water column.

Manual measurements made within the first half hour after algal addition show a strong positive bias. By mistake, 3 measurements on day 10 (morning) and 7 measurements on day 13 (morning) were done after algal addition and had to be discarded. This effect is especially noticeable because the tanks used in this experiment are small. In large, commercial scale tanks, the problem is likely to be less significant.

During tank cleaning, there is some upwelling of organic matter from the bottom into the water column. This matter includes a large amount of dead rotifers, which cause a positive bias in the automatic rotifer density measurements before resettling to the bottom.[3] The result can be a drop in densities after tank cleaning, which was observed especially on days 11 and 14. The best way to avoid this error may be to ignore measurements and add rotifers based on the process model only for a couple of hours after each tank cleaning. Commercial scale tanks are typically equipped with automatic cleaning arms running continuously, but more slowly, and will therefore not suffer from this problem.

4.5 Other sources of error

Manual measurements have statistical uncertainty, and a possibility of sampling or counting error. If sampling coincides with feeding, an error may occur if the sample contains substrate from the feeding tube. The water exchange rate is another potential source of error. It is adjusted manually, and may suffer some drift due to changes elsewhere in the water supply. A deviation in this rate affects the estimate of the feed intake rate, but has only a transient effect on the controlled density.

4.6 Conclusions and further work

The experiment has shown that the automatic feeding system works acceptably. However, due to some sources of error, deviations were observed in conjunction with events such as tank cleaning and algal addition. All errors that introduced bias worked in the same direction, causing densities lower than the set points. For this reason, observed densities in the experiment were too low on average for most tanks.

[3] When measuring density manually, dead rotifers can be distinguished visually, because only live rotifers ingest the strongly colored Lugol's solution. The automatic counter has no means to discriminate between them.

These problems can be partly avoided by temporarily disabling model corrections from measurements, e.g. after tank cleaning and algal addition. Due to differences between the experimental tanks and commercial scale tanks, some of these problems are not likely to occur in a commercial setting.

The manual work required for the feeding of rotifers is reduced to refilling the rotifer reservoir once per day when using the automatic feeding system, and the controller can provide either a constant feed availability, or a variation in feed density as chosen by the user. Choosing the optimal feed availability may have a positive effect on larval performance and on the predictability of the rearing process.

5 Acknowledgments

Thanks to Ingrid Overrein, Sunniva Kui and Tove Beate Leren who participated in the first feeding experiment.

This work is part of the university programme CODTECH, funded by the Research Council of Norway and the Norwegian University of Science and Technology.

References

Alver, M. O., Tennøy, T., Alfredsen, J. A., Øie, G., in press. Automatic measurement of rotifer *Brachionus plicatilis* densities in first feeding tanks. Aquacultural Engineering.

Holling, C. S., 1965. The functional response of predators to prey density and its role in mimicry and population regulation. Memoirs of the Entomological Society of Canada.

Jazwinsky, A., 1970. Stochastic processes and filtering theory. Academic Press.

Kolkovski, S., Curnow, J., King, J., Oct. 2004. Intensive rearing system for fish larvae research: I. marine fish larval rearing system. Aquacultural Engineering 31, 295–308.

Lubzens, E., Tandler, A., Minkoff, G., 1989. Rotifers as food in aquaculture. Hydrobiologia 186/187, 387–400.

Otterlei, E., Nyhammer, G., Folkvord, A., Stefansson, S. O., 1999. Temperature- and size-dependent growth of larval and early juvenile atlantic cod (*Gadus morhua*): a comparative study of norwegian coastal cod and northeast artctic cod. Canadian Journal of Fisheries and Aquatic Sciences 56, 2099–2111.

Papakostas, S., Dooms, S., Triantafyllidis, A., Deloof, D., Kappas, I., Dierckens, K., Wolf, T. D., Bossier, P., Vadstein, O., Kui, S., 2006. Evaluation of dna methodologies in identifying brachionus species used in european hatcheries. Aquaculture 255, 557–564.

Papandroulakis, N., Dimitris, P., Pascal, D., 2002. An automated feeding system for intensive hatcheries. Aquacultural Engineering 26, 13–26.

Puvanendran, V., Brown, J. A., 1999. Foraging, growth and survival of atlantic cod larvae reared in different prey concentrations. Aquaculture 175, 77–92.

Rabe, J., Brown, J. A., 2000. A pulse feeding strategy for rearing larval fish: an experiment with yellowtail flounder. Aquaculture 191, 289–302.

Shields, R. J., 2001. Larviculture of marine finfish in europe. Aquaculture 200, 55–88.

Skjermo, J., Vadstein, O., Jul. 1999. Techniques for microbial control in the intensive rearing of marine larvae. Aquaculture 177, 333–343.

Yoshimura, K., Hagiwara, A., Yoshimatsu, T., Kitajima, C., 1996. Culture technology of marine rotifers and the implications for intensive culture of marine fish in Japan. Marine & Freshwater Research 47, 217–222.